University of Sheffield

Don’t go out there! How interaction outside the host can affect the Rhizobia-Legume Symbiosis

Charlotte Pain

A thesis in partial fulfilment of the requirements for the degree of Doctor of Philosophy

The University of Sheffield

Faculty of Science

School of Biosciences

Submission Date

March 2025

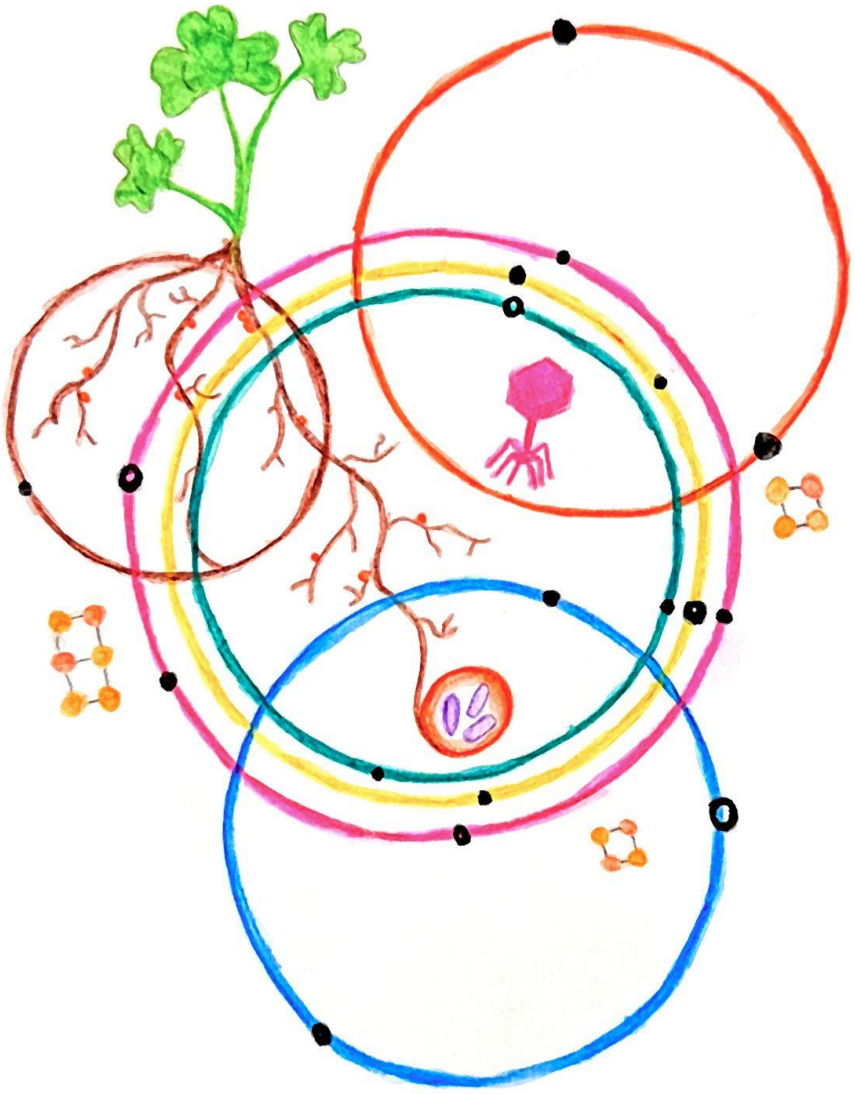

Illustration by Dr. Anne Williams (spoiler alert for thesis!).

For my Dad,

I love you,

… and you're lucky you got out of here before you had to read this!

Acknowledgements

Firstly, I'd like to say thank you to my supervisors, Dr Ellie Harrison, Dr Alex Best and Dr Ville Friman, all your advice and guidance has shaped me into the scientist I am today; 'thank you' seems too embarrassingly simple and completely inadequate to convey the depth of my gratitude to you all. Ellie and Alex, your knowledge, patience and kindness are unmatched. Your support has helped me believe in myself as a scientist in ways I never expected, and academia is a brighter place because of you both.

To everyone on f-floor corridor, you're some of the most brilliant like-minded people I've ever met, thank you for always providing the most wildly unproductive but deeply necessary conversations, questionable baked goods and making me laugh on an hourly basis. A special thanks to the Harrison lab - Conrad, Grace, Mary, Kat and Sol, it would have been a hard, lonely road without you all. Anne, thank you for pulling me away from work to enjoy life. Conrad, thank you for bringing all the colour to my life on the dullest of days. Hannah and Laura, thank you for always being two beautiful ears to rant to. And Rachele, I am lucky enough to have found a best friend amongst this chaos, to have gone through all this and more together, thank you for questioning our life choices together.

Again, thank you all for knowing when *not* to ask, and for encouraging me to the bitter end.

A thank you to my family for always supporting my endeavours - Dad, thank you for trekking through fields with me for samples and your continued excitement over digging up plants - despite still not knowing what I do with them. Gran, you'll be happy to hear, I've finally finished my '*exams*' and got a *'real job'*…

And last but never least, thank you to my ultimate partner in crime, Dave, for being the only thing that really matters. Thank you for everything you've done for me, you've truly kept me alive whilst doing this PhD and I could not have done it without you.

Stick a fork in me, I'm done.

Authors Declaration

I, Charlotte Pain, confirm that this thesis is my own work. I am entirely aware of the guidance of the University on the Practice of Unfair Means (www.sheffield.ac.uk/ssid/unfair-means). This work has never been previously presented for an award at this, or any other degree or any other university.

Thesis Summary

The interaction between rhizobia and their bacteriophage predators represents an understudied yet critical component of soil microbial ecosystems, with potential implications for the agriculturally important rhizobia-legume symbiosis. Little is understood about how phage-driven evolution of rhizobia in the soil influences their symbiotic relationships with legumes. Using experimental and mathematical modelling, this thesis aims to bridge this knowledge gap by investigating the evolutionary consequences of phage predation on rhizobia and the resulting impacts on symbiosis. We demonstrate that prolonged exposure of rhizobia to phage predation in the soil rapidly selects for phage-resistant bacterial strains. Although these resistant rhizobia did not exhibit direct symbiosis-specific trade-offs, phage-driven selection did induce genetic mutations that indirectly influenced symbiotic quality of evolved rhizobia. Genome sequencing revealed that phage-exposed rhizobia accumulated mutations predominantly affecting metabolic pathways and biofilm formation. Consequently, some of these mutations indirectly affected rhizobia's symbiotic quality, highlighting that phage coevolution can shape the functionality of the rhizobia-legume mutualism. Additionally, we show that the ability of rhizobia to escape phage exposure by colonizing root nodules creates an important ecological trade-off. Early nodule colonization allows rhizobia to evade phage-driven selection, preserving symbiotic efficiency, but renders them more susceptible to phage predation upon their return to the soil. Highlighting the interplay between symbiosis and coevolution, where the timing of host association can influence bacterial fitness and evolutionary trajectories. Mathematical modelling showed that plant-associated nodules serve as spatial refuges, influencing rhizobia-phage coevolution. Refuges promote stable coexistence between rhizobia and free-living phages, while trade-offs in phage resistance, particularly those tied to refuge use, are crucial for maintaining both resistant and susceptible strains in the soil. Collectively, this research emphasizes that bacteriophage predation not only shapes rhizobial evolution in the soil but has downstream consequences for their ecological interactions with legumes.

Table of Contents

List of Figures

Chapter 1

Chapter 2

Chapter 3

Chapter 4

Chapter 5

Chapter 6

Supplementary Figures

List of Tables

Chapter 2

Chapter 3

Supplementary Tables

Chapter 4

Chapter 5

Supplementary Tables

Chapter 6

Chapter 1: Introduction

1.1 Overview of Research Significance

Symbiotic interactions between plants and microbes are fundamental to ecosystem functioning and agricultural productivity, with the rhizobia-legume relationship serving as a critical example. Rhizobia, specialized nitrogen-fixing bacteria, convert atmospheric nitrogen into ammonia within legume root nodules, enhancing plant growth, soil fertility, and reducing reliance on environmentally harmful synthetic fertilizers (Sprent, 2007; Herridge, 2008; Oldroyd, 2013).

Understanding the diverse genetic and environmental factors that influence the effectiveness and evolution of this symbiosis is crucial for sustainable agriculture and ecosystem management. These factors range from host-symbiont genetic compatibility and soil nutrient availability to complex biotic interactions within the soil microbiome (Sprent, 2017). While much research has focused on the direct interaction between legumes and rhizobia, considerably less attention has been given to how the broader microbial community, particularly bacteriophages (phages), shapes rhizobial evolution and their mutualistic interactions (Koskella and Brockhurst, 2014; Pratama and Van Elsas, 2019). In soil ecosystems, rhizobia coexist with diverse microbial organisms, including fungi, protists, and other bacteria, alongside phages, which impose significant evolutionary pressures through predation, thereby influencing bacterial abundance, genetic diversity, and functionality (Kuzyakov and Blagodatskaya, 2015; Jansson and Hofmockel, 2018).

Phages are abundant, diverse viruses that significantly drive microbial evolution by mediating genetic exchange and selecting for resistance mechanisms ((Gómez and Buckling, 2011; Koskella and Brockhurst, 2014; Touchon, Moura de Sousa and Rocha, 2017). Given that rhizobia alternate between free-living states in soil and symbiotic states within nodules, phage-driven selection in soil could profoundly impact their symbiotic traits. Resistance adaptations, while advantageous against phages, might impose fitness costs that alter traits important for

the symbiosis, such as surface polysaccharide production, motility, or metabolic efficiency, potentially impairing rhizobial symbiotic capabilities (Oldroyd and Downie, 2008; Gómez and Buckling, 2011; Poole, Ramachandran and Terpolilli, 2018). This understanding is particularly important as alterations in rhizobial fitness, due to phage-rhizobia co-evolution, may have profound implications for agricultural sustainability, ecosystem productivity, and the management of legume crops.

Currently, the broader implications of phage-rhizobia interactions on symbiotic efficiency and legume productivity remain poorly understood. This thesis addresses this knowledge gap, integrating experimental and mathematical modelling approaches to investigate how coevolution between rhizobia and phages in the soil influences rhizobial functionality and consequently affects the rhizobia-legume mutualism. Additionally, it examines how the symbiosis itself shapes bacteria-phage interactions, particularly by providing refuges within nodules that may alter coevolutionary dynamics and resistance evolution.

1.2. Rhizobia-Legume Symbiosis

1.2.1 The Legume Host

Legumes, plants belonging to the family Fabaceae, are a cornerstone of global agriculture and natural ecosystems. This diverse family includes critical food crops such as beans (Phaseolus vulgaris), peas (Pisum sativum), lentils (Lens culinaris), soybeans (Glycine max), and alfalfa (Medicago sativa), as well as foundational ecosystem species like clover (Trifolium spp.) (Graham and Vance, 2003). A defining characteristic of most legumes is their ability to form a specialized root structure, the root nodule, which houses rhizobial bacteria. The development of this symbiosis is intrinsically linked to the legume's root system architecture. A typical legume root system consists of a primary root that grows vertically downward, with lateral roots branching off to explore the soil for water and nutrients (Forde and Lorenzo, 2001). The infection process resulting in nodulation predominantly occurs on root hairs, which are delicate, single-cell extensions of epidermal cells located on the primary and lateral roots

(Gage, 2004). Because root hairs occur on both primary and lateral roots, their developmental timing and density strongly influence where and when nodules form, The plant actively controls nodule development, initiating it in response to rhizobial signals and regulating nodule number through systemic processes to balance the carbon and nitrogen economy of the plant (Reid, Ferguson and Gresshoff, 2011).

1.2.2 The Rhizobial Symbiont

Rhizobia are a polyphyletic group of soil bacteria, most of which are classified as motile, Gram-negative Alphaproteobacteria (e.g., *Rhizobium*, *Sinorhizhobium*, *Mesorhizobium*, *Bradyrhizobium*) (Sprent, Ardley and James, 2017). They exist in a dual lifestyle, alternating between a free-living, saprophytic state in the soil and a symbiotic, nitrogen-fixing state within legume root nodules (Poole, Ramachandran and Terpolilli, 2018). In their free-living state, rhizobia compete for resources in the soil matrix. Most rhizobial species possess flagella, which provide motility essential for chemotaxis, the directed movement towards chemical gradients, such as the flavonoids and other root exudates released by potential host legumes (Al-Ghamdi et al., 2022). This ability is critical for locating a suitable host and initiating the symbiosis.

1.2.3 The mutualistic relationship

The rhizobia-legume interaction is a mutualism of global importance. Legumes provide rhizobia with carbon-rich nutrients derived from photosynthesis and a protective microaerobic environment within root nodules (Udvardi and Poole, 2013). In return, the rhizobia provide the plant with a bioavailable nitrogen source. Legumes, due to this interaction, are integral to crop rotation systems, enhancing agricultural sustainability (Herridge, 2008) in two ways , 1) by reducing reliance on synthetic nitrogen fertilizers that contribute to environmental degradation and 2) by improving soil fertility.

1.2.4 Mechanisms of Rhizobia-Legume Symbiosis

The symbiotic relationship between rhizobia and its host legume begins with a molecular communication, as described in 1.2.2..Flavonoids secreted by legume roots act as chemical signals, inducing the expression of rhizobial nodulation (*nod*) genes(Grundy *et al.*, 2023). These genes produce Nod factors, which are recognized by Nod factor receptors (NFRs; plant LysM receptor-like kinases, e.g., NFR1/NFR5 orthologues)on legume root hairs (D'Haeze and Holsters, 2002). This recognition triggers a, the plant's common symbiosis signalling pathway (Sym pathway). A key downstream effect of this pathway is the initiation of characteristic, periodic oscillations in calcium concentration, known as 'calcium spiking', within the nucleus of the root hair cell (Oldroyd et al., 2011). This calcium signal is essential for activating the full cascade of symbiotic events, including root hair curling, infection thread formation, and nodule organogenesis (Oldroyd and Downie, 2008; Cangioli *et al.*, 2022). Inside the nodules, rhizobia differentiate into bacteroids, specialized nitrogen-fixing cells that express nitrogenase enzymes. These enzymes catalyse the reduction of atmospheric nitrogen to ammonia under microaerobic conditions maintained by leghaemoglobin, a plant produced protein that sequesters oxygen (Udvardi and Poole, 2013). NFRs are plant receptors on root hairs, whereas on the bacterial side surface components such as LPS/EPS and flagella mediate attachment and infection-thread progression, and in many systems also serve as phage receptors. Together, Nod factor structure, host NFR specificity, Sym-pathway signalling, bacterial EPS/LPS architecture, and nitrogenase regulation. Together, Nod factor structure, host NFR specificity, Sym-pathway signalling, EPS/LPS architecture, and nitrogenase regulation constitute the core genetic and molecular determinants of compatibility and fixation efficiency. See **Figure 1** for a schematic overview.

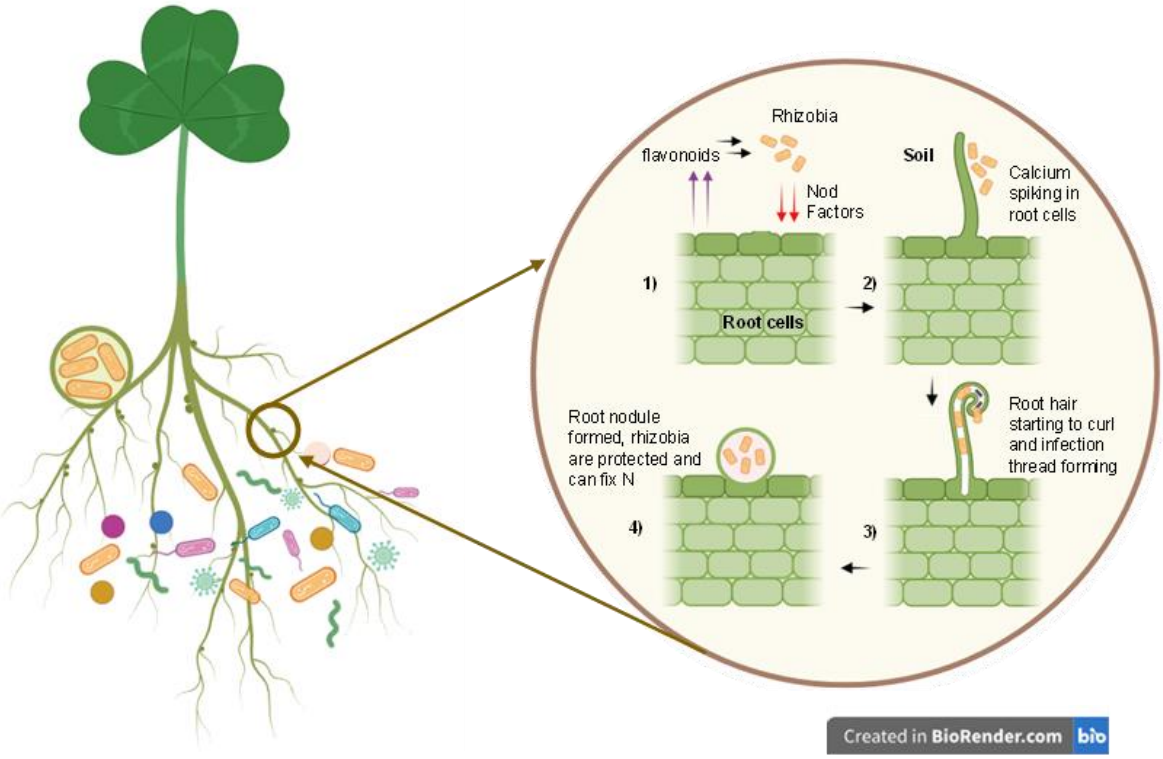

Figure 1: *Nodulation of legumes by Rhizobium.* ***1)*** *Signal Exchange and Symbiosis Activation: Flavonoids released by legume roots attract rhizobia, which produce nodulation factors (Nod factors). These are recognized by the plant, activating the symbiosis signalling pathway.* ***2)*** *Calcium Spiking and Infection Thread Formation: Nod factor recognition triggers a spike in calcium levels in root epidermal and cortical cells. Rhizobia enter root hair cells, causing them to curl, and an infection thread forms at the curl site for bacterial entry.* ***3)*** *Nodule Initiation and Infection Thread Growth: Nodule primordia form in the root cortex beneath the infection site, while the infection thread grows deeper and fuses with these developing nodules.* ***4)*** *Bacteroid Formation and Nitrogen Fixation Rhizobia are released into symbiosomes within the nodules, where they differentiate into bacteroids, specialized cells that fix atmospheric nitrogen for the plant. Image created using biorender.*

1.2.5 Selective Pressures on the Rhizobia-legume Symbiosis

The efficiency of the rhizobia-legume symbiosis depends on genetic compatibility of rhizobia and host and many external pressures. Genetic diversity within rhizobial populations influences nodule occupancy and nitrogen fixation efficiency, with highly efficient strains significantly enhancing legume growth (Denison, 2000; Sprent, Ardley and James, 2017) . This genetic diversity is extensive, often involving variations in key symbiosis genes (e.g., *nod*, *nif*, *fix* genes) that are frequently located on mobile genetic elements like symbiosis plasmids

(pSym) (Bailly et al., 2006). In their free-living soil phase, rhizobia also face environmental challenges, including pH, temperature, moisture, and nutrient availability, all of which impact survival and functionality (Alexandre and Oliveira, 2013; Zhang *et al.*, 2023; Yeremko *et al.*, 2025). For example, acidic soils and drought conditions can hinder rhizobial viability and limit nodulation and nitrogen fixation (Slattery, Coventry and Slattery, 2001; Ferguson and Mathesius, 2014).

In addition to environmental factors, microbial interactions significantly shape rhizobial populations. Among these, phages exert strong selective pressures through predation. Phage-driven evolution forces rhizobia to develop resistance mechanisms that enhance survival but may interfere with the molecular dialogue essential for symbiosis. Potential fitness costs of phage resistance are numerous and can directly impact symbiotic traits. For example, resistance often involves modifying or masking surface receptors like LPS or EPS (Montenegro-Gómez et al., 2022), which are also critical for root attachment, infection thread formation, and evading plant immune responses (Poole, Ramachandran and Terpolilli, 2018). Similarly, if flagella are used as phage receptors, down-regulation of motility to escape infection would simultaneously reduce chemotaxis towards root exudates, thus lowering the chances of nodulation (Al-Ghamdi et al., 2022).

Given that genetic variation in rhizobial mutualist quality is strongly influenced by host genotype and environmental conditions(Heath and Tiffin, 2007), selective pressures from phages may similarly contribute to variability in symbiotic efficiency. Studies suggest that phage resistance in bacteria can impose metabolic costs affecting key ecological functions, though direct evidence for reduced nitrogen fixation in rhizobia is lacking. For example, in *Escherichia coli*, resistance to phage lambda via modification of the LamB outer membrane protein comes at the cost of reduced maltose uptake (Bohannan and Lenski, 2000). In cyanobacteria, phage resistance has been linked to reduced nitrogen fixation ability (Kolan *et al.*, 2024), while phage-resistant *Pseudomonas syringae* and *Dickeya solani* mutants exhibit growth rate costs in plant hosts and compromised colonization or virulence, respectively

(Meaden and Koskella, 2017; Bartnik *et al.*, 2022). Bacterial immune strategies against phages often involve trade-offs between defence and fitness(van Houte, Buckling and Westra, 2016) , influencing physiology, metabolism (Martinez *et al.*, 2009), and broader ecological interactions (Bohannan and Lenski, 2000). Given that nutrient transport and metabolism are essential for effective nitrogen fixation in legume-rhizobia symbioses (van Houte, Buckling and Westra, 2016), it is plausible that phage resistance mechanisms could impact this process. This dynamic represents a coevolutionary arms race, where rhizobia evolve defences to evade phage predation, and phages counter-adapt to overcome these defences. Such interactions shape rhizobial traits critical for symbiosis, as the dual lifestyle of rhizobia, alternating between soil and legume nodules, exposes them to fluctuating selective pressures (**Van Houte et al., 2016**).

1.3. Bacteria-Phage Co-Evolution and their role in Soil Microbial Communities

Phages, the most abundant biological entities on Earth, are central drivers of microbial diversity and evolution (Clokie *et al.*, 2011; Hatfull, 2015). In soil ecosystems, phages regulate bacterial populations through predation, influencing community structure, gene flow, and ecosystem functionality (Abedon, 2008). Beyond population control, phages facilitate horizontal gene transfer (HGT) via transduction, contributing to bacterial adaptation and genetic innovation (Touchon, Moura de Sousa and Rocha, 2017)). Phages employ two primary infection strategies, lytic and temperate lifestyles (Olszak *et al.*, 2017). (**Figure 2**). Lytic phages rapidly infect and lyse their bacterial hosts, imposing strong selection pressures on bacterial populations and shaping their evolutionary trajectories (Koskella and Brockhurst, 2014). In contrast, temperate phages can integrate into the bacterial genome as prophages, entering a lysogenic state where they are replicated along with the bacterial host (Howard-Varona *et al.*, 2018). This lysogeny allows phages to persist within bacterial populations without immediate destruction, occasionally providing hosts with beneficial genes through lysogenic conversion (Touchon, Bernheim and Rocha, 2016). However, under stress conditions, temperate phages can be induced into the lytic cycle, leading to bacterial cell lysis and phage propagation.

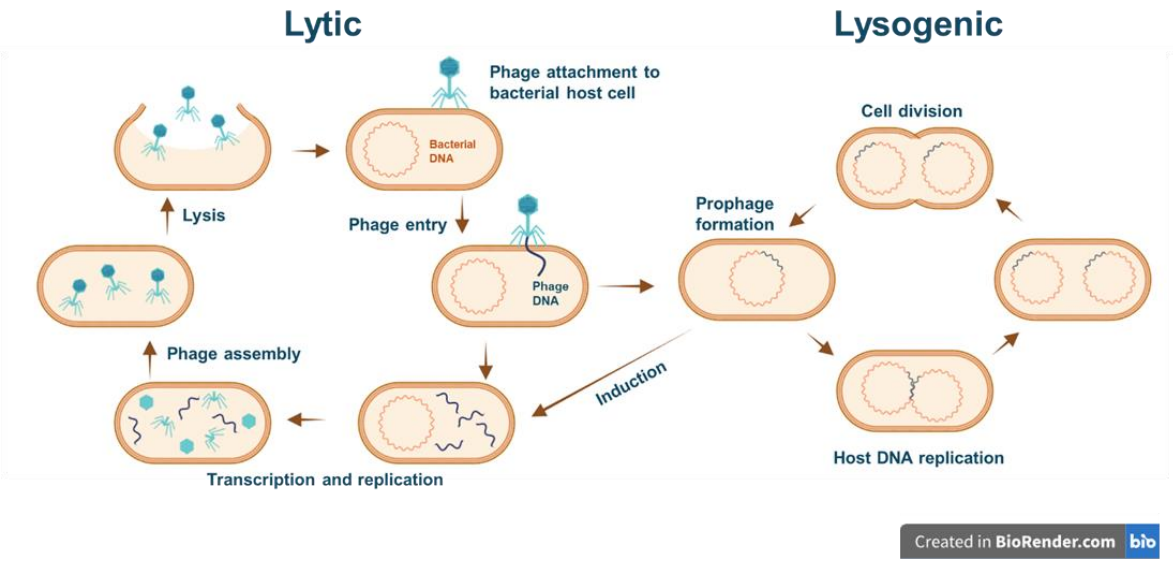

Figure 2: *Bacteriophage Lifecycle: Lytic phages attach and infect a bacterial cell which results in the reproduction of phages and lysis of the cell host and this lysogenic cycle results in the integration of a phage genome into the bacterial genome. Some lysogenic phages do not integrate into the genome and remain in the cell as a circular or linear plasmid (not depicted here). Image created using biorender.*

In the highly diverse and structured environments of soil, phages interact with numerous bacterial taxa and among these are nitrogen-fixing rhizobia. These interactions influence rhizobial abundance, survival, and evolutionary trajectories, with downstream effects on their symbiotic capacity and agricultural utility(Fierer, Bradford and Jackson, 2007)). Understanding these dynamics is essential to elucidate how microbial interactions shape mutualisms like the rhizobia-legume symbiosis.

1.3.1 Mechanisms of Bacteria-Phage Co-Evolution

Bacteria and phages are frequently engaged in a co-evolutionary arms race, where bacterial populations evolve defences to evade predation, and phages counter-adapt to overcome these barriers. However, this dynamic is not universal across all phage-bacteria interactions. In lysogenic cycles, where temperate phages integrate into bacterial genomes as prophages rather than immediately lysing their hosts, the selective pressures on both bacteria and phages can differ significantly from those observed in strictly lytic interactions(Bobay, Touchon and

Rocha, 2014)**.** Additionally, fluctuating negative frequency-dependent selection can influence the pace and nature of co-evolution, as the relative advantage of resistance and infectivity shifts over time (Gandon *et al.*, 2008; Westra *et al.*, 2015).

These variations highlight the complexity of bacteria-phage interactions, which can range from intense antagonistic co-evolution to more stable, integrated relationships depending on environmental conditions and bacterial host dynamics. For nitrogen-fixing rhizobia, we predict that these co-evolutionary pressures not only shape bacterial survival strategies during their free-living phase but also influence their ability to engage in mutualistic interactions with legumes. While previous studies have highlighted the role of genetic and molecular factors in determining symbiotic compatibility and nitrogen-fixing efficiency (Wang, Liu and Zhu, 2018), the impact of phage-driven evolution on rhizobial symbiosis remains largely unexplored. These factors include the high specificity of the Nod factor structures produced by the rhizobia, the corresponding host plant receptors (e.g., NFRs) that recognize them, and the complex signal exchange (e.g., NCR peptides) that occurs within the nodule to control bacteroid differentiation and persistence (Oldroyd et al., 2011). Phage resistance mechanisms, such as receptor modifications and altered surface polysaccharides, could therefore disrupt the successful establishment of symbiosis (Oldroyd *et al.*, 2011; Liu and Murray, 2016). Rather than interfering with intracellular flavonoid recognition (which is mediated by the NodD protein), phage resistance is more likely to create trade-offs at the cell surface. For example, modifications to surface receptors like Lipopolysaccharide (LPS) or Exopolysaccharide (EPS), which are known phage attachment sites in rhizobia (Montenegro-Gómez et al., 2022), could directly impair root attachment, infection thread formation, or the ability to evade the plant's immune response, all of which are essential for initiating symbiosis (Poole, Ramachandran and Terpolilli, 2018).

However, resistance to phages often comes with substantial trade-offs that can influence bacterial fitness and ecological functionality. One of the most common bacterial defences to phages is adsorption inhibition, where bacteria modify or mask the surface receptors that

phages use to attach and initiate infection. In Escherichia coli, mutations in LamB receptors confer resistance to lambda phages by preventing attachment; however, these modifications come at the cost of reduced maltose uptake, highlighting a trade-off between phage resistance and nutrient acquisition (Lenski, 1984; Bohannan and Lenski, 2000). As mentioned, similar mechanisms are likely at play in rhizobia, where surface receptor modifications that block phage binding could interfere with these essential symbiotic processes (Oldroyd and Downie, 2008; Poole, Ramachandran and Terpolilli, 2018). These disruptions could significantly reduce nodulation efficiency and nitrogen fixation capacity, underscoring the potential impact of phage-driven evolution on mutualistic functionality.

Other resistance strategies, such as biofilm formation, also come with costs. While biofilms provide protection against phage penetration, they can reduce bacterial motility and metabolic efficiency, limiting resource acquisition and competitive fitness (Gómez and Buckling, 2011). In rhizobia, these trade-offs are particularly relevant, reduced motility and altered EPS composition in biofilm-forming cells can hinder chemotaxis toward root exudates, slow infection-thread initiation, and lower the rate of nodulation (Poole, Ramachandran and Terpolilli, 2018). Although biofilms enhance survival under phage pressure, they can therefore impair symbiotic performance by preventing efficient root colonization and timely nodule formation. Likewise, flagellar suppression, another strategy to avoid phage adsorption, further diminishes rhizobial chemotaxis and root attachment, compounding the loss of symbiotic efficiency.(Poole, Ramachandran and Terpolilli, 2018). While phages can facilitate horizontal gene transfer (HGT) through transduction or lysogenic conversion, the relevance of these processes to rhizobia-phage interactions remains uncertain. In general, HGT contributes to bacterial adaptation by spreading beneficial traits; for example, phages can transfer genes for antibiotic resistance, metabolic enzymes that unlock new nutrient sources, or stress tolerance factors (Touchon et al., 2017).However, HGTcan also introduce maladaptive genetic elements or disrupt essential symbiotic genes (Touchon et al., 2017). Ultimately, these trade-offs mean that phage-driven selection can shape rhizobial populations beyond simply determining which

strains persist. In structured soil ecosystems, where phage pressure varies spatially and temporally, resistant strains may dominate in phage-rich environments, while susceptible strains with higher symbiotic efficiency thrive in legume-rich zones. Understanding how these pressures influence rhizobial evolution is essential for predicting their long-term ecological roles and their effectiveness as agricultural inoculants., affecting their ability to engage in and sustain mutualistic relationships with legumes.

1.4. Refuges in Ecological and Disease Systems/ Root nodules as refuges

If we build upon the insights into bacteria-phage co-evolution and the trade-offs associated with resistance mechanisms, it becomes evident that selective pressures imposed by phages could pose significant challenges for rhizobial populations (Naureen *et al.*, 2020; Puxty and Millard, 2023). Phages, as unique microbial predators, regulate bacterial populations in ways that go beyond abundance control. Their free-living nature allows them to target bacteria across diverse environments, driving bacterial evolution and maintaining genetic diversity (Abedon, 2008). For rhizobia, these pressures could be particularly impactful during their free-living phase in soil, where they must invest in resistance mechanisms that often come with significant trade-offs, such as reduced symbiotic efficiency.

Root nodules could serve as unique ecological refuges for rhizobia, offering a temporary escape from the intense selective pressures imposed by phages. Within the nodule environment, rhizobia are isolated from predation, allowing them to focus on nitrogen fixation without the burden of maintaining costly resistance mechanisms. This protection could preserve genetic diversity within rhizobial populations, ensuring the persistence of strains that might otherwise be lost to phage predation in the soil (Williams, 2013).However, this refuge is temporary and once nodules senesce, rhizobia are released back into the soil, where they are re-exposed to phage pressures, potentially reigniting the evolutionary arms race (Provorov and Vorobyov, 2000)**,** This release is a fundamental part of the rhizobial life cycle, allowing the bacteria that have multiplied within the nodule to repopulate the soil rhizosphere**.** (a schematic of this idea can be seen in **Figure 3**).

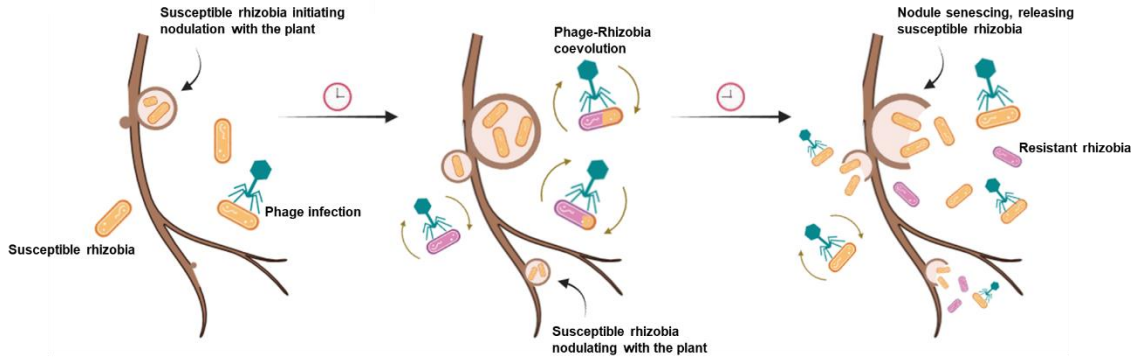

***Figure 3**: This schematic illustrates the role of legume root nodules in providing a temporary refuge for rhizobia from phage predation. In soil, free-living rhizobia are exposed to phages, leading to selective pressures that drive bacterial resistance evolution. However, once rhizobia successfully infect legume roots and form nodules, they are shielded from phage attack. Within nodules, rhizobia focus on nitrogen fixation without the cost of maintaining phage resistance. When nodules senesce, rhizobia are released back into the soil, where they once again face phage predation, potentially reigniting the co-evolutionary arms race. This cycle may contribute to the persistence of both susceptible and resistant strains in rhizobial populations.*

The concept of ecological refuges influencing predator-prey or host-antagonist dynamics has been widely observed across microbial and ecological systems. In microbial communities, biofilms act as protective structures, shielding bacteria from phage predation while promoting bacterial persistence and coexistence with phages (Simmons *et al.*, 2018; Attrill *et al.*, 2021). Within biofilms, embedded bacterial cells avoid direct attack, which reduces the intensity of selection for resistance mechanisms while still allowing phages to persist in the environment (Hall-Stoodley, Costerton and Stoodley, 2004; Gómez and Buckling, 2011). This moderation of selection pressure slows down the rate of bacterial evolution toward resistance, maintaining genetic diversity within microbial populations (Bohannan and Lenski, 2000). Similar refuge dynamics occur in marine ecosystems, where plankton exhibit diel vertical migration, moving into deeper waters during periods of high predation. This strategy temporarily disrupts predator-prey interactions, reducing the selective pressure on prey populations to develop costly defensive adaptations (Abrams, 2009). Likewise, in pathogen-host systems, some pathogens enter dormant or latent states within host cells to evade immune detection and persist within the population. Mycobacterium tuberculosis, for example, can survive inside

macrophages in a non-replicative state, allowing susceptible bacterial subpopulations to escape antibiotic treatment and immune clearance (Gengenbacher and Kaufmann, 2012). These studies demonstrate how temporary refuges can maintain susceptible populations within evolving systems, influencing co-evolutionary dynamics and preventing the rapid fixation of resistant phenotypes. If root nodules function as refuges in the rhizobia-phage system, they could have similar effects on microbial co-evolution. By halting direct antagonistic interactions between phages and rhizobia, nodules may slow the pace of co-evolution, allowing phage-susceptible rhizobia to persist without the immediate pressure to evolve resistance. This evolutionary stasis could help maintain symbiotic efficiency by preserving traits essential for nitrogen fixation, similar to how spatial or temporal refuges in other systems sustain functional diversity despite ongoing selection pressures (Holt and Hochberg, 1997). However, the release of rhizobia from nodules back into the soil reintroduces them to phage predation, potentially driving cycles of resistance and counter-adaptation, as observed in other bacteria-phage interactions (Gómez and Buckling, 2011; Hall *et al.*, 2011). These recurrent evolutionary shifts can be shaped by the costs of resistance (Best *et al.*, 2017) and environmental factors such as coinfections, which influence competitive interactions and selection pressures(Seppälä, Lively and Jokela, 2020). The repeated exposure of rhizobia to phages may contribute to population turnover and genetic diversity, ultimately impacting their symbiotic efficiency and nitrogen fixation. Phages, in turn, play a critical role in regulating rhizobial abundance, distribution, and genetic diversity, which in turn may affect the efficiency of the rhizobia-legume mutualism, influencing nitrogen fixation and agricultural productivity. Whether root nodules actively mediate these processes remains an open question, but if they do function as refuges, they could stabilize rhizobial populations by reducing selective pressures for phage resistance while preserving symbiotically beneficial traits. Understanding the role of nodules in modulating rhizobia-phage co-evolution will provide valuable insights into microbial ecology and symbiotic stability. If nodules indeed provide an escape from phage-driven evolutionary pressure, they may play a crucial role in sustainable agriculture by

ensuring the resilience of nitrogen-fixing rhizobia populations, ultimately supporting ecosystem productivity and long-term agricultural sustainability.

1.5. Research aims and overview

This research aims to advance our understanding of co-evolutionary dynamics between hosts and their antagonists by using the Rhizobia-Legume symbiosis as a system and investigating rhizobia-phage interactions. By addressing how external pressures influence symbiotic mutualisms, it provides insights into microbial ecology and the evolutionary consequences of refuge dynamics. To do this, this research integrates both experimental (wet lab) approaches and mathematical modelling. This combination allows us to bridge the gap between short-term evolutionary dynamics observed at the bacterial strain level and longer-term ecological and population-level consequences of these interactions. Experimental components of this study involve laboratory-based evolutionary experiments in which rhizobia and their associated phages are coevolved over multiple generations. These experiments enable us to directly observe the effects of coevolution on bacterial traits relevant to symbiosis, such as nodulation efficiency and nitrogen fixation capacity. By tracking changes in bacterial phenotypes and genotypes under phage pressure, we can assess trade-offs between resistance and symbiotic function. In parallel, mathematical modelling is used to investigate the broader ecological implications of phage-driven selection in rhizobia populations. Ecological models enable the simulation of long-term interactions between phage-resistant and susceptible rhizobia in the presence and absence of refuges (i.e., root nodules). By combining experimental approaches and mathematical modelling, this study takes an interdisciplinary approach to studying rhizobia-phage co-evolution. The experimental data provide direct evidence for how phage predation influences bacterial evolution at the genetic and phenotypic levels, while the models allow us to extend these insights to understand their long-term consequences on microbial populations and mutualistic interactions.

Figure 4, is a schematic overview of the themes that are investigated in this thesis, where the numbers correspond to the following sections:

1. Chapter 2 details main methodologies and how phage was isolated and selected for use in all experimental research.

2. Chapter 3 investigates the effects of co-evolution between rhizobia and phage, on their symbiont quality and genetic changes that may be affecting their symbiotic functions.

3. Chapter 4 focuses on how the presence of a refuge can influence population dynamics in ecological systems. Specifically, where susceptible hosts can escape predation from a free-living parasite.

4. Chapter 5 investigates the impact nodulation has on phage-rhizobia co-evolution, whether rhizobia can escape co-evolution and what impact this has on their resistance to phage.

5. Chapter 6 investigates competing susceptible and resistant strains and who can win in refuge and in the soil.

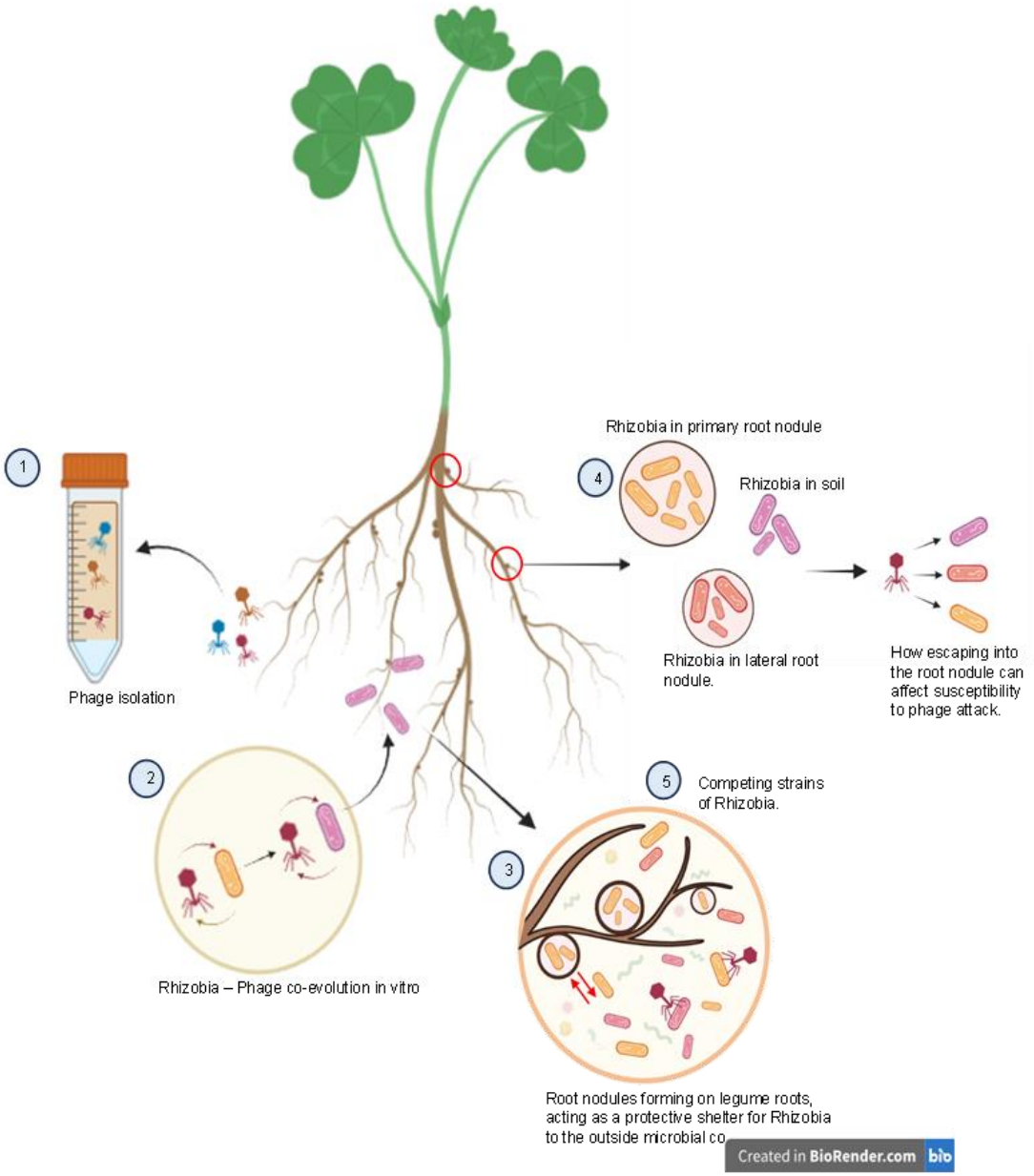

***Figure 4**: Schematic overview of the themes explored in this thesis. Created with Biorender.*

1.6. References

Abedon, S.T. (ed.) (2008) Bacteriophage ecology: population growth, evolution, and impact of bacterial viruses. Cambridge ; New York: Cambridge University Press (Advances in molecular and cellular microbiology, 15).

Abrams, P.A. (2009) 'Adaptive changes in prey vulnerability shape the response of predator populations to mortality', Journal of Theoretical Biology, 261(2), pp. 294–304. Available at: https://doi.org/10.1016/j.jtbi.2009.07.026.

Alexandre, A. and Oliveira, S. (2013) 'Response to temperature stress in rhizobia', Critical Reviews in Microbiology, 39(3), pp. 219–228. Available at: https://doi.org/10.3109/1040841X.2012.702097.

Attrill, E.L. et al. (2021) 'Individual bacteria in structured environments rely on phenotypic resistance to phage', PLOS Biology, 19(10), p. e3001406. Available at: https://doi.org/10.1371/journal.pbio.3001406.

Bartnik, P. et al. (2022) 'Resistance of Dickeya solani strain IPO 2222 to lytic bacteriophage ΦD5 results in fitness tradeoffs for the bacterium during infection', Scientific Reports, 12(1), p. 10725. Available at: https://doi.org/10.1038/s41598-022-14956-7.

Best, A. et al. (2017) 'Host–parasite fluctuating selection in the absence of specificity', Proceedings of the Royal Society B: Biological Sciences, 284(1866), p. 20171615. Available at: https://doi.org/10.1098/rspb.2017.1615.

Bobay, L.-M., Touchon, M. and Rocha, E.P.C. (2014) 'Pervasive domestication of defective prophages by bacteria', Proceedings of the National Academy of Sciences, 111(33), pp. 12127–12132. Available at: https://doi.org/10.1073/pnas.1405336111.

Bohannan, B. j. m. and Lenski, R. e. (2000) 'Linking genetic change to community evolution: insights from studies of bacteria and bacteriophage', Ecology Letters, 3(4), pp. 362–377. Available at: https://doi.org/10.1046/j.1461-0248.2000.00161.x.

Cangioli, L. et al. (2022) 'Differential Response of Wheat Rhizosphere Bacterial Community to Plant Variety and Fertilization', International Journal of Molecular Sciences, 23(7), p. 3616. Available at: https://doi.org/10.3390/ijms23073616.

Clokie, M.R. et al. (2011) 'Phages in nature', Bacteriophage, 1(1), pp. 31–45. Available at: https://doi.org/10.4161/bact.1.1.14942.

Denison, R.F. (2000) 'Legume Sanctions and the Evolution of Symbiotic Cooperation by Rhizobia', The American Naturalist, 156(6), pp. 567–576. Available at: https://doi.org/10.1086/316994.

D'Haeze, W. and Holsters, M. (2002) 'Nod factor structures, responses, and perception during initiation of nodule development', Glycobiology, 12(6), pp. 79R-105R. Available at: https://doi.org/10.1093/glycob/12.6.79r.

Ferguson, B.J. and Mathesius, U. (2014) 'Phytohormone Regulation of Legume-Rhizobia Interactions', Journal of Chemical Ecology, 40(7), pp. 770–790. Available at: https://doi.org/10.1007/s10886-014-0472-7.

Fierer, N., Bradford, M.A. and Jackson, R.B. (2007) 'Toward an ecological classification of soil bacteria', Ecology, 88(6), pp. 1354–1364. Available at: https://doi.org/10.1890/05-1839.

Gandon, S. et al. (2008) ‘Host–parasite coevolution and patterns of adaptation across time and space’, Journal of Evolutionary Biology, 21(6), pp. 1861–1866. Available at: https://doi.org/10.1111/j.1420-9101.2008.01598.x.

Gengenbacher, M. and Kaufmann, S.H.E. (2012) ‘Mycobacterium tuberculosis: success through dormancy’, FEMS microbiology reviews, 36(3), pp. 514–532. Available at: https://doi.org/10.1111/j.1574-6976.2012.00331.x.

Gómez, P. and Buckling, A. (2011) ‘Bacteria-Phage Antagonistic Coevolution in Soil’, Science, 332(6025), pp. 106–109. Available at: https://doi.org/10.1126/science.1198767.

Grundy, E.B. et al. (2023) ‘Legumes Regulate Symbiosis with Rhizobia via Their Innate Immune System’, International Journal of Molecular Sciences, 24(3), p. 2800. Available at: https://doi.org/10.3390/ijms24032800.

Hall, A.R. et al. (2011) ‘Host–parasite coevolutionary arms races give way to fluctuating selection’, Ecology Letters, 14(7), pp. 635–642. Available at: https://doi.org/10.1111/j.1461-0248.2011.01624.x.

Hall-Stoodley, L., Costerton, J.W. and Stoodley, P. (2004) ‘Bacterial biofilms: from the natural environment to infectious diseases’, Nature Reviews. Microbiology, 2(2), pp. 95–108. Available at: https://doi.org/10.1038/nrmicro821.

Hatfull, G.F. (2015) ‘Dark Matter of the Biosphere: the Amazing World of Bacteriophage Diversity’, Journal of Virology, 89(16), pp. 8107–8110. Available at: https://doi.org/10.1128/JVI.01340-15.

Heath, K.D. and Tiffin, P. (2007) ‘Context dependence in the coevolution of plant and rhizobial mutualists’, Proceedings. Biological Sciences, 274(1620), pp. 1905–1912. Available at: https://doi.org/10.1098/rspb.2007.0495.

Herridge, D.F. (2008) ‘Inoculation Technology For Legumes’, in M.J. Dilworth et al. (eds) Nitrogen-fixing Leguminous Symbioses. Dordrecht: Springer Netherlands (Nitrogen Fixation: Origins, Applications, and Research Progress), pp. 77–115. Available at: https://doi.org/10.1007/978-1-4020-3548-7_4.

Hirsch, P. (2002) ‘Sprent, J.I. Nodulation in legumes’, Annals of Botany, 89(6), pp. 797–798. Available at: https://doi.org/10.1093/aob/mcf128.

Holt, R.D. and Hochberg, M.E. (1997) ‘When Is Biological Control Evolutionarily Stable (or Is It)?’, Ecology, 78(6), pp. 1673–1683. Available at: https://doi.org/10.1890/0012-9658(1997)078[1673:WIBCES]2.0.CO;2.

van Houte, S., Buckling, A. and Westra, E.R. (2016) ‘Evolutionary Ecology of Prokaryotic Immune Mechanisms’, Microbiology and Molecular Biology Reviews, 80(3), pp. 745–763. Available at: https://doi.org/10.1128/mmbr.00011-16.

Howard-Varona, C. et al. (2018) ‘Multiple mechanisms drive phage infection efficiency in nearly identical hosts’, The ISME Journal, 12(6), pp. 1605–1618. Available at: https://doi.org/10.1038/s41396-018-0099-8.

Jansson, J.K. and Hofmockel, K.S. (2018) ‘The soil microbiome-from metagenomics to metaphenomics’, Current Opinion in Microbiology, 43, pp. 162–168. Available at: https://doi.org/10.1016/j.mib.2018.01.013.

Kolan, D. et al. (2024) ‘Tradeoffs between phage resistance and nitrogen fixation drive the evolution of genes essential for cyanobacterial heterocyst functionality’, The ISME Journal, 18(1), p. wrad008. Available at: https://doi.org/10.1093/ismejo/wrad008.

Koskella, B. and Brockhurst, M.A. (2014) ‘Bacteria–phage coevolution as a driver of ecological and evolutionary processes in microbial communities’, FEMS Microbiology Reviews, 38(5), pp. 916–931. Available at: https://doi.org/10.1111/1574-6976.12072.

Kuzyakov, Y. and Blagodatskaya, E. (2015) ‘Microbial hotspots and hot moments in soil: Concept & review’, Soil Biology and Biochemistry, 83, pp. 184–199. Available at: https://doi.org/10.1016/j.soilbio.2015.01.025.

Lenski, R.E. (1984) ‘Coevolution of bacteria and phage: Are there endless cycles of bacterial defenses and phage counterdefenses?’, Journal of Theoretical Biology, 108(3), pp. 319–325. Available at: https://doi.org/10.1016/S0022-5193(84)80035-1.

Liu, C.-W. and Murray, J.D. (2016) ‘The Role of Flavonoids in Nodulation Host-Range Specificity: An Update’, Plants, 5(3), p. 33. Available at: https://doi.org/10.3390/plants5030033.

Martinez, J.L. et al. (2009) ‘A global view of antibiotic resistance’, FEMS Microbiology Reviews, 33(1), pp. 44–65. Available at: https://doi.org/10.1111/j.1574-6976.2008.00142.x.

Meaden, S. and Koskella, B. (2017) ‘Adaptation of the pathogen, Pseudomonas syringae, during experimental evolution on a native vs. alternative host plant’, Molecular Ecology, 26(7), pp. 1790–1801. Available at: https://doi.org/10.1111/mec.14060.

Naureen, Z. et al. (2020) ‘Bacteriophages presence in nature and their role in the natural selection of bacterial populations’, Acta Bio-Medica: Atenei Parmensis, 91(13-S), p. e2020024. Available at: https://doi.org/10.23750/abm.v91i13-S.10819.

Oldroyd, G.E.D. et al. (2011) ‘The rules of engagement in the legume-rhizobial symbiosis’, Annual Review of Genetics, 45, pp. 119–144. Available at: https://doi.org/10.1146/annurev-genet-110410-132549.

Oldroyd, G.E.D. (2013) ‘Speak, friend, and enter: signalling systems that promote beneficial symbiotic associations in plants’, Nature Reviews. Microbiology, 11(4), pp. 252–263. Available at: https://doi.org/10.1038/nrmicro2990.

Oldroyd, G.E.D. and Downie, J.A. (2008) ‘Coordinating nodule morphogenesis with rhizobial infection in legumes’, Annual Review of Plant Biology, 59, pp. 519–546. Available at: https://doi.org/10.1146/annurev.arplant.59.032607.092839.

Olszak, T. et al. (2017) ‘Phage Life Cycles Behind Bacterial Biodiversity’, Current Medicinal Chemistry, 24(36), pp. 3987–4001. Available at: https://doi.org/10.2174/0929867324666170413100136.

Poole, P., Ramachandran, V. and Terpolilli, J. (2018) ‘Rhizobia: from saprophytes to endosymbionts’, Nature Reviews Microbiology, 16(5), pp. 291–303. Available at: https://doi.org/10.1038/nrmicro.2017.171.

Pratama, A.A. and Van Elsas, J.D. (2019) ‘The Viruses in Soil - Potential Roles, Activities, and Impacts’, in J.D. van Elsas et al. (eds) Modern Soil Microbiology. Boca Raton: CRC Press (Books in Soils, Plants, and the Environment). Available at: https://doi.org/10.1201/9780429059186-6.

Provorov, N.A. and Vorobyov, N.I. (2000) 'Population genetics of rhizobia: construction and analysis of an "Infection and Release" model', Journal of Theoretical Biology, 205(1), pp. 105–119. Available at: https://doi.org/10.1006/jtbi.2000.2051.

Puxty, R.J. and Millard, A.D. (2023) 'Functional ecology of bacteriophages in the environment', Current Opinion in Microbiology, 71, p. 102245. Available at: https://doi.org/10.1016/j.mib.2022.102245.

Seppälä, O., Lively, C.M. and Jokela, J. (2020) 'Coinfecting parasites can modify fluctuating selection dynamics in host–parasite coevolution', Ecology and Evolution, 10(18), pp. 9600–9612. Available at: https://doi.org/10.1002/ece3.6373.

Simmons, M. et al. (2018) 'Phage mobility is a core determinant of phage–bacteria coexistence in biofilms', The ISME Journal, 12(2), pp. 531–543. Available at: https://doi.org/10.1038/ismej.2017.190.

Slattery, J.F., Coventry, D.R. and Slattery, W.J. (2001) 'Rhizobial ecology as affected by the soil environment', Australian Journal of Experimental Agriculture, 41(3), pp. 289–298. Available at: https://doi.org/10.1071/ea99159.

Sprent, J.I. (2007) 'Evolving ideas of legume evolution and diversity: a taxonomic perspective on the occurrence of nodulation', The New Phytologist, 174(1), pp. 11–25. Available at: https://doi.org/10.1111/j.1469-8137.2007.02015.x.

Sprent, J.I., Ardley, J. and James, E.K. (2017) 'Biogeography of nodulated legumes and their nitrogen-fixing symbionts', New Phytologist, 215(1), pp. 40–56. Available at: https://doi.org/10.1111/nph.14474.

Touchon, M., Bernheim, A. and Rocha, E.P.C. (2016) 'Genetic and life-history traits associated with the distribution of prophages in bacteria', The ISME Journal, 10(11), pp. 2744–2754. Available at: https://doi.org/10.1038/ismej.2016.47.

Touchon, M., Moura de Sousa, J.A. and Rocha, E.P. (2017) 'Embracing the enemy: the diversification of microbial gene repertoires by phage-mediated horizontal gene transfer', Current Opinion in Microbiology, 38, pp. 66–73. Available at: https://doi.org/10.1016/j.mib.2017.04.010.

Udvardi, M. and Poole, P.S. (2013) 'Transport and metabolism in legume-rhizobia symbioses', Annual Review of Plant Biology, 64, pp. 781–805. Available at: https://doi.org/10.1146/annurev-arplant-050312-120235.

Van Houte, S., Buckling, A. and Westra, E.R. (2016) 'Evolutionary Ecology of Prokaryotic Immune Mechanisms', *Microbiology and Molecular Biology Reviews*, 80(3), pp. 745–763. Available at: https://doi.org/10.1128/mmbr.00011-16.

Wang, Q., Liu, J. and Zhu, H. (2018) 'Genetic and Molecular Mechanisms Underlying Symbiotic Specificity in Legume-Rhizobium Interactions', Frontiers in Plant Science, 9. Available at: https://doi.org/10.3389/fpls.2018.00313.

Westra, E.R. et al. (2015) 'Parasite Exposure Drives Selective Evolution of Constitutive versus Inducible Defense', Current biology: CB, 25(8), pp. 1043–1049. Available at: https://doi.org/10.1016/j.cub.2015.01.065.

Williams, H.T.P. (2013) 'Phage-induced diversification improves host evolvability', BMC evolutionary biology, 13, p. 17. Available at: https://doi.org/10.1186/1471-2148-13-17.

Yeremko, L. et al. (2025) ‘Role of Environmental Factors in Legume-Rhizobium Symbiosis: A Review’, Biomolecules, 15(1), p. 118. Available at: https://doi.org/10.3390/biom15010118.

Zhang, J. et al. (2023) ‘The Effect of Different Rhizobial Symbionts on the Composition and Diversity of Rhizosphere Microorganisms of Chickpea in Different Soils’, Plants, 12(19), p. 3421. Available at: https://doi.org/10.3390/plants12193421.

Chapter 2: Phinding Phages

2.1 Abstract

This chapter describes the isolation and characterisation of bacteriophages infecting Rhizobium ruizarguesonis bv. trifolii from agricultural soils in the UK. A total of 32 phages were isolated from 48 rhizosphere samples, and their host range and virulence were assessed across 16 Rhizobium leguminosarum strains. Host range analysis identified 29 unique infection profiles, highlighting extensive diversity among environmental phages. Based on host range, efficiency of plating, and genomic distinctness, three phages were selected for subsequent coevolution experiments. Whole-genome sequencing revealed that these phages share less than 70% nucleotide identity, representing separate viral genera. This chapter establishes a diverse and well-characterised phage panel that underpins later experimental chapters investigating phage–bacteria coevolution and its consequences for symbiosis.

2.2 Introduction and aims

Bacteriophages (phages) are major drivers of bacterial diversity, influencing microbial ecology and evolution in both free-living and symbiotic contexts. In legume–Rhizobium systems, phages have the potential to alter bacterial population structure and symbiotic performance, yet their diversity and biology remain poorly understood.

The primary aim of this chapter was to isolate and characterise phages capable of infecting Rhizobium ruizarguesonis bv. trifolii strain TRX19, a model strain associated with white clover (Trifolium repens). These phages were intended for use in subsequent experiments exploring how phage–bacteria interactions shape evolutionary outcomes and plant–microbe symbiosis.

Aim:

- To isolate and characterize diverse phages infecting R. ruizarguesonis bv. trifolii for use in subsequent coevolution experiments.

Objectives:

- Collect and process environmental rhizosphere soil samples from multiple UK sites.
- Isolate bacteriophages infecting strain TRX19.
- Determine host range, efficiency of plating, and effects on bacterial growth. **Figure 1** outlines the full screening and selection pipeline, that was used to narrow down the initial pool of phage to three highly distinct phages for use in subsequent work
- Sequence and compare phage genomes to assess genetic distinctness.

Hypothesis:

Soils associated with different leguminous hosts harbour genetically and phenotypically diverse Rhizobium phages that differ in infectivity and host range.

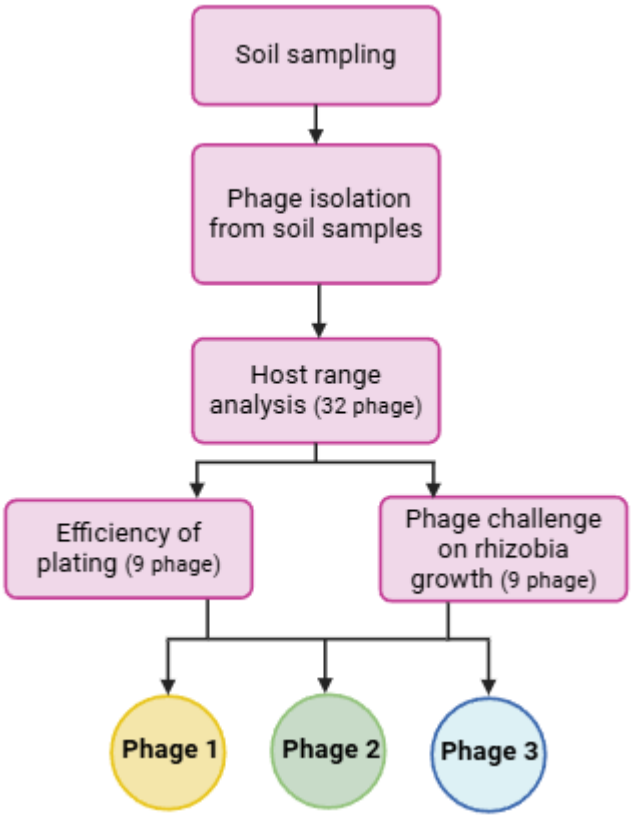

***Figure 1**: Flowchart outlining the phage isolation, screening, and selection process, narrowing the candidates from 32 isolates to 3 phages for subsequent experiments.*

2.3 Methods

2.3.1 Strains used

All experiments, unless stated otherwise, were conducted using *R. ruizarguesonis* bv. *trifolii* strain TRX19, previously isolated from *Trifolium repens* (white clover) in York, UK (Kumar et al., 2015) (Ford *et al.*, 2021; Turner *et al.*, 2021) and genetically labelled with gentamycin resistance and GFP markers (Mendoza-Suárez et al., 2020). TRX19 was chosen because it is a genetically tractable, well-characterised model strain with a sequenced genome and established use in legume symbiosis studies (Ford et al, 2021). Cultures were established in TY media (3 g/L yeast extract, 6 g/L tryptone, 0.5 g/L $CaCl_2$) in 6 ml volumes at 28°C with shaking (180 rpm); and maintained on TY agar (6 g L^{-1} tryptone, 3 g L^{-1} yeast extract, 0.5 g L^{-1} $CaCl_2 \cdot 2H_2O$, 15 g L^{-1} agar). Overnight cultures typically reached OD_{600} ~1.2 (~10^8 CFU mL^{-1}).

2.3.2 Sampling locations and rhizosphere collection

Environmental soil samples were collected in May 2022 from 8 different locations around the UK (**Figure 2**). Six replicates per site (total = 48 samples) were taken from each site, and stored at 4°C no later than 48hrs after collection. Sampling sites were selected based on the presence of leguminous plants. Where few legumes were present, all available plants within the area were used as replicates; in larger fields (e.g., *Vicia faba*), samples were taken at the edge, edge–middle, and centre.

Approximately 5 g of rhizosphere soil (soil tightly adhering to roots within ~ 5 cm) was collected; bulk soil (further than 5cm from roots) was avoided. Samples were kept in sterile 15ml falcon tubes. Host plants included white clover (Trifolium repens L.), red clover (T. pratense L.), vetch (Vicia sativa), and broad bean (Vicia faba L.).

2.3.3 Phage extraction from soil and enrichment on TRX19

To extract phages, 2g of soil were mixed with 2 ml of sterile SM buffer (50 mM Tris-HCl, 100 mM NaCl, 8 mM $MgSO_4$, 0.01% gelatin, pH 7.5) and 2 g of sterile 2mm glass beads. SM buffer was used for was used for phage resuspension and storage, as it provides osmotic stability and maintains phage particle integrity during handling and long-term preservation. The mixture was shaken at 180 rpm for 5 min and left to stand for 30 min. 2 ml of supernatant were collected, centrifuged at 10,000 × g for 5 min, and 200 µl filtered through 0.22 µm membranes using a 96-well plate centrifuged at 2000 × g for 5 min.

48 filtrates were obtained, each representing one soil replicate.

To amplify any phages infecting TRX19, 100 µl of the filtered lysate was added to 6 ml overnight culture of TRX19 culture (OD_{600} ≈ 1.2, ~10^8 CFU/ml) and incubated for 12 hours at 28°C with shaking (180 rpm). This was then filtered through a 0.22 µm filter using a 5 ml syringe, and the filtrate was stored at 4°C for up to 48 hours.

Figure 2: *Map of each sampling site within the UK. Each site details its location, the soil type, samples taken and from which host plant and how many phages were found at that site across replicates.*

2.3.4 Phage isolation from environmental samples

Phage presence were screened on TRX19 using soft agar overlays. 100 µl of an overnight TRX19 culture were mixed with 5 ml of 0.5% molten TY agar (45 °C) and poured onto 1% TY plates. Serial dilutions (10^{-1}–10^{-7}) of each lysate were spotted (5 µl per dilution). Plates were incubated at 28 °C for 24 h and then stored at 4 °C for ≤ 7 days. Occasional appearance of turbid zones after storage suggested potential emergence of phage-resistant colonies.

Individual plaques were picked using sterile 200 µL tips and resuspended in 200 µL SM buffer. When two distinct plaque morphologies were present, both were isolated. Clones were refiltered (0.22 µm) and stored at 4 °C. Care was taken to pick plaques that were spatially separated to minimise re-isolation of the same phage. These procedures were adapted from Jakočiūnė & Moodley (2018).

32 phages were isolated and kept for characterisation.

2.3.5 Phenotypic Characterisation of Isolated Phages

2.3.5.1 Host range analysis

Host range for the 32 isolated phage was assessed across 16 *R. leguminosarum* strains representing several genospecies (**Table 2**). Strains originated from the John Innes Centre culture collection, isolated between 2010–2019 from clover roots in Norfolk and Yorkshire. For each strain, 100 µl of culture were mixed with 5 ml soft TY agar (0.5%) and overlaid on solid TY. A 10^{-1} phage dilution (15 µl + 135 µl TY) was spotted in triplicate. Plates were incubated 24 h at 28 °C; infection was considered positive if plaques appeared in ≥ 2 of 3 replicates.

Table 1: *Strain panel (15-strains used in the host range analysis + our target strain TRX19 (highlighted in red.) genospecies and origin (as provided).*

Strain	Genospecies	Origin
TRX4	D	Clover
TRX9	E	Clover
TRX18	B	Clover
TRX19	C	Clover
TRX34	A	Clover
TRX20	C	Clover
SM41	C	Clover
SM159	E	Clover
SM137b	A	Clover
SM158	C	Clover
SM168A	A	Clover
WS53	Yet to be determined	Clover
WS119	Yet to be determined	Clover
WS84	Yet to be determined	Clover
WS276	Yet to be determined	Clover
WS11	Yet to be determined	Clover

2.3.5.2 Efficiency of plating analysis (EOP)

To quantify infectivity, nine phages showing the most variable host-range profiles were selected for EOP assays on the 16-strain panel. For each test strain, overlays were prepared

by mixing 5 mL soft TY (0.5%) with 120 µL overnight culture and pouring onto TY agar. Phage lysates were serially diluted (10^{-1}–10^{-8}), and 5 µL were spotted in triplicate. After incubation at 28°C for 24 hours, plaques were counted, and the titer (Plaque forming units, PFU/ml) was calculated as **formula 1** (Kutter, 2009).

Formula 1: $$PFU\ ml = \frac{Number\ of\ plaques * dilution\ factor}{Volume\ of\ phage\ plated}$$

EOP for each phage-strain combination was defined as (titre on test strain) ÷ (titre on reference host TRX19) An EOP value of 1 indicates equal efficiency, while lower values indicate reduced infectivity (Kutter, 2009)

2.3.5.3 Phage impact on TRX19 growth(virulence assay)

The same 9 phages were tested for their impact on TRX19 growth over 72 hours. TRX19 cultures were grown overnight in ~6 ml TY media at 28°C and 180 RPM. Cultures were standardized to 0.6 OD_{600}nm (~10^6 Colony Forming Units CFU/ml) and diluted 10^{-1} into a clear 96-well plate (135 µl per well). The plate was loaded into a Tecan Spark plate reader, which recorded OD_{600}nm readings every 30 minutes at 28°C with orbital shaking.

After 4 hours of initial growth, phage samples (diluted to 10^{-6}) were added (15 µl per well) to designated wells, while control wells received 15 µl of TY media. Growth was monitored for an additional 68 hours.

Phage virulence was assessed by calculating the reduction in bacterial growth (RBG) at two time points, 10 hours post-infection to estimate the initial impact of infection, and 40 hours to capture the overall effect including potential recovery, RBG was calculated using **formula 2**:

Formula 2: $$RBG = 1 - \left(\frac{OD600\ phage\ tn - OD600\ phage\ t0}{OD600\ phage\ free\ tn - OD600\ phage\ free\ t0}\right)$$

Where OD_{600} *phage* represents the absorbance cultures grown with phage. OD_{600} *phage-free* refers to the absorbance of cultures grown without phage. t0 is the starting time point (0 hours), and tn represents the time at n hours.

2.3.6 Phage DNA extraction, sequencing and genomics

Nine representative phages were processed for genome sequencing. Phage lysates (1 ml) were treated with DNase I and RNase A to remove contaminating host nucleic acids, followed by Proteinase K digestion to lyse capsids. DNA was extracted using the Qiagen DNeasy Blood & Tissue Kit. Libraries were sequenced using an Illumina MiSeq (2 × 150 bp) at the Centre for Genomic Research, University of Liverpool. Trimmed raw sequencing reads were preliminary assembled using pipelines from **(**Ford *et al.*, 2021 and Turner *et al.*, 2021). Reads were quality-filtered, assembled de novo with SPAdes, assessed with QUAST, mapped with BWA (Li, 2018) and coverage assessed in SAMtools (Danecek *et al.*, 2021). Pilon was used to polish assemblies where required. Average nucleotide identity (ANI) and inter-genomic similarity were estimated with VIRIDIC (Moraru et al., 2020). Taxonomic assignment was supported using the *taxmyPHAGE* web platform (Millard et al., 2024). Genome sequences will be deposited in NCBI (accessions pending).

2.4 Results

2.4.1 Isolation yield and site differences

Of 48 rhizosphere samples, 20 yielded detectable plaques, resulting in 32 distinct phage isolates (Figure 2). Isolation success was highest at the York and Norwich sites (eight isolates each). Plaque morphologies commonly ranged 1–3 mm and varied in clarity, indicating lytic diversity.

2.4.2 Host-range diversity across R. leguminosarum strains

Across the 16-strain panel (Table 2), 29 unique infection profiles were observed among the 32 phages (Figure 3). Three isolates shared identical profiles, suggesting clonal origin or similar microhabitats. Overall infection frequency averaged 41% ± 12 (SD) across strains. TRX19 was susceptible to all isolates (as intended by enrichment). Genospecies A, C, and E strains were most frequently susceptible, whereas several "WS" isolates (e.g., WS11, WS276) were largely resistant. The nine phage with the most variable host-ranges were carried forward.

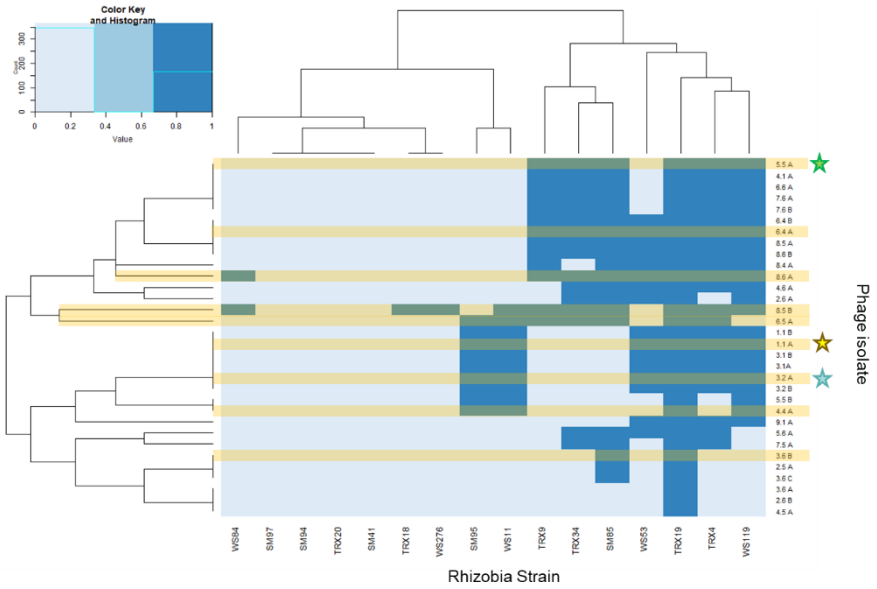

***Figure 3**: Heatmap indicating the strains each isolated phage can infect; dark blue indicates infection. Along the x axis are each of the strains used in the host range analysis (16), whilst the right y-axis lists all isolated phage samples (32) that were tested on each strain. Here phage is labelled as location: replicate. Those highlighted in yellow, were ones taken for further analysis due to variation and diversity in host range. To the left y-axis and top of the plot are dendrograms, showing the relationship/similarities between samples for phage and the rhizobia strains. Stars denote the 3 final phage that were selected*.

2.4.3 Efficiency of plating (EOP) quantifies infectivity differences

Among the nine representative phages, EOP values spanned 10^{-1} to 10^{-6} relative to TRX19 (Figure 4). Phages 1 and 2 showed higher EOPs on multiple susceptible hosts, consistent with efficient adsorption and replication, whereas Phage 3 typically showed lower EOPs ($<10^{-3}$) on non-TRX19 hosts, suggesting reduced infectivity or narrower effective range.

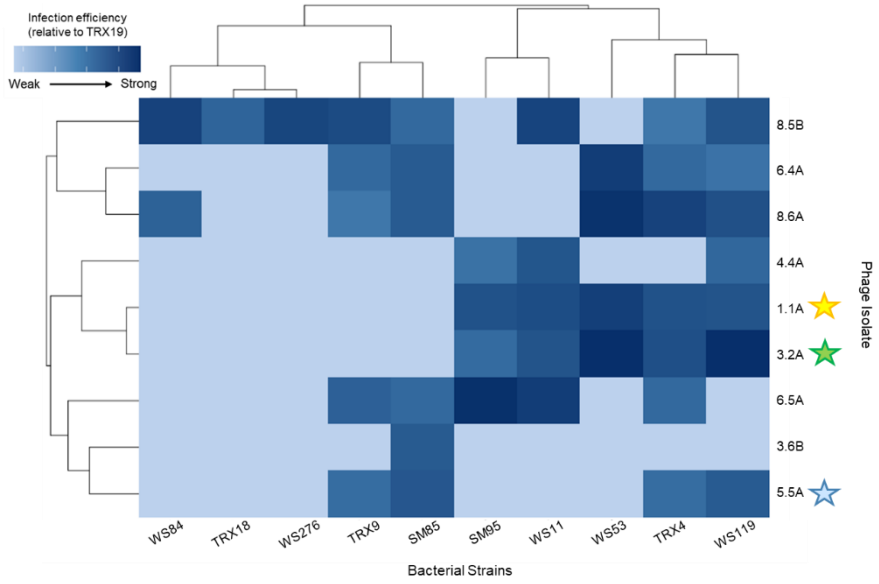

Figure 4: *Heatmap indicating the Efficiency Of Plating (EOP) for each phage on each strain of rhizobia. Along the x axis are each of the strains that the chosen phage collectively can infect (11), whilst the right y-axis lists all isolated phage samples (9) that were tested on each strain. Here phage are labelled as location:replicate. To the left y-axis and top of the plot are dendrograms, showing the relationship/similarities between samples for phage and the rhizobia strains. Stars denote the 3 final phage that were selected.*

2.4.4 Virulence on TRX19: growth-curve phenotypes

The same nine phages were next tested for their effects on TRX19 population growth over 72 hours (**Figure 5**). Distinct infection dynamics were observed.

Phage 3.2A caused the strongest and most sustained suppression of OD_{600}, with little recovery over 72 h, indicating a highly lytic interaction. Phage 1.1A produced a rapid initial decline followed by partial recovery around 40 h, consistent with incomplete lysis or the emergence of resistant subpopulations. Phage 5.5A produced a milder, transient effect, with bacterial growth resuming more rapidly. These were the 3 phages that were then chosen to carry on to experiments.

Across the nine tested phages, RBG at 10 h ranged from 0.45 to 0.83, and RBG at 40 h from 0.20 to 0.70, illustrating pronounced differences in virulence and persistence.

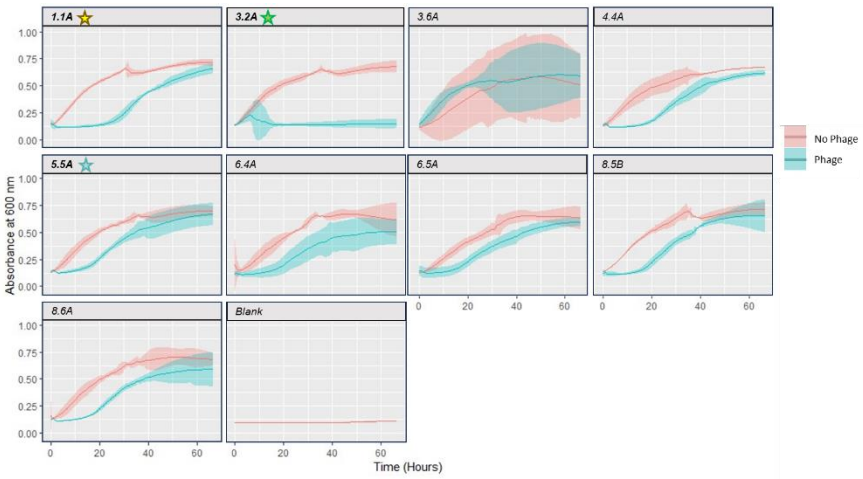

***Figure 5**: Growth curves of Rhizobia TRX19 strain over 72 hours, growing with(blue) and without (red) one of the 9 phage samples, plotted readings are after phage or TY control was added. Absorbance at OD_{600}nm readings were taken every 30 minuites over 72 hours. TRX19 were allowed to grow for 4 hours prior to phage being added. Stars denote the 3 final phage that were selected.*

2.4.5 Selection of three focal phages

Based on the combined results of host-range diversity (**Figure 3**), EOP variability (**Figure 4**), and virulence profiles (Figure 5), three phages, Phage 1 (1.1A) , Phage 2 (3.2A), and Phage 3 (5.5A), were selected for detailed genomic and taxonomic characterisation (see Figure 6 for full comparative results between these 3 phages).

These three were chosen to represent the range of infection behaviours observed:

- Phage 2 was the most virulent, causing sustained host suppression.
- Phage 1 showed moderate virulence and partial recovery, representing an intermediate phenotype.
- Phage 3 produced mild, transient inhibition, corresponding to low virulence.

Together, they span a gradient of infection strength and host-range breadth, providing ideal candidates for studying phage–bacterium coevolution under differing selective pressures.

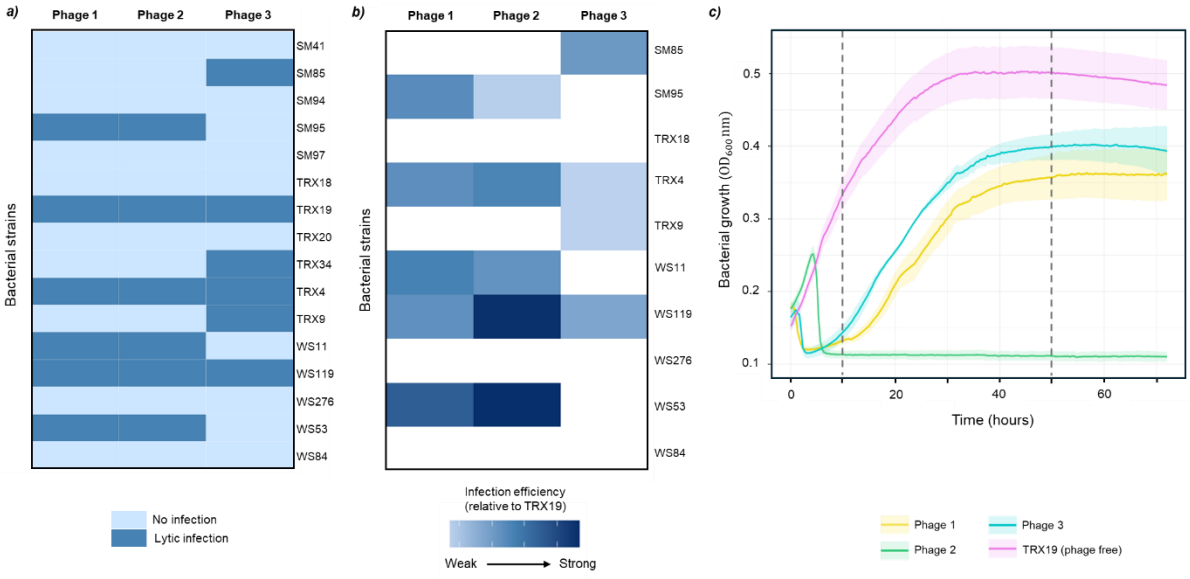

***Figure 6**: a) Host range profiles of Phage 1, 2 and 3 against a panel of 16 R. leguminosarum strains. Infection was scored as positive if plaques formed in ≥2 out of 3 replicates. Infectivity was graded as either no infection or infection;*

b) Efficiency of plating (EOP) of Phage 1,2 and 3 on the same strain panel, relative to the target host strain TRX19 (EOP = 1), only performed on strains that were able to infect those phages.

c) Phage virulence effects on growth of TRX19 in the presence of each phage over a 72-hour period. Phage infection was introduced at 4 hours post-inoculation, and OD_{600}nm was recorded every 30 minutes. Phage virulence was estimated with reduction in bacterial growth (RBG) relative to the phage-free control at 10 hours and 40 hours post infection. The lines show the average across 6 replicates with standard error.

2.4.6 Genomic features and taxonomic assignment

Pairwise intergenomic comparisons using VIRIDIC showed that the three focal phages shared less than 70 % nucleotide similarity, with variable aligned-genome fractions and unequal genome length ratios (**Figure 7a-b**). Phage 1, Phage 2, and Phage 3 assembled to 26.8 kb, 44.1 kb, and 42.9 kb, respectively, with GC contents between 58–60 %.

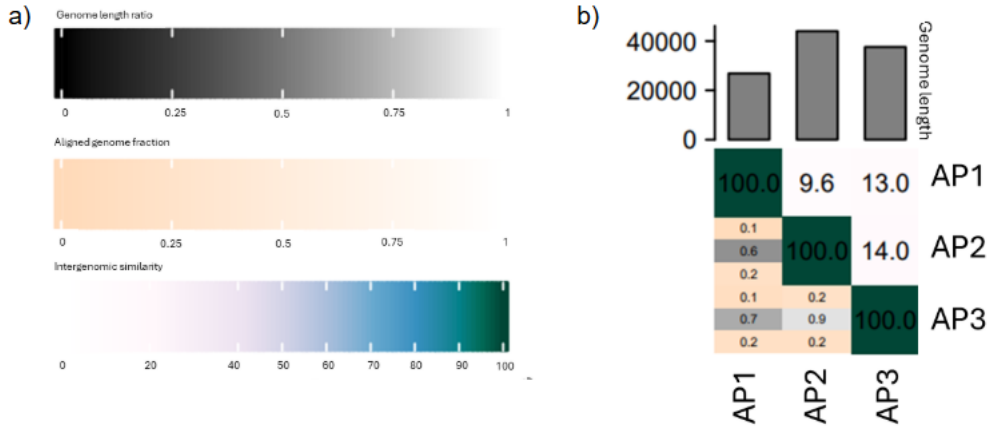

Figure 7: *Intergenomic relatedness of the three focal phages.. (a) VIRIDIC colour scales for genome length ratio, aligned-genome fraction, and intergenomic similarity.*

(b) Pairwise VIRIDIC matrix for Phage 1 (AP1), Phage 2 (AP2), and Phage 3 (AP3) with genome lengths shown above. All pairwise similarities are < 70 %, consistent with species-level separation.

2.5 Discussion

This chapter provides the first systematic isolation and comparative characterisation of Rhizobium ruizarguesonis phages from UK agricultural soils. Recovery of phages from 20 out of 48 rhizosphere samples demonstrates that legume-associated soils are active reservoirs of rhizobial viruses, supporting their potential ecological role in influencing bacterial abundance and diversity in the rhizosphere (Kuzyakov & Blagodatskaya, 2015).

The substantial variation observed in host range, efficiency of plating (EOP), and infection outcomes reveals high phenotypic diversity among natural Rhizobium-infecting phages. The identification of 29 unique infection profiles among 32 isolates indicates extensive local diversity, likely reflecting adaptation to heterogeneous rhizobial populations and plant-associated microhabitats. Such diversity is consistent with findings in other soil and symbiotic systems, where spatial structure and host variation maintain coexistence of multiple phage lineages (Gómez & Buckling, 2011; Koskella & Brockhurst, 2014).

From these isolates, three representative phages (Phages 1, 2, and 3) were chosen to capture the range of infection dynamics observed. Phage 2 exhibited the strongest and most persistent suppression of TRX19, Phage 1 showed an intermediate effect with partial recovery, and Phage 3 produced only transient inhibition. These contrasting patterns highlight differences in phage–host interaction strength, which could result from underlying variation in adsorption rate, replication kinetics, or burst size—parameters not directly measured in this study but valuable targets for future investigation (Abedon, 2012; De Smet et al., 2017).

Comparative genomic analysis confirmed that the three focal phages are genetically and taxonomically distinct, sharing less than 70 % average nucleotide identity (ANI) based on VIRIDIC and taxmyPHAGE analyses (Millard et al., 2024). Classification by taxmyPHAGE further suggested that Phage 1 belongs to the Podoviridae and Phages 2 and 3 to the Siphoviridae, consistent with their differing genome sizes (26.8 kb vs. ~43–44 kb). Although detailed genome annotation was beyond the scope of this study, differences in genome size and predicted morphology suggest variation in infection mechanisms and host specificity, as reported for other Rhizobium and Sinorhizobium phages (Ford et al., 2021; Turner et al., 2021). Further annotation, including searches for integrase, tRNA, or accessory genes, would refine our understanding of their functional potential and evolutionary relationships (Hatfull, 2015).

Collectively, these results establish a diverse and representative phage set for experimental studies of Rhizobium–phage interactions. By spanning a continuum from highly to weakly virulent infection types, the three focal phages provide an ideal comparative framework for exploring how differing phage pressures influence bacterial evolution and symbiotic performance (Koskella, 2019).

In the following chapter, these phages are employed in coevolution experiments to test how long-term phage exposure shapes bacterial resistance, fitness, and plant symbiotic traits, thereby linking viral–bacterial interactions with ecosystem-level outcomes.

2.6 References

Danecek, P. *et al.* (2021) 'Twelve years of SAMtools and BCFtools', *GigaScience*, 10(2), p. giab008. Available at: https://doi.org/10.1093/gigascience/giab008.

Ford, S. *et al.* (2021) 'Introducing a Novel, Broad Host Range Temperate Phage Family Infecting Rhizobium leguminosarum and Beyond', *Frontiers in Microbiology*, 12, p. 3375. Available at: https://doi.org/10.3389/fmicb.2021.765271.

Gómez, P. and Buckling, A. (2011) 'Bacteria-Phage Antagonistic Coevolution in Soil', Science, 332(6025), pp. 106–109. Available at: https://doi.org/10.1126/science.1198767.

Gurevich, A. *et al.* (2013) 'QUAST: quality assessment tool for genome assemblies', *Bioinformatics*, 29(8), pp. 1072–1075. Available at: https://doi.org/10.1093/bioinformatics/btt086.

Hatfull, G.F. (2015) 'Dark Matter of the Biosphere: the Amazing World of Bacteriophage Diversity', Journal of Virology, 89(16), pp. 8107–8110. Available at: https://doi.org/10.1128/JVI.01340-15.

Jakočiūnė, D. and Moodley, A. (2018) 'A Rapid Bacteriophage DNA Extraction Method', *Methods and Protocols*, 1(3), p. 27. Available at: https://doi.org/10.3390/mps1030027.

Koskella, B. and Brockhurst, M.A. (2014) 'Bacteria–phage coevolution as a driver of ecological and evolutionary processes in microbial communities', FEMS Microbiology Reviews, 38(5), pp. 916–931. Available at: https://doi.org/10.1111/1574-6976.12072.,

Kumar N., Lad G., Giuntini E., Kaye M. E., Udomwong P., Shamsani N. J., et al. (2015). Bacterial genospecies that are not ecologically coherent: population genomics of Rhizobium leguminosarum. Open Biol. 5:140133. 10.1098/rsob.140133

Kutter, E. (2009) 'Phage Host Range and Efficiency of Plating', in M.R.J. Clokie and A.M. Kropinski (eds) *Bacteriophages: Methods and Protocols, Volume 1: Isolation, Characterization, and Interactions*. Totowa, NJ: Humana Press, pp. 141–149. Available at: https://doi.org/10.1007/978-1-60327-164-6_14.

Kuzyakov, Y. and Blagodatskaya, E. (2015) 'Microbial hotspots and hot moments in soil: Concept & review', Soil Biology and Biochemistry, 83, pp. 184–199. Available at: https://doi.org/10.1016/j.soilbio.2015.01.025.

Li, H. (2018) 'Minimap2: pairwise alignment for nucleotide sequences', *Bioinformatics*, 34(18), pp. 3094–3100. Available at: https://doi.org/10.1093/bioinformatics/bty191.

Mendoza-Suárez, M.A. et al. (2020) 'Optimizing Rhizobium-legume symbioses by simultaneous measurement of rhizobial competitiveness and N2 fixation in nodules', Proceedings of the National Academy of Sciences of the United States of America, 117(18), pp. 9822–9831. Available at: https://doi.org/10.1073/pnas.1921225117.

Moraru, C., Varsani, A. and Kropinski, A.M. (2020) 'VIRIDIC—A Novel Tool to Calculate the Intergenomic Similarities of Prokaryote-Infecting Viruses', *Viruses*, 12(11), p. 1268. Available at: https://doi.org/10.3390/v12111268.

Turner, D. *et al.* (2021) 'Phage Annotation Guide: Guidelines for Assembly and High-Quality Annotation', *Phage*, 2(4), pp. 170–182. Available at: https://doi.org/10.1089/phage.2021.0013.

Chapter 3: Rhizobia-Phage co-evolution outside the host can drive loss of symbiotic function

3.1 Abstract

When not engaged in symbiosis with legumes, rhizobia live freely in the soil, where they will be exposed to predation from phages. Predation by phages can drive rapid selection for resistance, which could lead to trade-offs in rhizobial traits that are not under selection, including those useful during symbiosis. To test this, we experimentally evolved a free-living strain of *Rhizobium leguminosarum* bv. *trifolii* (Rlt) with and without 3 different lytic phages isolated from soil environments. Wecompared evolved, phage resistant clones to ancestral rhizobia in symbiosis with their host plants, T*rifolium repens* (white clover). Coevolution with all 3 phages resulted in significant changes to bacterial phenotypes, including biofilm and motility traits, but these did not correspond to significant changes to the symbiosis for 2/3 phage-evolved rhizobia. In contrast, association with one of the 3 phages led to the complete loss of symbiotic potential, highlighting the potential for complex and context-dependent interactions between phage predation and symbiont fitness.

3.2. Introduction

Bacteria-phage coevolution drives rapid adaptation through strong selection for traits such as increased biofilm formation or altered cell surface receptors (Labrie, Samson and Moineau, 2010; Koskella and Brockhurst, 2014; Hampton, Watson and Fineran, 2020). While beneficial in the presence of phages such changes can create fitness trade-offs in other environments (i.e. antagonistic pleiotropy). For example, changes in lipopolysaccharide (LPS) structures or outer membrane proteins, which can prevent phage adsorption, may reduce nutrient uptake or impair bacterial interaction with hosts (Lenski, 1984; Meyer *et al.*, 2012). While increased biofilm production can physically block phage access to cells, it may also reduce motility and colonization ability(Lenski, 1984; Gómez and Buckling, 2011). As a result, these trade-offs significantly influence microbial community dynamics and bacterial fitness in natural environments. The impact of trade-offs is likely to be especially strong for bacteria switching between very different lifestyles, such as facultative symbionts which move between free-living environments and intimate symbiotic interactions. Examples of such facultative symbionts are widespread and include the bioluminescent *Vibrio fischeri*, which colonizes the light organs of squid, and numerous plant-associated bacteria like *Pseudomonas fluorescens* that can promote plant growth (Nishiguchi, 2002; Haas and Défago, 2005).

Rhizobia are nitrogen-fixing bacteria that can exist freely in the soil or as symbionts within legume root nodules (Sprent, 2007; Poole, Ramachandran and Terpolilli, 2018). This symbiosis is critical for soil fertility and agricultural productivity, as rhizobia fix atmospheric nitrogen into ammonia in exchange for carbon from the plant (Oldroyd and Downie, 2008; Poole, Ramachandran and Terpolilli, 2018). By supplying plants with bioavailable nitrogen, rhizobia play a key role in reducing reliance on synthetic fertilizers and enhancing ecosystem sustainability (van Brussel *et al.*, 2002).

The effectiveness of this symbiosis depends on rhizobia's ability to colonize plant roots, initiate nodule formation, and efficiently fix nitrogen, a process that requires substantial energy investment from the bacterial partner. These processes are governed by a complex signalling

network that facilitates bacterial attraction to the host and mediates the exchange of molecular cues necessary for infection and nodule development (Oldroyd and Downie, 2008; Roy *et al.*, 2020).

However, the symbiosis is facultative, and bacteria spend a considerable portion of their life in the soil where they face environmental pressures, including competition for nutrients and predation by phages. Given the intricacy of the rhizobia-legume interaction it is likely that phage-bacteria coevolution could drive changes affecting rhizobia's fitness and symbiotic capabilities. For instance, mutations conferring phage resistance may also alter surface structures critical for nodule formation, potentially reducing nitrogen fixation efficiency or preventing symbiosis altogether (Kiers *et al.*, 2003; Westhoek *et al.*, 2017). In the rhizobia-legume system, such trade-offs might result in reduced nitrogen content and lower plant biomass (Denison, 2000; Oldroyd and Downie, 2008). Given the agricultural and ecological importance of this symbiosis, we used this system to test the hypothesis that coevolution with phages in the soil drives trade-offs with symbiotic competence. Our findings show that exposure to phages in the soil can lead to divergent evolutionary outcomes, in some cases preserving symbiotic function, and in others, completely disrupting it. Different phages imposed distinct impacts on rhizobial performance, highlighting the unpredictable and context-dependent nature of phage pressure on symbiotic traits.

3.3. Methods

3.3.1 Bacterial and phage strains

All experiments were conducted on *Rhizobium ruizarguesonis* bv *trifolii* (Rlt) strain TRX19, a member of the *R. leguminosarum* species complex. This 'species complex' refers to a group of very closely related bacteria that are phenotypically similar but genetically diverse, often classified into biovars (bv.) based on their specific legume host range (Poole, Ramachandran and Terpolilli, 2018). For instance, the biovar *trifolii* (used in this study) infects *Trifolium*, while the biovar *viciae* infects *Vicia* (vetch) and *Pisum* (peas). This strain was

isolated from the root nodules of Trifolium repens (White Clover) growing in York, UK (Kumar et al., 2015). The strain was labelled with gentamycin resistant markers and Green Fluorescent Protein (GFP) (Mendoza-Suárez *et al.*, 2020) to allow for recovery from plant microcosms.

Phage strains used, '*Phage 1', 'Phage 2'* and '*Phage 3'*, were all isolated from environmental soils in the UK (**Chapter 2**). Phages were isolated from the rhizosphere of Trifolium repens (clover) a known host of R. leguminosarum. These phages were deliberately selected to represent a range of infection profiles, including variation in host range, lytic activity, and their ability to disrupt rhizobial growth in vitro (see **Chapter 2** for full detail).

All bacterial culturing was performed in TY media in 6 ml culture volumes under shaken (180 rpm) conditions at 28◦C. Colony forming units (CFUs) were enumerated on solid TY agar (13 g/L) and plaque forming units (PFUs) on soft TY agar overlays after cells were removed through filtration (using 0.45 µM syringe filters). Soft agar overlays consist of 5ml solid TY agar (13 g/L) with 5 ml of 6 g/L agar overlay, containing 100 µl of a growing culture of phage free TRX19.

3.3.2 Evolution

TRX19 evolved with each isolated phage (*Phage 1*,*2* and *3*) as well as on its own. For each phage treatment, six replicate microcosms were established. Additionally, three phage-free control microcosms were set up per phage treatment, resulting in a total of 18 phage–rhizobia coevolving populations and 9 rhizobia-only populations. A transfer experiment was carried out for a total of 20 transfers.

For each population, single TRX19 colonies were grown for 72 hours, in 5 mL of TY media to ensure the culture reached a standardised stationary phase. These cultures were diluted 1:100 into fresh media, and incubated for 4 hours, to allow the bacteria to exit lag phase and enter logarithmic growth. Bacterial Optical Density (OD) was then measured at a wavelength of 600nm, using a Tecan Spark microplate reader, and estimated to be ~ 10^6 CFU/mLPhage

was added at a multiplicity of infection (MOI) of approximately 1, to achieve a 1:1 ratio of phage to bacteria. This marks Transfer 0 (T0).

Rhizobia and phage populations were then transferred at a dilution of 1:100 every 72 hours for a total of 20 transfers; 60ul of each population was transferred to fresh 6ml TY. A 1:100 dilution was performed every transfer to replenish nutrients and ensure a new cycle of growth and selection. Each transfer was sampled for population densities and 500ul stocked in 15% glycerol at -70C. 100ul of population density samples were serially diluted and 30ul plated to quantify CFU and PFU.

3.3.3 Measuring resistance

Evolved strains from each population in each phage treatment, were assessed for resistance to evolved and ancestral phage populations. Evolved populations were plated onto TY agar, 10 clones were randomly selected, and inoculated into 150ul of TY media in a 96 well plate and left to grow for 72 hours to reach stationary phase. Cultures were then diluted 1 in 10 and each clone was subjected to the following conditions:

- Mock infected with TY media.
- End-evolved phage (Pn-): The coevolved T20 phage population
- Ancestral phage: The respective ancestral phage.
- Other ancestral phages: The ancestral phages from other treatments.

As a control, the nine no-phage populations were grouped (three populations per group), and each group was matched to one of the three phage treatments. Meaning, the control clones were also tested against the same panel of ancestral and evolved phages, which allowed to check for any lab resistance that might have evolved in the absence of direct phage selection.

Each of the clones were grown for 72 hours at 28’C/180RPM and at hours 0, 10, 20, 40 and 60, the(OD) at a wavelength of 600nm, was measured. Bacterial susceptibility to infection was measured as Reduction in bacterial growth (RBG) for each strain, using **formula 1**:

Formula 1: $$RBG = 1 - \left(\frac{OD600\ phage\ tn - OD600\ phage\ t0}{OD600\ phage\ free\ tn - OD600\ phage\ free\ t0}\right)$$

Where *OD600 phage* represents the absorbance cultures grown with phage. *OD600 phage-free* refers to the absorbance of cultures grown without phage. t0 is the starting time point (0 hours), and tn represents the time at n hours.

The clone with the most evolved resistance to their ancestral phage (lowest RBG value) was chosen from each population within each treatment for subsequent analysis, leaving 6 evolved clones from each *Phage 1, Phage 2* and *Phage 3* treatment, then 9 from the *No Phage* treatment.

3.3.4. Phenotype assays

Phenotypes potentially associated with root colonisation - biofilm production and motility - were measured in vitro in evolved clones.

3.3.4.1 Biofilm formation

A microtiter plate assay was used to quantify biofilm formation (Coffey and Anderson, 2014). Rhizobia were grown to stationary phase, diluted 10-fold into TY media into a 96-well plate, and the density standardised to within 0.05 OD600 of each other. The plate was incubated at 28'C/180RPM for 72 hours to allow biofilm to form then rinsed with sterile dH20 to remove non-adherent bacteria. The wells were left to dry and then stained with 0.1% crystal violet for 10 minutes, then rinsed again to remove excess stain. The stained biofilm was solubilized using 30% acetic acid, and absorbance (OD) was measured at 550nm in a Tecan Spark microplate reader.

3.3.4.2 Motility assays

Motility assays were carried out to investigate the swimming and swarming abilities of the evolved clones. TY plates were made at 0.3% (swimming) and 0.5% agar (swarming). Plates

were left to dry under a laminar flow hood, 10cm at least from the back of the hood and turned 90 degrees every 30 mins for 4 hours to ensure uniform drying. Rhizobia were grown to stationary phase (72 hours) inTY media, diluted 1:10 and 5ul dropped into the middle of a 0.3% or 0.5% TY agar plate. Plates were then incubated at 28'C for 72 hours. At end point 72-hours, plates were photographed in order of plating and the radius and area of growth measured in Image J

*3.3.4.3 Nutrient-dependent susceptibility assay (1% vs 100% TY)*To test whether phage resistance depended on nutrient availability, susceptibility was measured in low (1% TY) and high (100% TY) nutrient media. 1% TY was prepared as a 1:100 dilution of standard TY (6 g/L tryptone, 3 g/L yeast extract, 0.5 g/L $CaCl_2$) in sterile dH_2O..Clones from 3.3.3 and no-phage controls were tested against their contemporary phage. Clones were grown for 72 hours at 28°C and 180 RPM, standardised to OD_{600} = 0.6, diluted 1:10 into either 1% or 100% TY, and 135 µl dispensed into clear 96-well plates. After 4 hours of incubation, 15 µl of ancestral phage was added (MOI ≈ 1), and plates were incubated for 72 hours at 28°C with OD_{600} readings taken every 30 minutes in a Tecan Spark.

Susceptibility (RBG) was calculated at 10 and 40 hours post-infection to compare resistance between nutrient environments and determine whether resistance was maintained under low-nutrient conditions.

3.3.5 Plant assays

3.3.5.1 Experimental design

A pot experiment was designed to test the symbiont quality of evolved rhizobia clones in partnership with clover . The clones selected for this assay were the single most resistant clones chosen from each of the replicate populations, as described in 3.3.3. In total there were 6 clones for each phage treatment group, 9 from the *No Phage* controls, 3 ancestral controls (unevolved TRX19) and 3 uninoculated control plants. Each clone was replicated 3 times.

3.3.5.2 Germination, planting, inoculation and culture conditions

White clover plants (variety = Avoca, DLF seeds Ltd., a standard commercial variety chosen for its common use in agricultural and experimental settings) were grown in 1L ‘tricorn’ pots (three-cornered pots designed for optimal root growth and observation), containing 900 g of twice autoclaved vermiculite and sharp sand mix (2:3 ratio). Seeds were sterilised by immersing and shaking in 3% household (HH) bleach for 30 minutes at room temperature (RT). The seeds were washed 4 times with sterile dH20, spread on sterile filter paper, watered with 5ml of sterile dH20 and left to germinate for 5 days at RT. Single seedlings were randomly selected and placed in the tricorn pots, along with 5ml sterile, nitrogen free,Jensen media (Howieson and Dilworth, no date) and 5ml sterile dH20. Jensen media provides all essential macro- and micronutrients *except* nitrogen, ensuring that any plant growth is dependent on nitrogen fixed by the rhizobial symbiont. Each tricorn pot was sealed inside a sterile sunbag, equipped with a sterile polypropylene tube that extended from the soil to the top, functioning as a watering tube with a screw cap; all pots were placed in a controlled environment chamber (16/8-hour day/night cycle at 22 0C/20 0C, 500 µmol/m2/s1 light).

After one week of growth, pots were inoculated with 800ul of bacterial culture. Bacterial cultures were grown for 72 hours in TY media, standardised 0.6 at OD600nm, centrifuged at 13,000 x g and resuspended in 800ul of rhizobia wash buffer (10mM MgSO4 and 0.01% Tween 40). The bacterial suspension was pipetted directly onto the vermiculite/sand mix at the base of the seedling.

The plants were watered with 20mL of sterile water and Jensen’s media mix every week, with Jensen increasing 1ml extra per week. Plants were grown for a further 7 weeks after inoculation.

3.3.5.3 Harvest

At harvest, root nodules were removed and counted. To estimate CFUs from nodule populations nodules from each plant were pooled, sterilised (3 mins at 70% EtOH, 6 sterile dH20 washes) and crushed in 750ul of rhizobia wash buffer before plating on TY + 3mg/ml

gentamicin. Shoot biomass was separated from roots and both were and dried at 80'C for 48 hours then weighed.

To estimate free living populations 10g of rhizosphere soil was washed with 10ml rhizobia wash buffer (10mM MgSO4 and 0.1% Tween) and 5g of sterile glass bead mix (diameters 2mm and 4mm). Soil was vortexed for 1 minute, left to stand for 30 minutes and vortexed again for 1 minute before plating.

3.3.5.4 Total Nitrogen

Aboveground and belowground biomass from the plants were used to estimate biologically fixed N using 15N Natural abundance (Unkovich and Baldock, 2008; Maluk *et al.*, 2022). Dried root and shoot biomass were milled in Qiagen tissue lyser II using 5mm tungsten beads and analysed for 15N and %N on an isotope ratio mass spectrometer (IRMS) (ANCA GSL 20-20 Mass Spectrometer; Sercon, Cheshire).

Aboveground N biomass accumulation (g) was calculated as follows:

Formula 2: $\left(\frac{\%N}{100}\right) \times (shoot\ biomass)$

3.3.6 DNA extraction

DNA from evolved clones was extracted using the Qiagen DNeasy PowerSoil Pro kit following kit instructions using 250mg of input material (approx. 6ml of saturated culture) and quality checked on a Nanodrop 8000 (Nanodrop $_{TM}$) and Qubit 4 fluorometer (Qubit $_{TM}$). Rhizobia evolved clone samples were used to generate whole genome sequences for each clone. Whole genome sequencing was performed using Illumina MiSeq (2 × 150 bp) at Centre for Genomic Research (University of Liverpool).

3.3.7 *Lysogeny detection by PCR*

Lysogeny was confirmed by PCR amplification of an integrated prophage in *Phage 3*–evolved clones. A primer pair was designed against a highly variable genomic region showing strong

sequence similarity to phage vTRX32-1, enabling specific amplification of the integrated element (Forward: CAGTCCTGCCACCTCAATGT; Reverse: ACGAAGAAATCCGTTGCCCT) (Mary Eliza, 2023, p16-17).

3.3.8 Analysis

Data were analysed in R (v4.1.3) with R studio (R Studio Team 2020) using tidyverse packages (Wickham, et al. 2019).

For phenotypic traits, two-way ANOVAs assessed the impact of phage presence and phage treatment, after checking the model conformed to assumptions. Tukey post-hoc comparison tests were employed to find groups that differed significantly.

Coefficients (t and p-values) within linear models are compared to the Ancestral strain TRX19 unless stated otherwise. Linear mixed effects (lmer, in lm4 (Bates et al., 2015)) models were used for plant biomass to test for effects of phage presence, treatment and plant replicate.

Mutations in evolved rhizobia clone genomes were predicted using Breseq v0.37.0 (Deatherage and Barrick, 2014) aligned to the reference genome. Mutations that appeared in 100% of the samples were assumed to be ancestral and filtered out (**Table S1**).

3.4 Results/Discussion

3.4.1 Experimental evolution

All populations in all phage and no-phage treatments persisted over the 20-transfer experimental period (**Figure 1**), displaying fluctuations in population densities for both phages and rhizobia.. The phage-treated populations showed reciprocal fluctuations characteristic of antagonistic coevolution. The no-phage controls also fluctuated, likely reflecting esource depletion and replenishment with each 72-hour transfer. All populations, including controls, show a notable drop in density around T10, possibly due to a plating error in the lab, as after their respective population dynamics resumed.

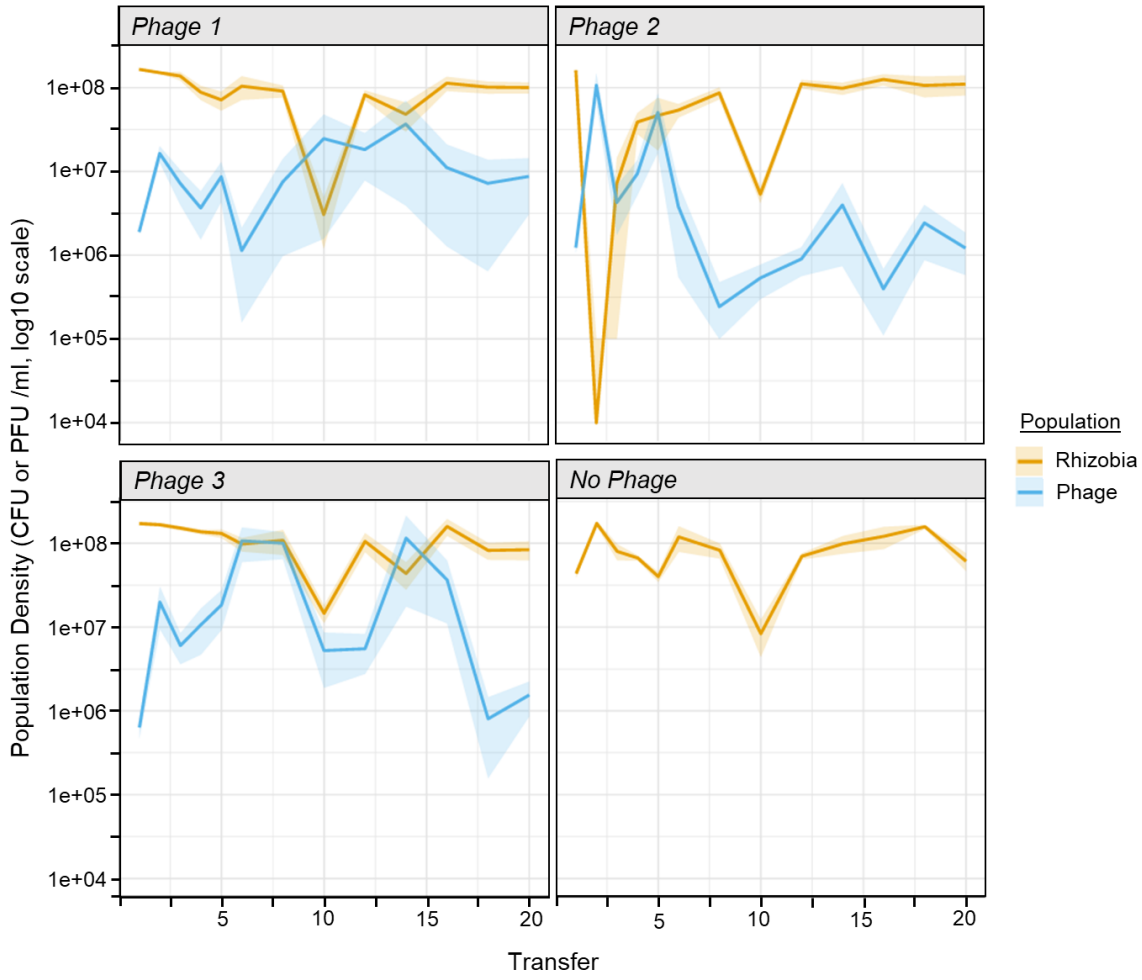

***Figure 1**: Showing Phage and Rhizobia populations, (Plaque forming units PFU and Colony Forming Units CFU) from each 72-hour transfer across all 20 transfers (T0 – T20). Each panel represents the Phage treatments the Rhizobia co-evolved with.*

To measure the extent of phage resistance evolution 10 randomly selected clones from each population in each treatment were exposed to both their coevolved phages and their ancestral phage. All phage-evolved bacteria exhibited resistance to their ancestral phage while bacteria evolved in the absence of phages remained largely (though not entirely) susceptible (**Figure 2**). Among the 90 no-phage control clones tested, all were highly susceptible to infection by the evolved phages, with RBG values remaining above 1.2 across treatments, indicating little or no resistance. When challenged with the ancestral phages, 89 of these clones remained strongly susceptible (RBG > 1.1), while 11 clones showed intermediate susceptibility (RBG between 0.4 and 1.1). Because higher RBG values represent greater inhibition of bacterial

growth, these results confirm that resistance did not evolve in the absence of direct phage selection, with only minor variation likely reflecting spontaneous mutations. Resistance to coevolved phages was lower, than resistance to ancestral phages, indicating that phages had evolved increased infectivity.. Testing evolved bacteria against ancestral phages from other treatments, revealed cross-resistance between phages 1 and 2, but not *Phage 3*. This means that clones evolved against Phage 1 were also resistant to Phage 2 (and vice-versa), suggesting these two phages may use a similar infection mechanisms. In contrast, resistance to Phage 3 was specific, and clones resistant to Phages 1 or 2 were still susceptible to Phage 3. (with the exception of one population which was strongly resistant to all phages).

Figure 2 clearly illustrates these patterns, where, the y-axis shows the individual bacterial clones, grouped by the population they evolved in (e.g., P1-1 to P1-6 are the 6 replicate populations from the Phage 1 treatment). The x-axis shows the specific phage they were challenged with. The colour scale from white (high resistance) to dark red (high susceptibility) shows the outcome. A clear band of white/light red is visible in the ‘Ancestor’ columns for all phage-evolved treatments (AP1, AP2 and AP3), confirming evolved resistance. In contrast, the ‘Ancestor’ columns for the No Phage treatment are dark red, confirming continued susceptibility.

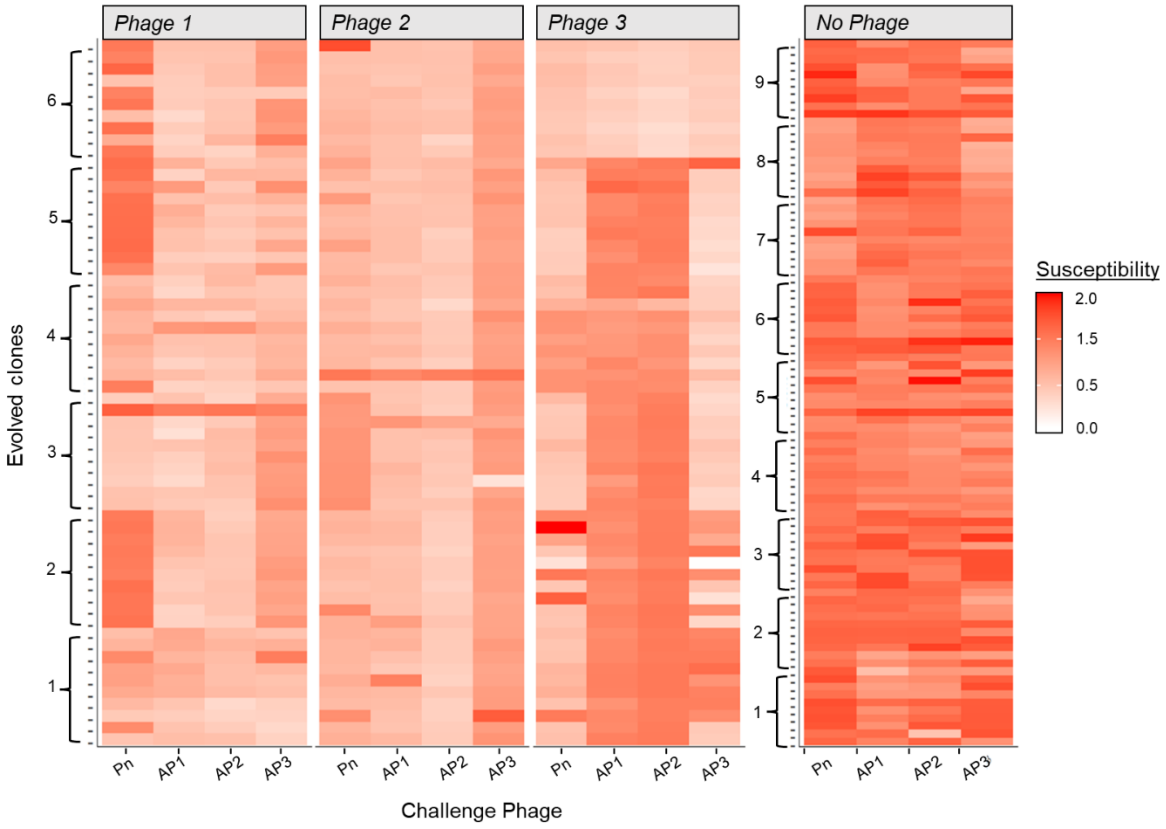

***Figure 2**: Heatmap showing susceptibility scores (RBG values) for 10 clones from each evolved rhizobial population. Each row represents a single bacterial clone. Clones are grouped on the y-axis by the replicate population they were isolated from. The facets (top labels) indicate the treatment group each population evolved under (No Phage, Phage 1, etc.). The No Phage clones were tested against all phage treatment.*

3.4.2 Molecular evolution

Single evolved clones from each replicate population were sequenced; meaning 6 clones from the Phage 1 treatment, 6 from Phage 2 treatment, 6 from Phage 3 treatment and 9 from the No phage controls, for a total of 27 sequenced individuals. We identified a total of 61 mutations identified in 51 unique loci across the 27 sequenced individuals (**Figure 3a-b, Table S1 and S3**). We identified 15 gene targets shared between both phage-treated and no-phage populations, 4 gene targets unique to the no-phage group, and 26 gene targets exclusive to phage-treated populations (**Figure 3a**). Six gene targets and one exact nucleotide change were shared across multiple phage treatments. Phage-evolved clones exhibited a greater

number of mutations per genome (26, 15 and 13 for *phages 1-3* respectively) than no-phage controls (7) (**Figure 3a, Table S2**), supporting the expectation that antagonistic coevolution accelerates genetic change (Paterson *et al.*, 2010).

Mutations in the phage-treated group predominantly targeted genes associated with exopolysaccharide (EPS) biosynthesis, metabolism, and regulatory pathways, suggesting that surface modifications and metabolic rewiring are key routes of adaptation in response to phage pressure. Several of these gene targets were notable for their level of parallelism or clear association with phage resistance:

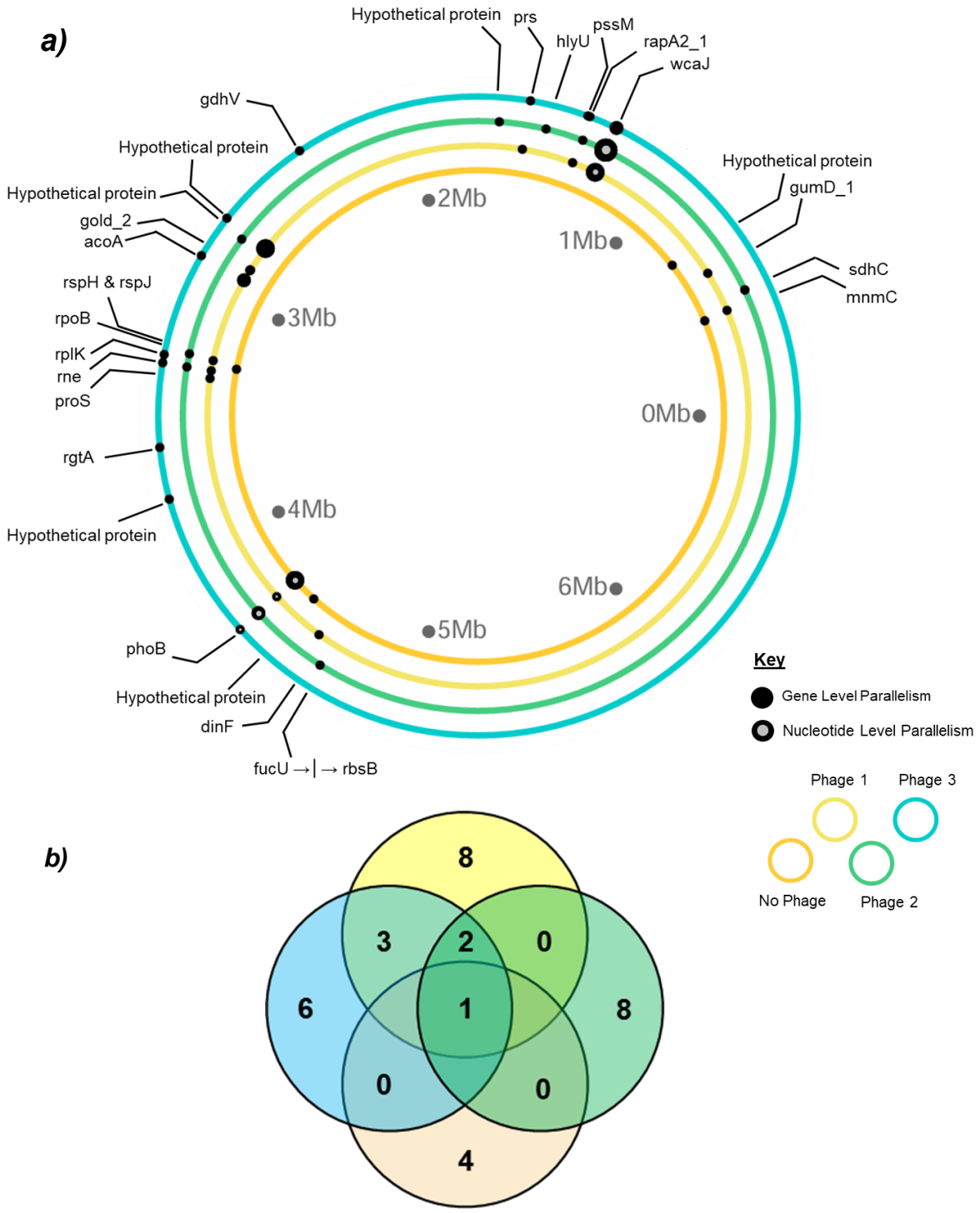

***Figure 3**: **a)** A summary of mutations identified in evolved clones across all treatments (No Phage, Phage 1, Phage 2 and Phage 3). The four inner rings represent the TRX19 bacterial genome, with each ring representing the four evolved treatment groups. Mutations are shown as dots, where the size of the dots represents how frequently a given gene was mutated across replicates within treatments. Grey dots denote nucleotide level parallelism (NLP). These clones were those chosen based on RBG values and those that were put into symbiosis with their plant hosts. **b)** Shared loci, at the gene level, between evolved bacterial clones across different treatments.*

3.4.2.1 wcaJ

wcaJ was mutated in 9/18 clones across all three phage treatments (**Table S2, Figure 3a**) but did not appear in any of the 9 *No Phage* evolved clones. Most of these mutations were frameshifts (7/9) (an insertion or deletion of nucleotides that shifts the genetic reading frame, usually resulting in a non-functional protein); while 2 were non-synonymous substitutions (a single nucleotide change that results in a different amino acid being coded). Notably, we observed parallel mutations at the nucleotide-level within *Phage 2* samples (3/4 clones containing *wacJ* mutations) and across treatments, with one *Phage 1* sample sharing the same mutation as occurred in the *Phage 2* clones (**Figure 3b**).

wcaJ encodes a glycosyltransferase involved in EPS biosynthesis, specifically the assembly of colanic acid, a key component of cell surface structures and biofilms (Tan et al., 2020). Mutations in *wacJ* can lead to altered EPS composition (Tan *et al.*, 2020), affecting both the structure and functionality of biofilms. This modification can enhance bacterial adhesion and aggregation, key traits that contribute to the robustness of biofilms as a defence mechanism. Importantly, mutations in *wacJ*, documented in other bacteria-phage systems, can modify cell surface glycoconjugates, reducing phage adsorption and effectively blocking access to receptor sites. For example, in *Klebsiella pneumoniae*, *wacJ* mutations disrupt capsule formation, providing resistance to phages but reducing virulence (Song *et al.*, 2021; Bain *et al.*, 2024). In *Pseudomonas aeruginosa*, similar mutations in other glycosyltransferase genes alter lipopolysaccharide (LPS) structure, reducing susceptibility to phage attack (Latino *et al.*, 2019).

3.4.2.2 acoA

Mutations in *acoA* were observed in the *Phage 1 (3/6 clones)* and *Phage 3 (1/6 clones)* treatments, with 3 clones carrying non-synonymous mutations and one clone in the *Phage 1* treatment exhibiting a large deletion spanning this locus. *acoA* encodes aconitate hydratase, a key enzyme in the tricarboxylic acid (TCA) cycle that is central to bacterial energy

metabolism. In other bacteria-phage systems, metabolic rewiring has been implicated in phage resistance, often accompanied by fitness trade-offs. For example, in *Pseudomonas fluorescens*, adaptive changes in metabolic genes under phage pressure reduced fitness in non-phage environments (Hall, Scanlan and Buckling, 2011).

3.4.2.3 Phage integration

In addition to identifying parallel mutations in key loci, we observed phage integration into the bacterial genome in all clones evolved with *Phage 3*. A nucleotide BLAST analysis of the evolved phage revealed 96.5% similarity to the temperate phage vTRX32-1 (Ford *et al.*, 2021). This high similarity suggests that Phage 3 possesses the necessary genetic machinery for lysogeny (e.g., genes for an integrase and repressor), which would explain its ability to integrate, however this is yet to be confirmed for this phage. Phages were selected for their inability to form prophages on the target strain, suggesting that the phage had transitioned from a purely lytic to a lysogenic lifestyle during the experiment.

To confirm the presence of lysogeny, we performed PCR analysis on evolved clones and found that phage integration was detectable in all populatduring*3* treatment as early as transfer 4 (**Figure S1**). We further verified lysogeny by inducing the evolved phage from these clones, spotting the lysates onto ancestral TRX19, and confirming successful phage integration via PCR. We then tested whether the integrated phage conferred resistance to infection. We assessed whether phage integration provided resistance by comparing growth of TRX19, TRX19+*Phage3*, and an evolved *Phage 3* clone, with and without phage. Only the ancestral strain showed reduced growth in the presence of phage, indicating that integration conferred protection (**Figure S2**). This protection, is known as superinfection immunity: the integrated prophage produces repressor proteins that prevent new, incoming phages from replicating, thus protecting the host cell from further lytic infection. In the presence of phage, TRX19 showed significantly reduced AUC ($t = 3.41$, $p = 0.0067$), while both TRX19+*Phage3* and *evolved Phage 3* maintained growth, with no significant difference between them. This indicates that phage integration confers protection against lytic infection. This switch from a

lytic to a lysogenic lifestyle has important implications for host–phage dynamics. Lysogeny allows phage genomes to persist within bacterial hosts while providing immunity to superinfection by related phages (Chibani-Chennoufi et al., 2004). This integration likely contributed to the evolved resistance observed in *Phage 3*-evolved clones (**Figure 2**) and may also help stabilize host fitness by modulating key cellular processes or influencing the host's ability to acquire or rearrange genetic material (genome plasticity) (Labrie et al., 2010).

3.4.3 Phenotype testing

To investigate how genetic changes translate to phenotypic adaptations, we measured biofilm formation, swimming, and swarming abilities in evolved clones from each treatment and compared these traits to the ancestral strain. These phenotypic changes provide insights into the broader adaptive strategies of *Rhizobium leguminosarum* under phage pressure and their potential consequences for symbiosis.

3.4.3.1 Biofilm

Biofilm formation is a well-documented bacterial response to phage predation (Hosseinidoust, Tufenkji, and van de Ven, 2013; Henriksen et al., 2019), often serving as a protective mechanism against phage infection. By creating a physical barrier, biofilms limit phage access to host cells, allowing bacteria to survive and persist under phage pressure. This response is particularly advantageous in environments with high phage density, where biofilm production can shield bacteria not only from phage adsorption but also from other environmental stressors such as nutrient deprivation or antibiotics (Simmons et al., 2020).

Biofilm formation was significantly affected by treatment (ANOVA, $F(4, 84) = 37.66$, $p < 0.001$), with evolved clones from *Phage 1*, *Phage 2*, and *Phage 3* treatments producing more biofilm than the ancestral strain ($t(9.38) = 3.40$, $p = 0.0075$; $t(9.93) = 2.56$, $p = 0.0286$; $t(9.93) = 2.21$, $p = 0.0483$) (**Figure 4**). *No Phage* treatments were not significantly different from the ancestral strain ($t(8.35) = -0.25$, $p = 0.807$). This suggests that phage exposure is a major driver of increased biofilm formation (Fernández et al., 2017).

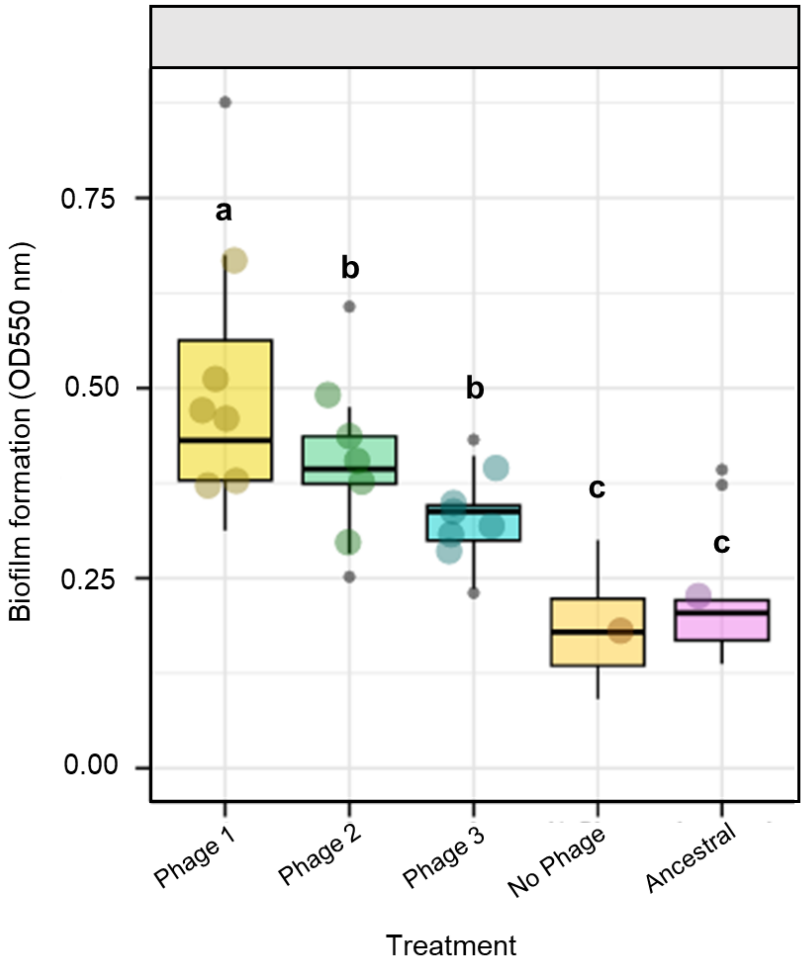

***Figure 4**: Biofilm formation quantification relative to OD550nm for each chosen resistant clone from each Phage treatment. Plot shows the data distribution for each Treatment, along with each population within that treatment (technical reps within bio rep). Two-way ANOVA and post hoc Tukey performed, where there is a different letter $p < 0.05$.*

Biofilm formation can provide phage resistance through two potential mechanisms: (1) a mass effect, where biofilms physically shield bacteria from phage attack, or (2) modifications to surface receptors involved in both biofilm formation and phage adsorption. If biofilm-mediated resistance primarily arises from physical shielding, we would expect it to be density-dependent, with stronger effects in high-nutrient environments that support robust biofilm growth. Conversely, if resistance stems from receptor modifications, it should be less affected by cell density. To test these possibilities, we examined whether phage resistance was consistent across nutrient environments by measuring susceptibility (RBG values) in low (1% TY) and high (100% TY) media across phage treatments (**Figure S3**). Allowing us to

distinguish between context-dependent mechanisms, such as biofilm-based protection, and fixed resistance mechanisms like receptor modification. Mixed-effects modelling revealed a significant effect of media concentration on susceptibility ($F(1, 25) = 17.78$, $p < 0.001$), with clones showing higher susceptibility in low-nutrient conditions. There was also a significant main effect of phage treatment ($F(2, 25) = 3.41$, $p = 0.049$). Indicating that resistance is not fully maintained in low-nutrient environments, consistent with a density-dependent resistance mechanism. Such a pattern supports the idea that biofilms contribute to resistance by acting as a physical barrier, which is compromised under nutrient-limited conditions where biofilm formation is reduced. If resistance were instead conferred solely via receptor-level modifications, susceptibility would be expected to remain low regardless of media concentration, which was not observed.

3.4.3.2 Motility

Motility plays a central role in rhizobia-host interactions, enabling bacteria to reach plant roots, colonize host tissues, and establish symbiosis (Miller *et al.*, 2007; Zheng *et al.*, 2015). Swimming refers to the movement of individual cells through liquid using flagella, whereas swarming is a coordinated surface-based movement of bacterial groups across semi-solid media. Given the prevalence of surface mutations in phage-evolved clones, we next examined swimming and swarming motility:

3.4.3.2.1 Swimming

Swimming ability was significantly influenced by treatment ($F(4, 84) = 21.58$, $p = 2.85e\text{-}12$). All evolved treatments, including the *No Phage* group, exhibited significantly greater swimming ability than the ancestral strain (Tukey's HSD, $p < 0.001$ for all pairwise comparisons) (**Figure 5a**). However, clones from the *Phage 1* and *Phage 2* treatments showed significantly lower swimming ability than the *No Phage*-evolved clones ($p < 0.05$), suggesting that adaptation to phage pressure constrained the broader evolution of swimming motility. While not linked to a single specific gene, this constraint is likely a pleiotropic cost of the various surface-modifying

mutations (e.g., *wacJ*) and metabolic changes (e.g., *acoA*) selected by these phages. This highlights a trade-off, where phage resistance limited the extent to which motility could evolve, a trait likely advantageous in the liquid broth environment. In contrast, clones from the *Phage 3* treatment did not show significantly reduced swimming relative to *No Phage* controls. Since *Phage 3* was found to be lysogenic, integrating into the bacterial genome, in all 6/6 clones, early during evolution, it is possible that this reduced the selective pressure for costly resistance mutations, allowing these clones to retain higher swimming ability.

3.4.3.2.2 Swarming

Swarming motility, surface-based movement, was also significantly influenced by treatment ($F(4, 84) = 9.086$, $p = 3.79e\text{-}06$), but the patterns differed from swimming. Clones from the *Phage 1* ($p = 0.0102$) and *Phage 2* ($p = 0.0034$) treatments exhibited significantly reduced swarming ability compared to the ancestral strain, while clones from the *Phage 3* ($p = 0.9999$) and *No Phage* ($p = 0.8691$) treatments showed no significant differences (**Figure 5b**).

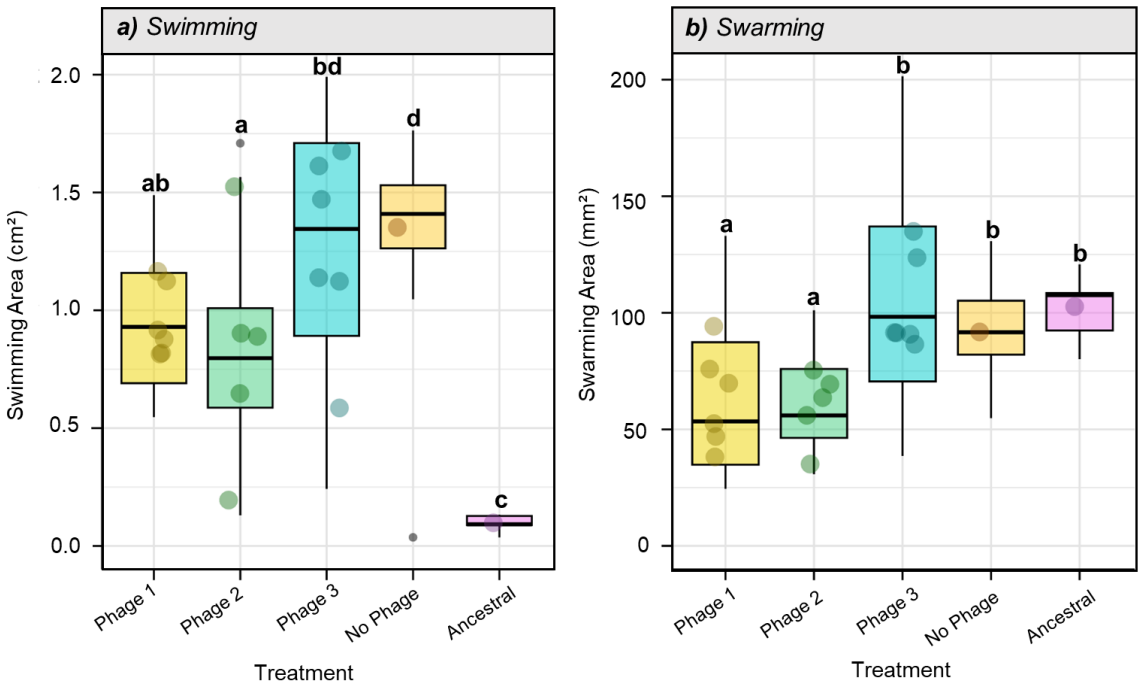

***Figure 5**: Shows phenotypic assays. **a)** shows Swimming ability in 0.3% Agar and **b)** shows Swarming ability in 0.5% agar. Two-way ANOVA and post hoc Tukey performed, where there is a different letter $p < 0.05$.*

The reduction in swarming observed in the *Phage 1* and *Phage 2* treatments is likely linked to changes in cell surface properties, particularly mutations in *wacJ*, which have been previously associated with impaired swarming motility (Chung, Sim and Cho, 2012). Our data support this, as evolved clones without *wacJ* mutations exhibited significantly greater swarming ability compared to those with the mutation (**Figure S4**). However, the prevalence of *wacJ* mutations across phage treatments does not fully explain the observed differences, suggesting that additional genetic factors may contribute to the variation in swarming motility.

By contrast, the lack of significant changes in swarming in *Phage 3* clones may reflect the stabilizing effects of lysogeny. Temperate phages are known to modulate bacterial behaviour by regulating stress responses and phenotypic changes through mechanisms such as lysogenic conversion, where prophages provide adaptive traits to their hosts, including biofilm formation (Feiner et al., 2015) and potentially motility. Indeed, previous work on the closely related vTRX32-1 phage has shown that lysogeny is associated with widespread changes in gene expression (Mary Eliza, 2023, p12-27), supporting the idea that *Phage 3* integration likely influenced bacterial physiology. Alternatively, lysogeny may have effectively ended the arms race, reducing the selective pressure for mutations in motility-related genes. Without ongoing phage predation, there was no strong evolutionary pressure to alter swarming behaviour, which may explain why *Phage 3*-evolved clones did not exhibit the same reductions in swarming seen in *Phage 1* and *Phage 2* treatments. Furthermore, population-level heterogeneity in phage induction, driven by environmental conditions, helps lysogenic populations survive under stress without completely losing essential behaviours (Imamovic et al., 2016). This suggests that rather than requiring compensatory mutations, *Phage 3* clones may have retained motility traits simply because selection for resistance was no longer a major constraint.

3.4.4 Symbiotic performance

Finally, we tested whether phage-driven adaptations affected rhizobia's ability to form symbiosis with plants. The 27 selected clones (6 from each phage treatment and 9 from no-phage controls) weretested in symbiosis with a host plant, clover (Trifolium repens) along with ancestral controls. Symbiont quality was assessed by measuring total plant biomass and nitrogen fixation efficiency (% total N).

Compared to the ancestral strain, there were no significant differences in biomass or nitrogen fixation when plants were inoculated with rhizobia evolved in the phage-free treatment ($p = 0.092$, $p=0.973$, respectively). Similarly, rhizobia evolved in the *Phage 2* ($p = 0.958$) or *Phage 3* ($p = 0.979$) treatments showed no reduction in symbiotic performance (**Figure 6a-b**). This important result tells us that under these conditions, rhizobia can evolve resistance to phages (like Phage 2 and Phage 3) without suffering a trade-off in their symbiotic effectiveness. However, partnerships with rhizobia evolved with *Phage 1* exhibited drastically reduced symbiotic performance, as they produced significantly lower biomass and nitrogen fixation compared to both the ancestral strain ($p < 0.001$) and the other phage treatments ($p < 0.05$, $p < 0.05$; vs *Phage 2* and *Phage 3* respectively). Indeed, plants inoculated with *Phage 1*-evolved strains were not significantly different from the uninoculated controls.

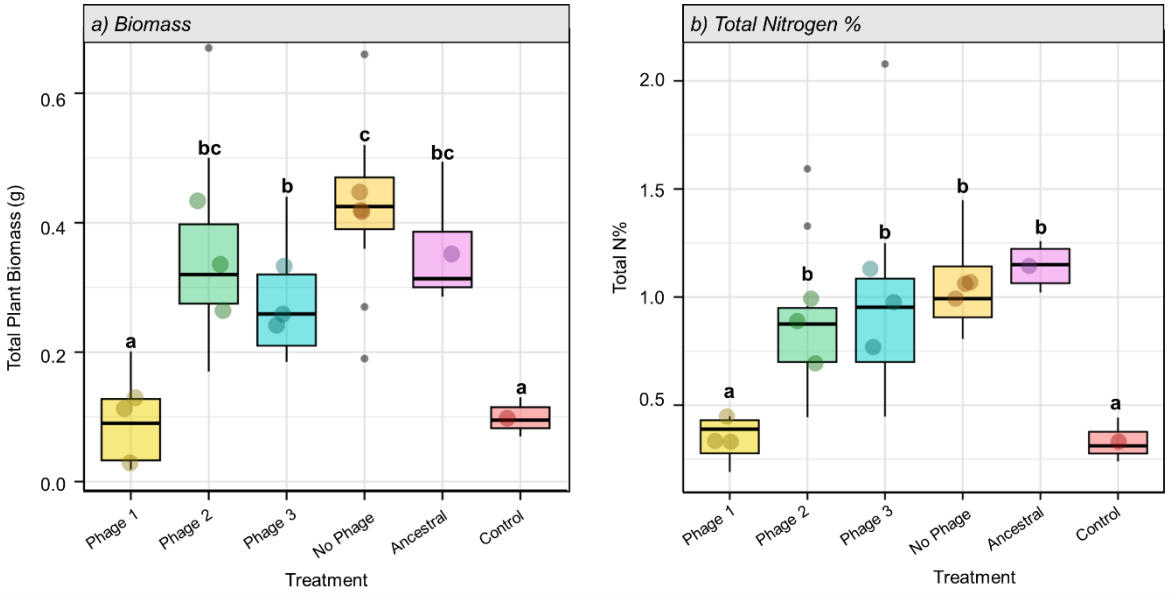

Figure 6: *Data from plant symbiosis assay. Chosen resistant Rhizobia clones, from each phage treatment were put into symbiosis with their host plant Clover (Trifolium repens).* ***a)*** *Total plant biomass (root+shoot dry);* ***b)*** *Nitrogen % for dry shoot biomass. For each treatment, where there is a different letter $p < 0.05$.*

Comparison between symbiotic performance and the presence of notable mutations found mutations in *wcaJ*, despite their prevalence across phage-evolved clones, were not associated with significant differences in plant biomass ($p = 0.0818$; **Figure S4e**). This suggests that while *wcaJ* mutations provided resistance against phage infection, they did not directly impact symbiotic traits such as nitrogen fixation or plant growth. This is consistent with the finding that symbiosis was not compromised in the majority of clones. However, there was an association with *acoA*-mutated clones which were strongly correlated with reduced plant biomass ($p = 0.0255$; **Figure S4f**). Whilst this association is confounded by the prevalence of *acoA* mutations in the *Phage 1* treatment, notably, a reduction in plant biomass was also observed in the only *Phage 3*-evolved clone to carry an *acoA* mutation (**Figure S5**). This specific finding strengthens the link between acoA and symbiotic failure, suggesting the metabolic disruption, not the phage it evolved with, is the causal factor.. *acoA* encodes aconitate hydratase, a key enzyme in the tricarboxylic acid (TCA) cycle essential for ATP

production and energy metabolism (Dunn, 1998; Soto, Sanjuan and Olivares, 2001). Previous studies have shown that disruptions in the TCA cycle can impose significant fitness costs on bacteria (Kwong, Zheng and Moran, 2017; MacLean, Legendre and Appanna, 2023). In E. coli, mutations in key TCA cycle enzymes have been linked to reduced colonization ability and impaired growth, especially under nutrient-limited conditions (Himpsl *et al.*, 2020). Similarly, experimental disruption of the oxidative TCA cycle in *Methylomicrobium buryatense* led to severe growth defects, underscoring the essential role of central metabolism in supporting bacterial fitness (Fu, Li and Lidstrom, 2017). In rhizobia, nitrogen fixation is one of the most energy-intensive processes, requiring substantial ATP and reducing power to sustain nitrogenase activity (Poole et al., 2018). As such, disruptions to central metabolism, such as *acoA* mutations, are likely to impose direct fitness costs by limiting energy availability for symbiosis.

3.5. Conclusions

Our study highlights the potentially profound impact of phage-driven evolution on Rhizobium leguminosarum, demonstrating that resistance to phages can lead to drastically different outcomes for symbiosis, ranging from total loss of symbiotic function to no measurable change, depending on the evolutionary trajectory imposed by different phages. This diversity of outcomes underscores how phages can act as powerful but unpredictable forces shaping bacterial evolution.

A striking result was the divergence in evolutionary responses between phages. The absence of symbiotic costs in *Phage 2* and *Phage 3* evolved clones suggests that resistance mechanisms in these treatments were either less disruptive to host interactions or that compensatory mutations(secondary mutations that alleviate the fitness cost of the primary resistance mutation) mitigated negative effects. Interestingly, *Phage 3* integration into the rhizobial genome likely played a stabilizing role by reducing the selective pressure for costly resistance strategies. The fact that *Phage 3* populations showed less pronounced biofilm formation may indicate that lysogeny buffers against costly resistance strategies, further

distinguishing it from its lytic counterparts. This aligns with previous findings on the lysogenic phage vTRX32-1, which does not impact symbiotic effectiveness (Mary Eliza, 2023, p12-27). In contrast, *Phage 1* and *Phage 2* maintained lytic interactions. Cross resistance between the ancestral phages suggests that, initially, the selective response to these phages may be similar, yet *Phage 2*, did not impose the same symbiotic cost, potentially suggesting either weaker selection or alternative resistance mechanisms at later stages in the coevolutionary arms race. A possible explanation is that *acoA* mutations, found in multiple *Phage 1*-evolved clones, disrupted the TCA cycle, limiting energy production needed for nitrogen fixation and thereby reducing symbiotic performance. While we cannot fully explain this discrepancy, it highlights the complexity of phage-host interactions and suggests that even similar selection pressures can drive distinct evolutionary paths.

Ultimately, these findings emphasize that phage-driven evolution is highly context-dependent, with different phages shaping bacterial ecology and symbiosis in distinct ways. The ability of phages to either drive host-pathogen arms races or disrupt them through lysogeny has major implications for microbial community stability, evolutionary dynamics, and even the potential application of phages in agriculture or biotechnology. Overall, our findings emphasize the need to consider both genetic and ecological factors when studying phage interactions in microbial symbioses. These interactions can lead to diverse evolutionary outcomes, influencing the ecological roles of symbiotic bacteria and their broader implications for ecosystem dynamics. Future work should explore the broader ecological consequences of these trade-offs, particularly in mixed microbial communities where phage interactions are likely even more complex.

3.6 Supplementary Materials

***Table S1**: Full mutation list and frequency of mutation occurring in each gene within Phage or No Phage treatment groups. The list is populated with each genes GO category and function.*

Gene	No Phage Frequency /9	Phage Frequency /18	Phage Treatment mutation occurred with	GO Category	GO Function
acoA	0	3	1, 3	Biosynthesis	Enzyme activity
hlyU_2	0	1	2	Biosynthesis	Enzyme activity
proS	0	1	1	Biosynthesis	Enzyme activity
rgtA	0	1	3	Biosynthesis	Enzyme activity
rpsH	0	1	1, 2	Biosynthesis	Enzyme activity
wcaJ	0	9	1, 2, 3	Biosynthesis	Initiates colanic acid biosynthesis for biofilm formation
dinF	0	1	1	DNA Damage Response	Protects against oxidative stress and enhances survival in biofilm conditions
gumD	0	2	1	Exopolysaccharide Biosynthesis	Initiates biofilm polysaccharide synthesis, aiding adhesion and stress protection
gdhIV	0	1	3	Metabolic process	Oxidation-reduction activity
phoB	3	4	1, 2, 3, NP	Metabolic process	Oxidation-reduction activity
fucU_2	0	1	2	Metabolic process	Oxidation-reduction activity
prs_2	0	2	1, 3	Metabolic process	Oxidation-reduction activity
rne	0	3	1, 2, 3	Metabolic process	Oxidation-reduction activity
sdhC	0	1		Metabolism	Part of the succinate dehydrogenas

			3		e complex, crucial for TCA cycle and biofilm support
rpoB	0	1	1, 2, 3	Transcription	Encodes the beta subunit of RNA polymerase, affecting gene transcription and biofilm adaptation
rapA2_1	0	1	2, 3	Transcription Regulation	ATP-dependent helicase aiding transcription and biofilm matrix regulation
rpsJ	0	1	1, 2, NP	Translation	Encodes ribosomal protein S10, essential for mRNA decoding and involved in antibiotic resistance
golD_2	0	2	1	Transport	Ion transmembrane transporter activity
rplK	1	0	1, 3	Transport	Ion transmembrane transporter activity
mnmC_3	1	0	1, NP	tRNA Modification	Supports translational fidelity and biofilm survival under stress
ILBCKJEK_00573	0	1	1	Unknown	Further research required
ILBCKJEK_00687	1	0	NP	Unknown	Further research required
ILBCKJEK_00688	1	0	NP	Unknown	Further research required
ILBCKJEK_01943	0	1	1	Unknown	Further research required
ILBCKJEK_01953	0	1	2	Unknown	Further research required
ILBCKJEK_02255	0	1	3	Unknown	Further research required

ILBCKJEK_03344	0	4	1, 2	Unknown	Further research required
ILBCKJEK_03368	0	1	2	Unknown	Further research required
ILBCKJEK_04377	0	1	1	Unknown	Further research required
ILBCKJEK_05037	0	1	3	Unknown	Further research required
ILBCKJEK_05038	1	0	NP	Unknown	Further research required

***Table S2**: Summary of all mutation stats.*

Metric	Summary / Value
Total Number of Mutations	61
Total Number of unique Mutations	51
Total Number of unique Genes Affected	27 genes with mutations across all samples
Total Number of Shared Genes	1 gene shared between Phage and No Phage groups
Total Number of Unique Genes in Phage Group	25 genes unique to the Phage group
Total Number of Unique Genes in No Phage Group	4 genes unique to the No Phage group
Number of Mutations by Phage Group	- No Phage group: 7 - Phage group: 54 - Phage 1: 26 - Phage 2: 15 - Phage 3: 13
Parallel Mutations at Loci	3 loci where mutations occurred in multiple samples - Position 1250805 had 4 mutations - Position 2914248 had 2 mutations - Position 4315591 had 7 mutations
Parallel Mutations at Loci by Phage Group	- No Phage group: 1 locus had parallel mutations - Phage group: 2 loci had parallel mutations
Mutation types	Phage group - Frameshift: 12 - Intergenic: 16 - Non-synonymous: 23 - Synonymous: 1 - Nonsense: 2 No Phage group - Frameshift: 1 - Intergenic: 5 - Non-synonymous: 1

Table S3: Full list of all mutation for each sample.

Type	Sequence	Position	Mutation	Annotatio	Gene	Description	Sample	Phage	Treatment	Mutation Type
SNP	contig_2	2914229	G→A	T214I (AC(	acoA ←	Acetoin:2,6-dichlorophenolindophenol oxidoreductase subunit alpha	Sample_24.3_6	phage	p3	synonymous
SNP	contig_2	2914248	T→C	T208A (AC	acoA ←	Acetoin:2,6-dichlorophenolindophenol oxidoreductase subunit alpha	Sample_4.1_4	phage	p1	synonymous
SNP	contig_2	2914248	T→C	T208A (AC	acoA ←	Acetoin:2,6-dichlorophenolindophenol oxidoreductase subunit alpha	Sample_6.1_6	phage	p1	synonymous
SNP	contig_2	4550413	G→A	V407I (GTC	dinF →	DNA damage-inducible protein F	Sample_3.1_3	phage	p1	synonymous
DEL	contig_2	4621004	(T)6→5	intergenic	fucU_2 → /	L-fucose mutarotase/Ribose import binding protein RbsB	Sample_10.2_1	phage	p2	intergenic
SNP	contig_2	2865476	C→G	A256A (GC	golD_2 →	NAD-dependent glycerol dehydrogenase	Sample_6.1_6	phage	p1	synonymous
SNP	contig_2	2865478	G→A	*257* (TG	golD_2 →	NAD-dependent glycerol dehydrogenase	Sample_6.1_6	phage	p1	nonsense
SNP	contig_2	2865482	T→C	intergenic	golD_2 → /	NAD-dependent glycerol dehydrogenase/IS21 family transposase ISRel5	Sample_6.1_6	phage	p1	intergenic
SNP	contig_2	2865486	A→G	intergenic	golD_2 → /	NAD-dependent glycerol dehydrogenase/IS21 family transposase ISRel5	Sample_6.1_6	phage	p1	intergenic
SNP	contig_2	2865491	C→G	intergenic	golD_2 → /	NAD-dependent glycerol dehydrogenase/IS21 family transposase ISRel5	Sample_6.1_6	phage	p1	intergenic
SUB	contig_2	2865497	2 bp →CG	intergenic	golD_2 → /	NAD-dependent glycerol dehydrogenase/IS21 family transposase ISRel5	Sample_6.1_6	phage	p1	intergenic
SUB	contig_2	2865508	2 bp →CA	intergenic	golD_2 → /	NAD-dependent glycerol dehydrogenase/IS21 family transposase ISRel5	Sample_6.1_6	phage	p1	intergenic
SNP	contig_2	2865517	A→G	intergenic	golD_2 → /	NAD-dependent glycerol dehydrogenase/IS21 family transposase ISRel5	Sample_6.1_6	phage	p1	intergenic
SNP	contig_2	2865523	A→G	intergenic	golD_2 → /	NAD-dependent glycerol dehydrogenase/IS21 family transposase ISRel5	Sample_6.1_6	phage	p1	intergenic
SNP	contig_2	491921	A→T	L75H (CTT	gumD_1 ←	UDP-glucose:undecaprenyl-phosphate glucose-1-phosphate transferase	Sample_11.2_2	phage	p2	synonymous
SNP	contig_2	492157	A→G	intergenic	gumD_1 ←	UDP-glucose:undecaprenyl-phosphate glucose-1-phosphate transferase/hypothetical protein	Sample_15.2_6	phage	p2	intergenic
DEL	contig_2	1490663	(AG)4→3	coding (15	hlyU_2 ←	Transcriptional activator HlyU	Sample_14.2_5	phage	p2	frameshift
SNP	contig_1	619471	G→A	A19V (GCA	ILBCKJEK_	HTH-type transcriptional regulator	Sample_4.1_4	phage	p1	synonymous
SNP	contig_1	735565	T→C	intergenic	ILBCKJEK_	hypothetical protein/hypothetical protein	Sample_27.C3_3	nophage	nophage	intergenic
SNP	contig_2	1345543	C→T	P88L (CCC	ILBCKJEK_	hypothetical protein	Sample_13.2_4	phage	p2	synonymous
DEL	contig_2	1351872	Δ33206 bp	NA	ILBCKJEK_	32 genes; ILBCKJEK_01948, prsD_1, prsE_1, ILBCKJEK_01951, ILBCKJEK_01952, ILBCKJEK_01953, ILBCK	Sample_5.1_5	phage	p1	non-synonymous
SNP	contig_2	1358864	C→A	G15C (GG	ILBCKJEK_	hypothetical protein	Sample_24.3_6	phage	p3	synonymous
INS	contig_2	1669429	(G)8→9	coding (36	ILBCKJEK_	hypothetical protein	Sample_10.2_1	phage	p2	frameshift
SNP	contig_2	2409285	G→A	intergenic	ILBCKJEK_	hypothetical protein/Glucose 1-dehydrogenase 4	Sample_20.3_2	phage	p3	intergenic
SNP	contig_2	2755960	G→T	T151N (AC	ILBCKJEK_	hypothetical protein	Sample_1.1_1	phage	p1	synonymous
SNP	contig_2	2756239	A→G	L58P (CTG	ILBCKJEK_	hypothetical protein	Sample_22.3_4	phage	p3	synonymous
SNP	contig_2	2755967	G→A	Q149* (CA	ILBCKJEK_	hypothetical protein	Sample_4.1_4	phage	p1	nonsense
INS	contig_2	2756338	+G	coding (74	ILBCKJEK_	hypothetical protein	Sample_6.1_6	phage	p1	frameshift
SNP	contig_2	2783934	C→T	E222E (GA	ILBCKJEK_	hypothetical protein	Sample_11.2_2	phage	p2	synonymous
SNP	contig_2	3793539	C→T	E2K (GAA→	ILBCKJEK_	hypothetical protein	Sample_19.3_1	phage	p3	synonymous
INS	contig_2	4315591	(C)11→12	intergenic	ILBCKJEK_	hypothetical protein/Phosphate regulon transcriptional regulatory protein PhoB	Sample_14.2_5	phage	p2	intergenic
INS	contig_2	4315591	(C)11→12	intergenic	ILBCKJEK_	hypothetical protein/Phosphate regulon transcriptional regulatory protein PhoB	Sample_15.2_6	phage	p2	intergenic
INS	contig_2	4315591	(C)11→12	intergenic	ILBCKJEK_	hypothetical protein/Phosphate regulon transcriptional regulatory protein PhoB	Sample_18.C2_3	nophage	nophage	intergenic
INS	contig_2	4315591	(C)11→12	intergenic	ILBCKJEK_	hypothetical protein/Phosphate regulon transcriptional regulatory protein PhoB	Sample_20.3_2	phage	p3	intergenic
INS	contig_2	4315591	(C)11→12	intergenic	ILBCKJEK_	hypothetical protein/Phosphate regulon transcriptional regulatory protein PhoB	Sample_25.C3_1	nophage	nophage	intergenic
INS	contig_2	4315591	(C)11→12	intergenic	ILBCKJEK_	hypothetical protein/Phosphate regulon transcriptional regulatory protein PhoB	Sample_4.1_4	phage	p1	intergenic
INS	contig_2	4315591	(C)11→12	intergenic	ILBCKJEK_	hypothetical protein/Phosphate regulon transcriptional regulatory protein PhoB	Sample_7.C1_1	nophage	nophage	intergenic
SNP	contig_2	4435591	G→A	intergenic	ILBCKJEK_	hypothetical protein/hypothetical protein	Sample_27.C3_3	nophage	nophage	intergenic
INS	contig_4	442923	(ACCGGC	coding (93	mnmC_3 →	tRNA 5-methylaminomethyl-2-thiouridine biosynthesis bifunctional protein MnmC	Sample_17.C2_2	nophage	nophage	frameshift
DEL	contig_2	3344654	(T)9→8	intergenic	proS ← / ←	Proline--tRNA ligase/hypothetical protein	Sample_5.1_5	phage	p1	intergenic
SNP	contig_2	1566423	C→T	D62N (GA(	prs_2 ←	Ribose-phosphate pyrophosphokinase	Sample_1.1_1	phage	p1	synonymous
SNP	contig_2	1566017	T→C	E197G (GA	prs_2 ←	Ribose-phosphate pyrophosphokinase	Sample_24.3_6	phage	p3	synonymous
SNP	contig_2	1351548	A→G	intergenic	rapA2_1 ←	Calcium-binding lectin RapA2/hypothetical protein	Sample_19.3_1	phage	p3	intergenic
DEL	contig_2	3609873	Δ81 bp	coding (10	rgtA →	Lipopolysaccharide core galacturonosyltransferase RgtA	Sample_24.3_6	phage	p3	frameshift
SNP	contig_2	3312786	T→C	S10P (TCT	rne →	Ribonuclease E	Sample_1.1_1	phage	p1	synonymous
SNP	contig_2	3313936	G→T	R393L (CG	rne →	Ribonuclease E	Sample_10.2_1	phage	p2	synonymous
SNP	contig_2	3313606	G→A	G283D (GC	rne →	Ribonuclease E	Sample_22.3_4	phage	p3	synonymous
SNP	contig_2	3286882	T→C	N119S (AA	rplK ←	50S ribosomal protein L11	Sample_25.C3_1	nophage	nophage	synonymous
SNP	contig_2	3284275	G→A	R94C (CG(	rpoB ←	DNA-directed RNA polymerase subunit beta	Sample_22.3_4	phage	p3	synonymous
SNP	contig_2	3263480	C→G	V73V (GTG	rpsH ←	30S ribosomal protein S8	Sample_14.2_5	phage	p2	synonymous
SNP	contig_2	3270379	T→C	M88V (ATG	rpsJ ←	30S ribosomal protein S10	Sample_4.1_4	phage	p1	synonymous
DEL	contig_2	447170	Δ6 bp	coding (65	sdhC →	Succinate dehydrogenase cytochrome b556 subunit	Sample_5.1_5	phage	p1	frameshift
INS	contig_2	1250760	+G	coding (18	wcaJ ←	UDP-glucose:undecaprenyl-phosphate glucose-1-phosphate transferase	Sample_1.1_1	phage	p1	frameshift
DEL	contig_2	1250805	Δ1 bp	coding (14	wcaJ ←	UDP-glucose:undecaprenyl-phosphate glucose-1-phosphate transferase	Sample_10.2_1	phage	p2	frameshift
SNP	contig_2	1250769	A→C	L60R (CTC	wcaJ ←	UDP-glucose:undecaprenyl-phosphate glucose-1-phosphate transferase	Sample_13.2_4	phage	p2	synonymous
DEL	contig_2	1250805	Δ1 bp	coding (14	wcaJ ←	UDP-glucose:undecaprenyl-phosphate glucose-1-phosphate transferase	Sample_14.2_5	phage	p2	frameshift
DEL	contig_2	1250805	Δ1 bp	coding (14	wcaJ ←	UDP-glucose:undecaprenyl-phosphate glucose-1-phosphate transferase	Sample_15.2_6	phage	p2	frameshift
INS	contig_2	1250692	+G	coding (25	wcaJ ←	UDP-glucose:undecaprenyl-phosphate glucose-1-phosphate transferase	Sample_22.3_4	phage	p3	frameshift
DEL	contig_2	1250691	Δ1 bp	coding (25	wcaJ ←	UDP-glucose:undecaprenyl-phosphate glucose-1-phosphate transferase	Sample_24.3_6	phage	p3	frameshift
DEL	contig_2	1250805	Δ1 bp	coding (14	wcaJ ←	UDP-glucose:undecaprenyl-phosphate glucose-1-phosphate transferase	Sample_4.1_4	phage	p1	frameshift
SNP	contig_2	1250757	G→C	P64R (CC(	wcaJ ←	UDP-glucose:undecaprenyl-phosphate glucose-1-phosphate transferase	Sample_6.1_6	phage	p1	synonymous

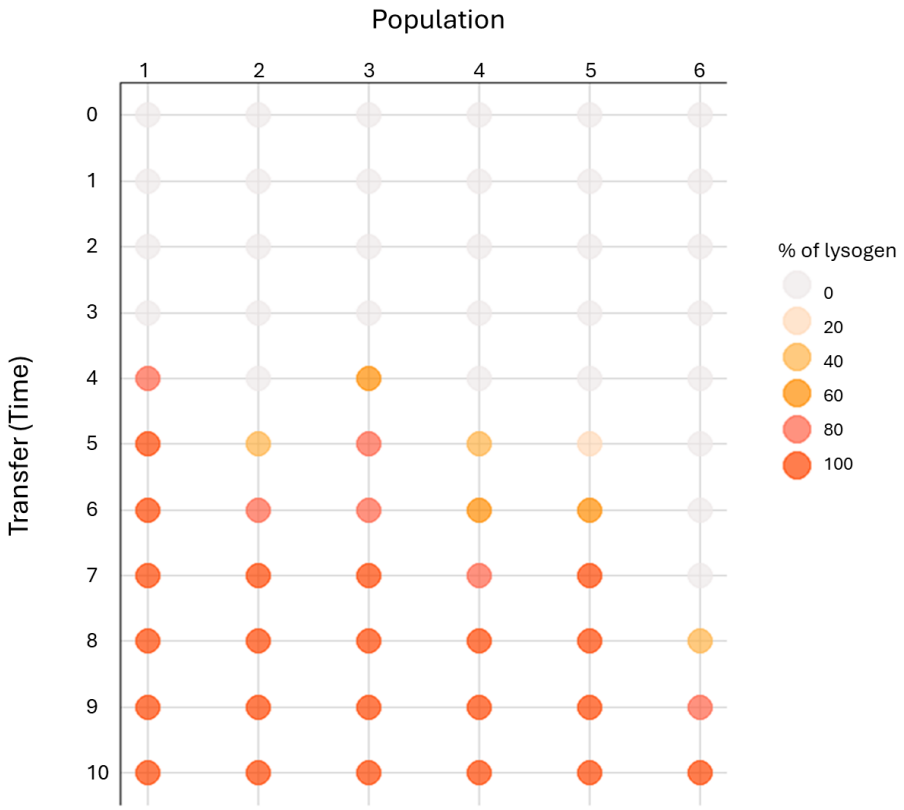

Figure S1: *Plot showing when each population of Rhizobia starts to display signs of phage integration. The orange point indicates that the phage is present in the rhizobia genomes. The plot displays up to 10 transfers out of 20, as the phage was present in all population after transfer 8.*

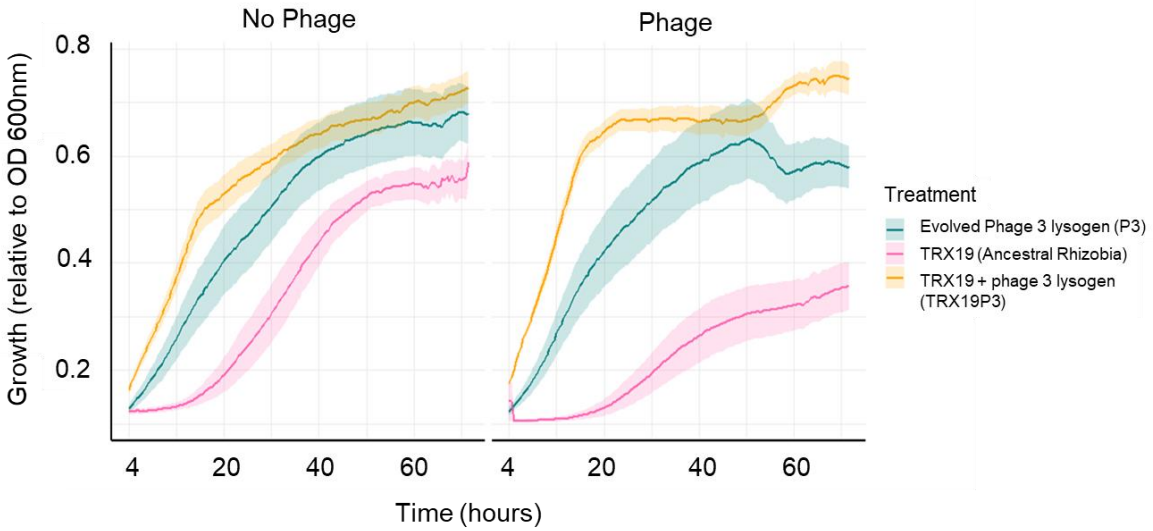

Figure S2*: Growth curve taken at OD600nm over 72 hours growth time; to see growth dynamics between the Evolved rhizobia with Phage 3 integrated (P3), the ancestral strain with integrated Phage 3 (TRX19+phage3), and the ancestral strain*

ANOVA and Tukey's HSD post hoc (where appropriate) were used to test the effects of Treatment, Phage presence and population on Area Under Curve (AUC). A linear mixed-effects model was fitted to the AUC data to look at interactions between Treatment and Phage presence (population as a mixed effect).

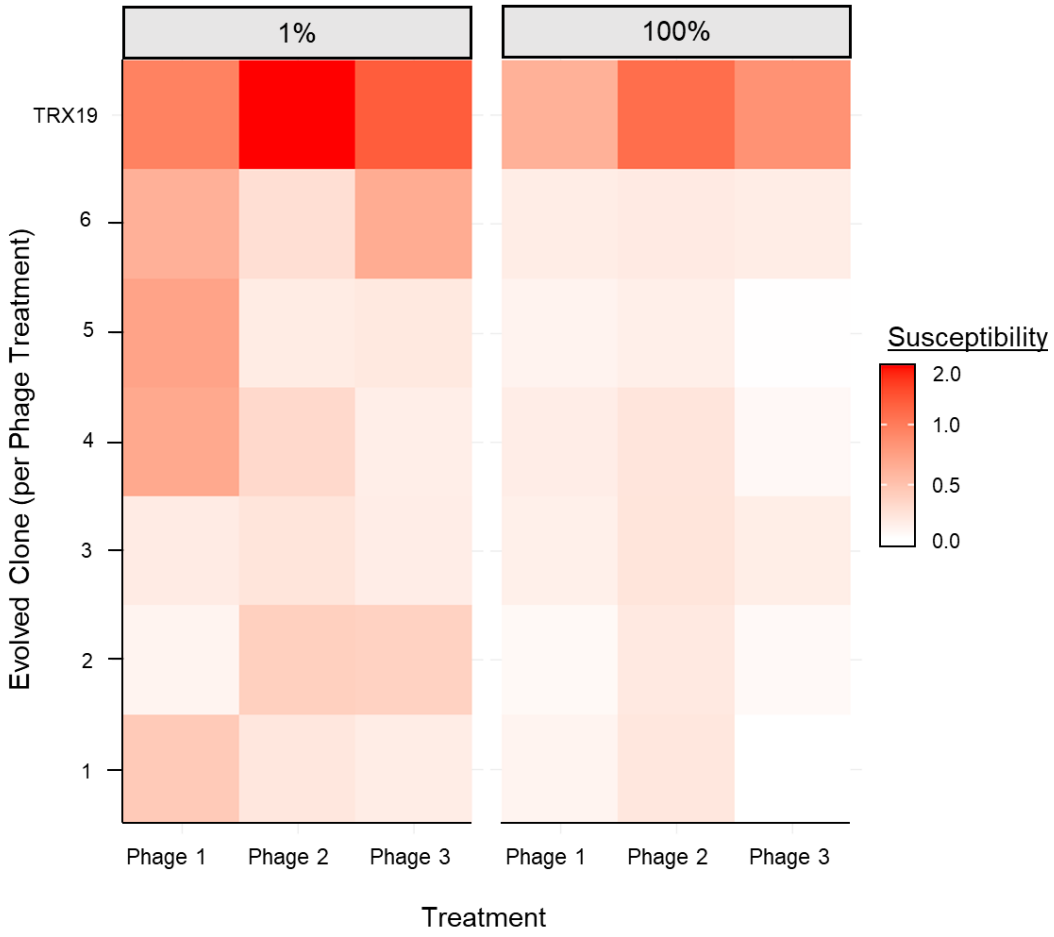

***Figure S3**: Heatmap showing bacterial susceptibility (measured as RBG) of evolved rhizobial clones from each phage treatment (Phage 1, Phage 2, Phage 3) when challenged with their respective ancestral phages under two nutrient conditions: 1% TY (low nutrient) and 100% TY (high nutrient). Each row represents a single evolved clone (labelled 1–6), tested against the phage it evolved with. The ancestral strain (TRX19) is included for reference to show baseline susceptibility to each phage.*

Each clone was tested in triplicate, and values shown represent the mean susceptibility score for each clone. Mixed-effects modelling revealed a significant effect of media concentration ($F(1,25) = 17.78$, $p < 0.001$), and a significant effect of phage treatment ($F(2,25) = 3.41$, $p = 0.049$.

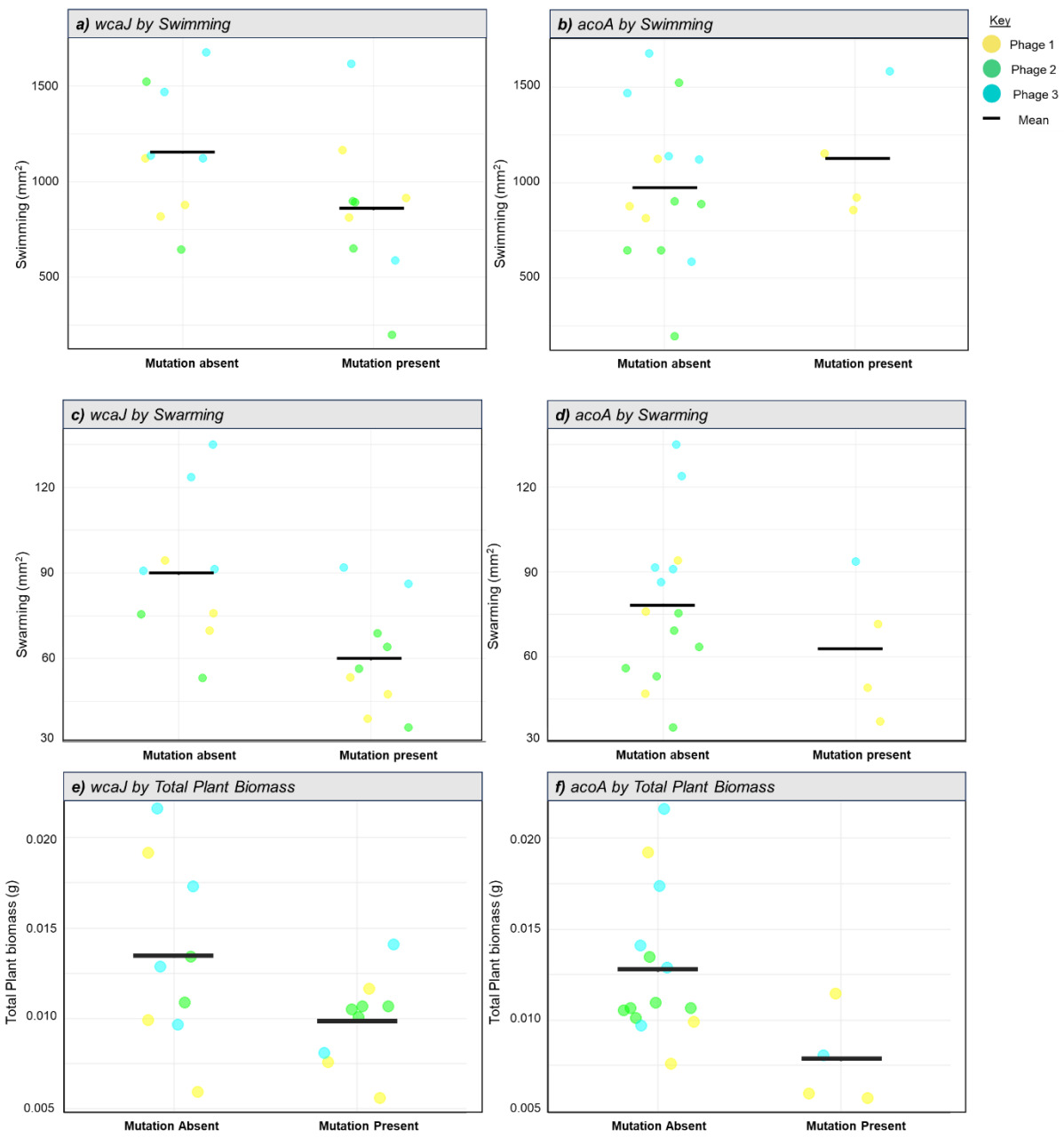

Figure S4: *T-test Comparison of Phenotype by Presence or Absence of mutations in the evolved clones of phage treatments, on the genes wacJ and acoA. Separated by Phage-only treatments, Phage 1 (yellow), Phage 2 (green) and Phage 3 (blue);* ***a)*** *Swimming and wacJ;* ***b)*** *Swimming and acoA;* ***c)*** *Swamring and wcaJ;* ***d)*** *Swarming and acoA. Where there is a * p=<0.05 and there is a significant difference between where the mutation is present for that phenotype;* ***e)*** *wcaJ and Total Plant Biomass (g)l;* ***f)*** *acoA and Total Plant Biomass (g).*

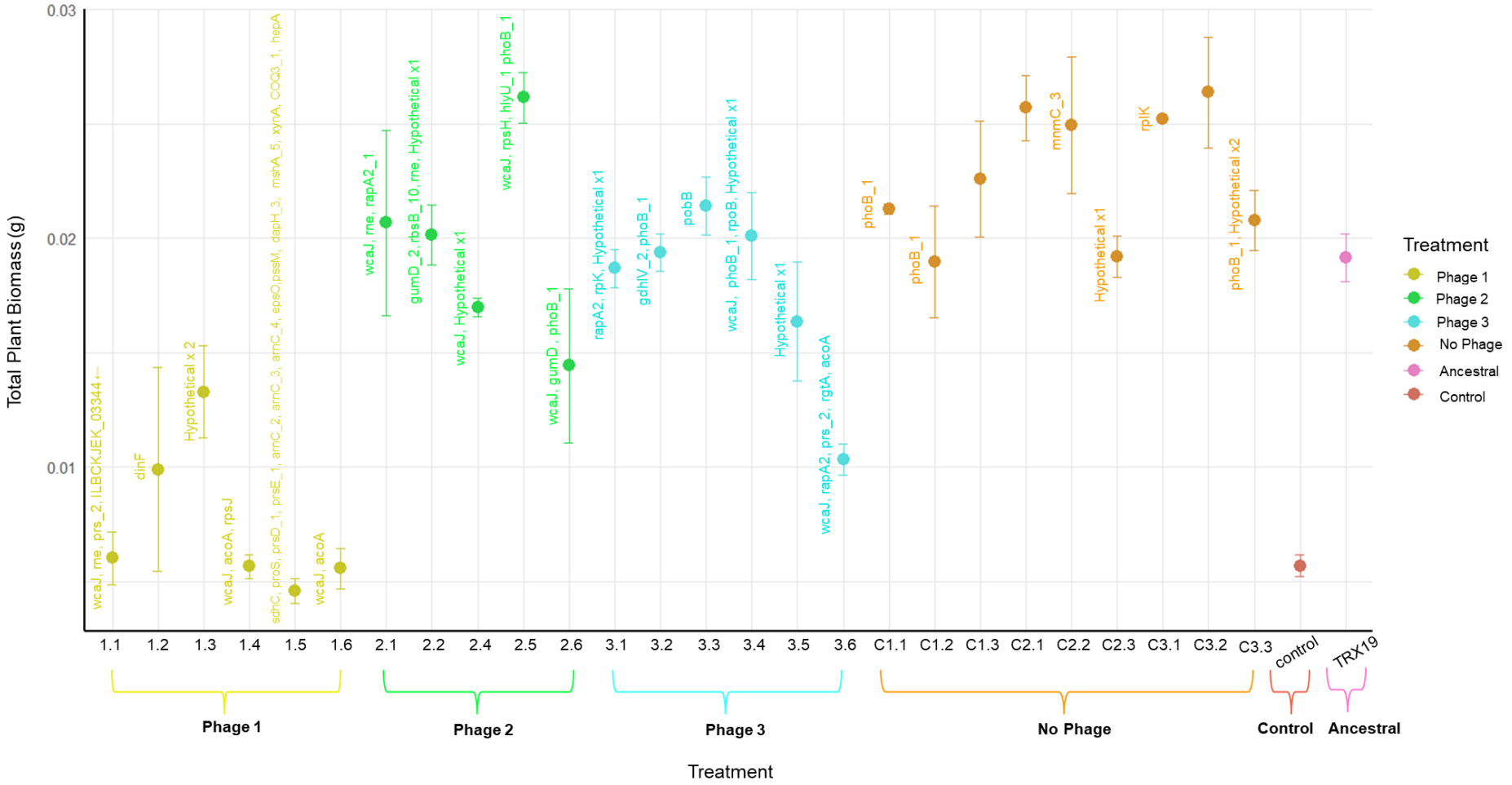

Figure S5: *The mean Total Plant biomass of each clone within each Treatment group. Written next to each clone is each gene-level mutation. A '*' is above each sample that has a mutation in 'wcaJ', and '**' is above each clone that has a mutation in 'acoA'.*

3.7. References

Bain, W. *et al.* (2024) 'In Vivo Evolution of a Klebsiella pneumoniae Capsule Defect With *wacJ* Mutation Promotes Complement-Mediated Opsonophagocytosis During Recurrent Infection', *The Journal of Infectious Diseases*, 230(1), pp. 209–220. Available at: https://doi.org/10.1093/infdis/jiae003.

Bates, D. *et al.* (2015) 'Fitting Linear Mixed-Effects Models Using lme4', *Journal of Statistical Software*, 67, pp. 1–48. Available at: https://doi.org/10.18637/jss.v067.i01.

Bowra, B.J. and Dilworth, M.J. (1981) 'Motility and Chemotaxis towards Sugars in Rhizobium leguminosarum', *Microbiology*, 126(1), pp. 231–235. Available at: https://doi.org/10.1099/00221287-126-1-231.

Chibani-Chennoufi, S. *et al.* (2004) 'Phage-host interaction: an ecological perspective', *Journal of Bacteriology*, 186(12), pp. 3677–3686. Available at: https://doi.org/10.1128/JB.186.12.3677-3686.2004.

Chung, I.-Y., Sim, N. and Cho, Y.-H. (2012) 'Antibacterial Efficacy of Temperate Phage-Mediated Inhibition of Bacterial Group Motilities', *Antimicrobial Agents and Chemotherapy*, 56(11), pp. 5612–5617. Available at: https://doi.org/10.1128/AAC.00504-12.

Coffey, B.M. and Anderson, G.G. (2014) 'Biofilm formation in the 96-well microtiter plate', *Methods in Molecular Biology (Clifton, N.J.)*, 1149, pp. 631–641. Available at: https://doi.org/10.1007/978-1-4939-0473-0_48.

Das, J. and Jha, G. (2020) 'Bacteriophages: co-evolving with bacteria to provide useful traits', *Polymorphism*, 4, pp. 72–82.

Deatherage, D.E. and Barrick, J.E. (2014) 'Identification of mutations in laboratory-evolved microbes from next-generation sequencing data using breseq', *Methods in Molecular Biology (Clifton, N.J.)*, 1151, pp. 165–188. Available at: https://doi.org/10.1007/978-1-4939-0554-6_12.

Dunn, M.F. (1998) 'Tricarboxylic acid cycle and anaplerotic enzymes in rhizobia', FEMS microbiology reviews, 22(2), pp. 105–123. Available at: https://doi.org/10.1111/j.1574-6976.1998.tb00363.x.

Feiner, R. *et al.* (2015) 'A new perspective on lysogeny: prophages as active regulatory switches of bacteria', *Nature Reviews. Microbiology*, 13(10), pp. 641–650. Available at: https://doi.org/10.1038/nrmicro3527.

Fernández, L. *et al.* (2017) 'Low-level predation by lytic phage phiIPLA-RODI promotes biofilm formation and triggers the stringent response in Staphylococcus aureus', *Scientific Reports*, 7(1), p. 40965. Available at: https://doi.org/10.1038/srep40965.

Ford, S. *et al.* (2021) 'Introducing a Novel, Broad Host Range Temperate Phage Family Infecting Rhizobium leguminosarum and Beyond', *Frontiers in Microbiology*, 12, p. 3375. Available at: https://doi.org/10.3389/fmicb.2021.765271.

Fu, Y., Li, Y. and Lidstrom, M. (2017) 'The oxidative TCA cycle operates during methanotrophic growth of the Type I methanotroph Methylomicrobium buryatense 5GB1', Metabolic Engineering, 42, pp. 43–51. Available at: https://doi.org/10.1016/j.ymben.2017.05.003.

Gillis, A. and Mahillon, J. (2014) 'Influence of lysogeny of Tectiviruses GIL01 and GIL16 on Bacillus thuringiensis growth, biofilm formation, and swarming motility', *Applied and Environmental Microbiology*, 80(24), pp. 7620–7630. Available at: https://doi.org/10.1128/AEM.01869-14.

Gurney, J. *et al.* (2020) 'Phage steering of antibiotic-resistance evolution in the bacterial pathogen, Pseudomonas aeruginosa', *Evolution, Medicine, and Public Health*, 2020(1), pp. 148–157. Available at: https://doi.org/10.1093/emph/eoaa026.

Hall, A.R., Scanlan, P.D. and Buckling, A. (2011) 'Bacteria-Phage Coevolution and the Emergence of Generalist Pathogens.', *The American Naturalist*, 177(1), pp. 44–53. Available at: https://doi.org/10.1086/657441.

Henriksen, K. *et al.* (2019) 'P. aeruginosa flow-cell biofilms are enhanced by repeated phage treatments but can be eradicated by phage-ciprofloxacin combination', *Pathogens and Disease*, 77(2), p. ftz011. Available at: https://doi.org/10.1093/femspd/ftz011.

Himpsl, S.D. et al. (2020) 'The oxidative fumarase FumC is a key contributor for E. coli fitness under iron-limitation and during UTI', PLOS Pathogens, 16(2), p. e1008382. Available at: https://doi.org/10.1371/journal.ppat.1008382.

Hosseinidoust, Z., Tufenkji, N. and van de Ven, T.G.M. (2013) 'Formation of biofilms under phage predation: considerations concerning a biofilm increase', *Biofouling*, 29(4), pp. 457–468. Available at: https://doi.org/10.1080/08927014.2013.779370.

Howieson, J.G. and Dilworth, M.J. (no date) 'Working with rhizobia'.

Imamovic, L. *et al.* (2016) 'Heterogeneity in phage induction enables the survival of the lysogenic population', *Environmental Microbiology*, 18(3), pp. 957–969. Available at: https://doi.org/10.1111/1462-2920.13151.

Knöppel, A. *et al.* (2018) 'Genetic Adaptation to Growth Under Laboratory Conditions in Escherichia coli and Salmonella enterica', *Frontiers in Microbiology*, 9. Available at: https://doi.org/10.3389/fmicb.2018.00756.

Koskella, B. *et al.* (2011) 'Using experimental evolution to explore natural patterns between bacterial motility and resistance to bacteriophages', *The ISME Journal*, 5(11), pp. 1809–1817. Available at: https://doi.org/10.1038/ismej.2011.47.

Kwong, W.K., Zheng, H. and Moran, N.A. (2017) 'Convergent evolution of a modified, acetate-driven TCA cycle in bacteria', Nature Microbiology, 2, p. 17067. Available at: https://doi.org/10.1038/nmicrobiol.2017.67.

Latino, L. *et al.* (2019) 'Investigation of Pseudomonas aeruginosa strain PcyII-10 variants resisting infection by N4-like phage Ab09 in search for genes involved in phage adsorption', *PLOS ONE*, 14, p. e0215456. Available at: https://doi.org/10.1371/journal.pone.0215456.

MacLean, A., Legendre, F. and Appanna, V.D. (2023) 'The tricarboxylic acid (TCA) cycle: a malleable metabolic network to counter cellular stress', Critical Reviews in Biochemistry and Molecular Biology, 58(1), pp. 81–97. Available at: https://doi.org/10.1080/10409238.2023.2201945.

Maluk, M. *et al.* (2022) 'Fields with no recent legume cultivation have sufficient nitrogen-fixing rhizobia for crops of faba bean (Vicia faba L.)', *Plant and Soil*, 472(1), pp. 345–368. Available at: https://doi.org/10.1007/s11104-021-05246-8.

Mary Eliza, (2023) ' *Utilizing the soil microbiome for sustainable agriculture in the UK: Drawing from rhizobial inoculants and farmer knowledge'*, PhD, University of Sheffield.

Mendoza-Suárez, M.A. *et al.* (2020) 'Optimizing Rhizobium-legume symbioses by simultaneous measurement of rhizobial competitiveness and N2 fixation in nodules', *Proceedings of the National Academy of Sciences of the United States of America*, 117(18), pp. 9822–9831. Available at: https://doi.org/10.1073/pnas.1921225117.

Miller, L.D. *et al.* (2007) 'The major chemotaxis gene cluster of Rhizobium leguminosarum bv. viciae is essential for competitive nodulation', *Molecular Microbiology*, 63(2), pp. 348–362. Available at: https://doi.org/10.1111/j.1365-2958.2006.05515.x.

Ottemann, K.M. and Miller, J.F. (1997) 'Roles for motility in bacterial-host interactions', *Molecular Microbiology*, 24(6), pp. 1109–1117. Available at: https://doi.org/10.1046/j.1365-2958.1997.4281787.x.

Parker, D.J., Demetci, P. and Li, G.-W. (2019) 'Rapid Accumulation of Motility-Activating Mutations in Resting Liquid Culture of Escherichia coli', *Journal of Bacteriology*, 201(19), pp. e00259-19. Available at: https://doi.org/10.1128/JB.00259-19.

Paterson, S. *et al.* (2010) 'Antagonistic coevolution accelerates molecular evolution', *Nature*, 464(7286), pp. 275–278. Available at: https://doi.org/10.1038/nature08798.

Simmons, E.L. *et al.* (2020) 'Biofilm Structure Promotes Coexistence of Phage-Resistant and Phage-Susceptible Bacteria', *mSystems*, 5(3), pp. e00877-19. Available at: https://doi.org/10.1128/mSystems.00877-19.

Song, L. *et al.* (2021) 'Phage Selective Pressure Reduces Virulence of Hypervirulent Klebsiella pneumoniae Through Mutation of the wzc Gene', *Frontiers in Microbiology*, 12. Available at: https://doi.org/10.3389/fmicb.2021.739319.

Soto, M.J., Sanjuan, J. and Olivares, J. (2001) 'The disruption of a gene encoding a putative arylesterase impairs pyruvate dehydrogenase complex activity and nitrogen fixation in Sinorhizobium meliloti', Molecular plant-microbe interactions: MPMI, 14(6), pp. 811–815. Available at: https://doi.org/10.1094/MPMI.2001.14.6.811.

Tambalo, D.D., Yost, C.K. and Hynes, M.F. (2010) 'Characterization of swarming motility in Rhizobium leguminosarum bv. viciae', *FEMS microbiology letters*, 307(2), pp. 165–174. Available at: https://doi.org/10.1111/j.1574-6968.2010.01982.x.

Tan, D. *et al.* (2020) 'A Frameshift Mutation in *wacJ* Associated with Phage Resistance in Klebsiella pneumoniae', *Microorganisms*, 8(3), p. 378. Available at: https://doi.org/10.3390/microorganisms8030378.

Tremblay, J. *et al.* (2007) 'Self-produced extracellular stimuli modulate the Pseudomonas aeruginosa swarming motility behaviour', *Environmental Microbiology*, 9(10), pp. 2622–2630. Available at: https://doi.org/10.1111/j.1462-2920.2007.01396.x.

Unkovich, M. and Baldock, J. (2008) 'Measurement of asymbiotic N2 fixation in Australian agriculture', *Soil Biology and Biochemistry*, 40(12), pp. 2915–2921. Available at: https://doi.org/10.1016/j.soilbio.2008.08.021.

Wickham H, Averick M, Bryan J, Chang W, McGowan LD, François R, Grolemund G, Hayes A, Henry L, Hester J, Kuhn M, Pedersen TL, Miller E, Bache SM, Müller K, Ooms J, Robinson D, Seidel DP, Spinu V, Takahashi K, Vaughan D, Wilke C, Woo K, Yutani H (2019). "Welcome to the tidyverse." *Journal of Open Source Software*, **4**(43), 1686. doi:10.21105/joss.01686.

Zheng, H. *et al.* (2015) 'Flagellar-dependent motility in Mesorhizobium tianshanense is involved in the early stage of plant host interaction: study of an flgE mutant', *Current Microbiology*, 70(2), pp. 219–227. Available at: https://doi.org/10.1007/s00284-014-0701-x.

Chapter 4: Refuge Impact on Population Dynamics in Free-living Disease Systems

4.1 Abstract

Refuges play an important role in shaping population dynamics by providing protection against external threats. While the influence of refuges on predator-prey systems is well-established, their impact on disease dynamics in systems with free-living parasites, remains largely unexplored. Similar to predator-prey interactions, disease systems involving environmentally acquired infections (i.e., free-living parasites) can promote stable population fluctuations. In this study, we explore the consequences of a refuge for susceptible individuals from disease on population dynamics and disease transmission. We develop a model based on a Susceptible-Infected (SI) framework, incorporating a free-living parasite population and a refuge accessible only to susceptible hosts. Our results demonstrate that refuges can both suppress and amplify disease outbreaks, depending on a critical refuge threshold. By offering insights into disease management and enhancing our understanding of parasite transmission in isolated systems, this research contributes to the broader understanding of ecological systems and has practical implications for public health and conservation.

4.2 Introduction

Disease outbreaks hinge on complex interactions between hosts, infectious agents, and the environment. A crucial element in these dynamics are the free-living stages of parasites, where the pathogens exist outside their hosts during transmission (McCallum, Barlow and Hone, 2001). Despite often appearing passive, these stages exert a substantial influence on the relationship of transmission cycles and population fluctuations, ultimately shaping disease outbreaks. Theoretical models incorporating the dynamics of this free-living phase reveal feedback loops that drive these fluctuations, often leading to stable negative frequency/density dependant cycles within the host and parasite populations (Anderson and May, 1981; Briggs *et al.*, 1995). High infection rates drive reductions in host availability, resulting in fewer free-living transmission stages being able to find hosts. Reduced infections then allow for host recovery, which can be exploited by the parasite (Otten, Bailey and Gilligan, 2004). This pattern can be observed for diverse parasites from soil-borne, spore-forming fungal pathogens to aquatic parasites with free-swimming larval stages, such as trematodes (Lafferty *et al.*, 2015). This cyclic pattern underscores the critical role of the free-living stage in driving disease dynamics.

Models typically assume a homogenous exposure to free-living parasites, however, the presence of refuges, allowing hosts to temporarily escape parasite infection, are likely to disrupt these cycles. For example, freshwater mussels burrow into the sediment to escape encounters with parasitic trematodes using the sediment as a physical refuge that the parasite cannot enter (Vaughn and Hakenkamp, 2001). Other similar examples include newts exposed to with the deadly fungal disease chytridiomycosis, which seek out drier terrestrial habitats that are uninhabitable for the disease (Daversa *et al.*, 2018). Beyond these behavioural adaptations, refuges can also emerge from biological structures. Microbial biofilms, for example, act as protective shelters for microorganisms by providing physical barriers, concentrating nutrients, and offering chemical protection against harmful substances like antibiotics or predation from bacteriophages (Costerton, Stewart and Greenberg, 1999; López,

Vlamakis and Kolter, 2010). Symbiosis itself can act as a refuge in certain systems; for instance, bio-eroding sponges harbour symbiotic algae (Symbiodinium) within their tissues. These algae are vital for the sponge's health and survival (Schoenberg and Ortiz, 2009), and in return offer the algae protection them from predators and harmful bacteria (Cervino *et al.*, 2004); Cohen *et al*., 2023) . Likewise, the legume symbiosis with Rhizobia occurs within protected root nodules, where the bacteria fix nitrogen in exchange for nutrients and protection e.g. from bacteriophages in the soil (Van Cauwenberghe *et al.*, 2021). Additionally, refuges are not always spatial; they can also arise from life stages or physiological changes. For example, some amphibians, such as tree frogs, avoid infections by periodically shedding their skin, effectively removing fungal pathogens like Batrachochytrium dendrobatidis (Bd) before they can cause severe disease (Rollins-Smith, Reinert and Burrowes, 2015).This physiological adaptation serves as a biological refuge by temporarily reducing infection risk, similar to spatial refuges that limit pathogen exposure. By providing shelter from external threats, refuges can profoundly alter the relationship between susceptible populations and those that predate, prey on, or parasitize them. Currently, we have little understanding of how these types of refuges within a free-living disease system can affect population dynamics.

Previous models, primarily exploring predator-prey interactions, have investigated the impact of refuges on prey survival rates and predator-prey interactions. Collectively, these studies have shown that a refuge can have a stabilizing effect on populations by providing a safe haven for prey when predator populations are high (Hassell and May, 1973). This reduces predation pressure, allowing the prey population to recover and eventually dampen the peak predator population in the next cycle. Early attempts to model refuge effects often relied on a single parameter, such as the proportion of the prey population the refuge could hold. This simplistic approach limited the ability to capture the nuances of refuge use. Later models incorporated more nuanced mechanisms, including the level of predation risk reduction within the refuge, the number of individuals the refuge can accommodate (refuge capacity), and its accessibility to both prey and(Oaten and Murdoch, 1975; Ruxton, 1995). Studies showed that

refuges with higher levels of protection from predators and restricted access for predators compared to prey could significantly dampen population cycles and optimize the refuge's effectiveness in stabilizing populations (Murdoch, Chesson and Chesson, 1985; Holt and Hochberg, 1997).

While previous studies have explored the role of refuges in predator-prey dynamics, their effects on disease systems, especially those involving free-living parasites, remain underexplored. The primary aim of this chapter is to use a theoretical model to explore how a refuge, accessible only to susceptible hosts, alters the population dynamics of a host-parasite system driven by a free-living parasite. Most existing models assume homogenous exposure to free-living parasites and do not account for how dynamic susceptible host movement into and out of refuges alters infection patterns.

We hypothesize that refuges are not inherently stabilizing. Instead, we predict that a refuge's impact will be conditional on its properties, specifically: (1) low movement rates will stabilize host-parasite cycles and reduce disease prevalence, but (2) high movement rates or large refuge capacities will paradoxically amplify outbreaks by creating a protected reservoir of susceptible hosts that are periodically released. Our study addresses this gap by explicitly modelling movement to and from the refuge, allowing us to determine the conditions under which refuges stabilize populations, promote equilibrium, or unexpectedly amplify disease outbreaks.

4.3 Methods

To investigate how refuges affect host-parasite dynamics in a system with a free-living parasite population, we constructed a model based on an S-I (Susceptible-Infected) framework, where the host population consists of susceptible (S) and infected (I) individuals. We extend this model by incorporating a free-living parasite population (P) and a refuge population (R), which represents the subset of susceptible individuals that move into the refuge. While individuals enter the refuge from the susceptible population, the refuge population has its own growth

dynamics, with a defined growth rate and carrying capacity. In this scenario, the refuge is spatial, and only susceptible individuals can enter, where they are protected from infection by free-living parasites.

The SI model with free-living parasite can be shown as:

$$\frac{dS}{dt} = r\left(1 - \frac{S+I}{k}\right)(S + fI) - cS - \beta SP)$$

$$\frac{dI}{dt} = \beta SP - cI - \gamma I$$

$$\frac{dP}{dt} = \gamma nI - bP$$

The susceptible (*S*) population has a growth rate of *r,* with a carrying capacity of *k*, and all susceptible (*S*) and infected (*I*) die at a natural rate of *c.* The infection is spread by direct contact between susceptible and the parasite (*P*) population with coefficient *β*, and the infected hosts will die at an additional accelerated death of *γ*, infected hosts cannot recover. In this system when infected hosts die at an accelerated death due to the infection, this directly increases the parasite population by *n*. Natural parasite death is represented by *b*.

Additionally, we included the effect of infected individuals on the density of the susceptible population. This is captured in the term $r\left(1 - \frac{S+I}{k}\right)(S + fI)$ which describes the combined contribution of both susceptible and infected individuals to the overall growth of the susceptible population. The parameter f represents the fecundity rate of infected individuals compared to the susceptibles, specifically describing the extent to which infected individuals can still contribute to the population growth by producing susceptible offspring. Initially, we assume f=0, meaning that infected individuals do not reproduce and do not contribute to the production of new susceptibles. However, in further model analyses, this parameter was adjusted to explore scenarios where infected individuals maintain some reproductive capacity. This assumes that in some scenarios infection does not necessarily result in complete sterility

and that offspring of infected individuals are born uninfected, which aligns with disease systems where vertical transmission is absent or negligible.

We then added a separate equation for the refuge population.

The SI model with free-living parasite and the addition of the refuge (R) can be shown as:

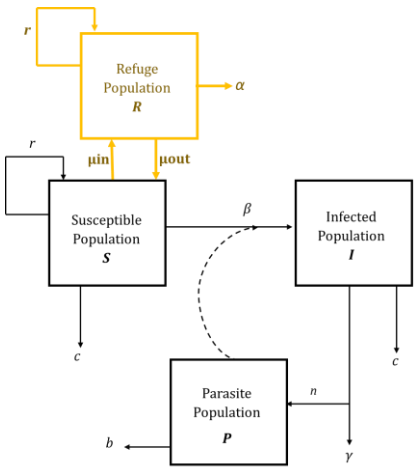

$$\frac{dS}{dt} = r\left(1 - \frac{S+I}{k}\right)(S + fI) - cS - \beta SP - \boldsymbol{\mu_{in}S + \mu_{out}R}$$

$$\frac{dI}{dt} = \beta SP - cI - \gamma I$$

$$\frac{dP}{dt} = \gamma nI - bP$$

$$\boldsymbol{\frac{dR}{dt} = r\left(1 - \frac{R}{m}\right)R + \mu_{in}S - \mu_{out}R - \alpha R}$$

***Figure 1**: Schematic of the SI , and free living model with a refuge.*

Here, the refuge (*R*) population has a growth rate *r*, which is assumed to be the same as for the external susceptible population, and a carrying capacity *m*. The refuge population experiences a natural death rate *α*. The rate at which susceptible individuals move into the refuge is represented by μ_{in}, while μ_{out} denotes the rate at which individuals leave the refuge and return to the susceptible population outside. Unlike in some predator-prey systems, where refuge use is often behaviourally adaptive, movement in our model is entirely passive and biologically constrained, meaning individuals do not adjust their refuge use in response to parasite prevalence. These rates reflect the speed/frequency at which individuals from the susceptible population migrate to and from the refuge. Both movement rates (μ_{in} *and* μ_{out}) are assumed to be completely passive, where there is no choice or decision to enter a refuge based on infection prevalence.

To investigate the impact of refuges on population dynamics in an isolated free-living disease system, we simulated host-parasite dynamics under different conditions. The default parameters used for these simulations are outlined in **Table 1**, and additional analyses were conducted to examine the effects of varying key parameters on population cycling and equilibrium states.

***Table 1**: Default parameters used in the model to obtain results for each figure, unless stated otherwise. Units: Rates (r, c, γ, b, μin, μout, α) are per unit time. Population sizes (S, I, P, R) and carrying capacities (k, m) are measured in individuals. The infection rate (β) has units of 1 / (time × individuals). n is unitless and represents the number of parasites released per infected death. f is the relative fecundity of infected hosts compared to susceptibles.*

Parameter	Description	**Default value**
S	Susceptible Population	
I	Infected Population	
P	Parasite Population	
R	Refuge Population	
r	Growth rate	2
c	Natural host death rate	1
β	Infection from exposure	0.02
γ	Infection induced death rate	0.3
n	Parasite growth	5
k	Carrying capacity	1000
b	Natural parasite 'death'	0.3
μ_{in}	Movement rate of susceptible hosts into the refuge	0.01
μ_{out}	Movement rate of susceptible host out of the refuge	0.01
α	Natural host death in the refuge	1
m	Carrying capacity of refuge	1000
f	Fecundity of infected individuals	0

4.4 Results

We find that the presence of a refuge significantly alters host-parasite population dynamics, shifting the system from cyclic fluctuations to equilibrium under certain conditions. When no refuge is present, host and parasite populations exhibit sustained oscillations, whereas the introduction of a refuge disrupts these cycles, leading to stabilization. However, as movement rates increase, cyclic dynamics re-emerge. Below, we examine how different movement rates and refuge characteristics shape these outcomes.

Figure 2a illustrates that with no refuge present ($\mu_{in} = 0$, $\mu_{out} = 0$), the free-living parasite stage drives cyclic population fluctuations. While the parasite population initiates these cycles, it also indirectly regulates them by limiting host availability at peak infection times, preventing extreme outbreaks or collapses. As a result, the system remains in a fluctuating but constrained dynamic state rather than reaching equilibrium. However, introducing a refuge (**Figure 2b**, $\mu_{in} = 0.01$, $\mu_{out} = 0.01$), dramatically alters this dynamic shifting it from cycling to equilibrium. Increasing movement rates further reintroduces cyclic patterns, as seen in **Figure 2c** ($\mu_{in} = 1$, $\mu_{out} = 3$), where peaks in the susceptible population precede parasite peaks, typical of host-parasite interactions. The population in the refuge also follows these cycles, peaking just after the susceptible population as individuals move into the refuge, temporarily reducing the pool of exposed susceptibles. This suggests that higher movement rates between the refuge and the main population push the system beyond the stabilizing effects observed at lower rates, restoring cyclic dynamics.

Exploring a wider parameter space for μ_{in} and μ_{out} reveals distinct thresholds separating regions of equilibrium from cycling (**Figure 2e**). The transition between these states is not solely dependent on one movement parameter but on their interaction. When μ_{out}: remains sufficiently low, equilibrium is maintained regardless of $\mu in.$ However, at extremely low values of μ_{in} cycles persist regardless of μ_{out} (**Figure 2f**). At higher μ_{out} values, the sensitivity to μ_{in} increases (**Figure 2e**), leading to shifts in cycle dynamics. For example, when μ_{out} is high and μ_{in} is low (illustrated by **Figure 2c**), the time between disease cycles is reduced. In contrast,

when both μ_{out} and μ_{in} are high, the system experiences larger amplitude disease cycles, corresponding to more intense outbreaks (**Figure 2d**).

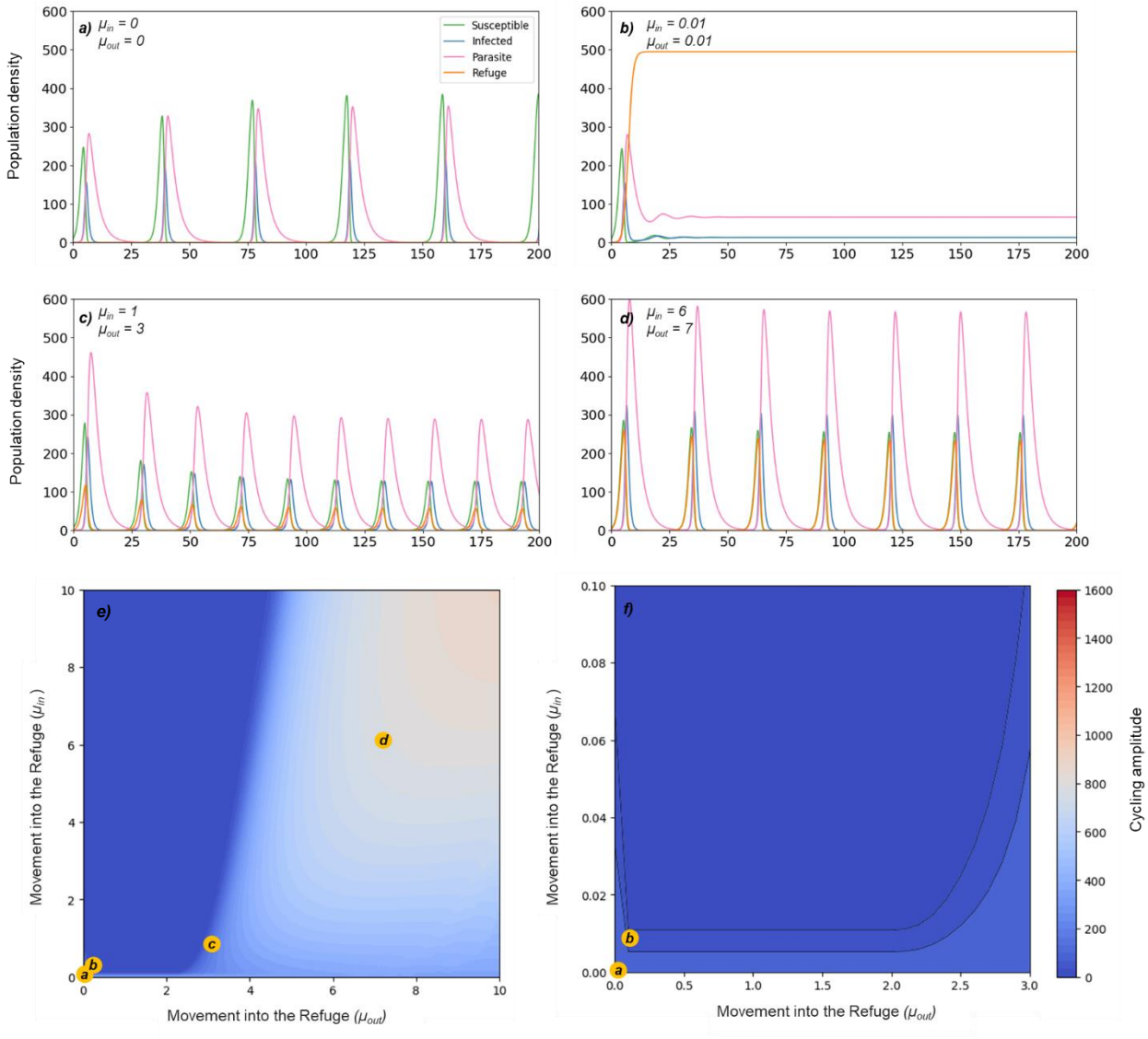

***Figure 2**: Time course of the model with varying μin and μout values. **a)** A time course of the dynamics between susceptible, free-living parasite and infected populations with no refuge, μin = 0 and μout = 0. **b)** A time course with the refuge added showing equilibria, where susceptible individuals can move at a rate of μin = 0.01 and μout = 0.01. **c)** where μin = 1 and μout = 3. **d)** where μin =6, μout = 7. **e)** A heatmap depicting the intensity of cycles within the free-living parasite population as the parameters are varied for μin and μout. The above time courses **(a-d)** are also shown for their corresponding μin and μout parameters. **f)** A zoomed-in section of the heatmap clearly showing that cycles persist at very low rates of μin and μout.*

All heatmaps presented in this study use a consistent colour scale to facilitate direct comparison across figures; therefore, some individual heatmaps do not utilize the entire colour range displayed.

Tracking the average prevalence of infection across varying rates of μ_{in} and μ_{out} shows that at low (but non-zero) μ_{in}, infection prevalence remains high, regardless of μ_{out} (**Figure 3**). This indicates that when movement into the refuge is minimal, infection persists even as μ_{out} increases. This pattern holds whether the system follows a limit cycle (high μ_{out}) or remains at a point equilibrium (low μ_{out}) (**Figure 2e**). As μ_{in} increases, the prevalence of infection decreases, even if μ_{out} stays low. This likely occurs because more susceptible individuals enter the refuge, reducing the number of hosts available for infection in the main population. Additionally, when μ_{out} is low, individuals that enter the refuge remain there for longer periods, reinforcing the stabilizing effect by further reducing the pool of susceptibles available for transmission. In contrast, when μ_{out} is high and μ_{in} is low, infection prevalence remains high because susceptibles are frequently reintroduced into the population without being removed into the refuge in sufficient numbers (**Figure 3**). However, when both μ_{in} and μ_{out} are high, the overall infection prevalence remains lower than in the no-refuge scenario, even though the system exhibits more intense population cycling (**Figure 2e**). While it might initially seem that high μ_{out} would increase infection prevalence by returning more susceptibles to the main population, the dynamics reduce overall disease prevalence because the continual flow of individuals into and out of the refuge limits the time susceptibles spend exposed to infection, leading to a net reduction in new infections.

It is important to note that the frequency and intensity of disease cycles do not always correlate directly with long-term infection prevalence. Although larger outbreaks can occur when μ_{out} is high, the average infection prevalence (**Figure 3**) is moderated by the fraction of susceptibles that remain in the refuge at any given time. The movement between refuge and non-refuge populations results in a net reduction in the number of infected individuals per unit time, which, in turn, decreases overall disease prevalence compared to the no-refuge case.

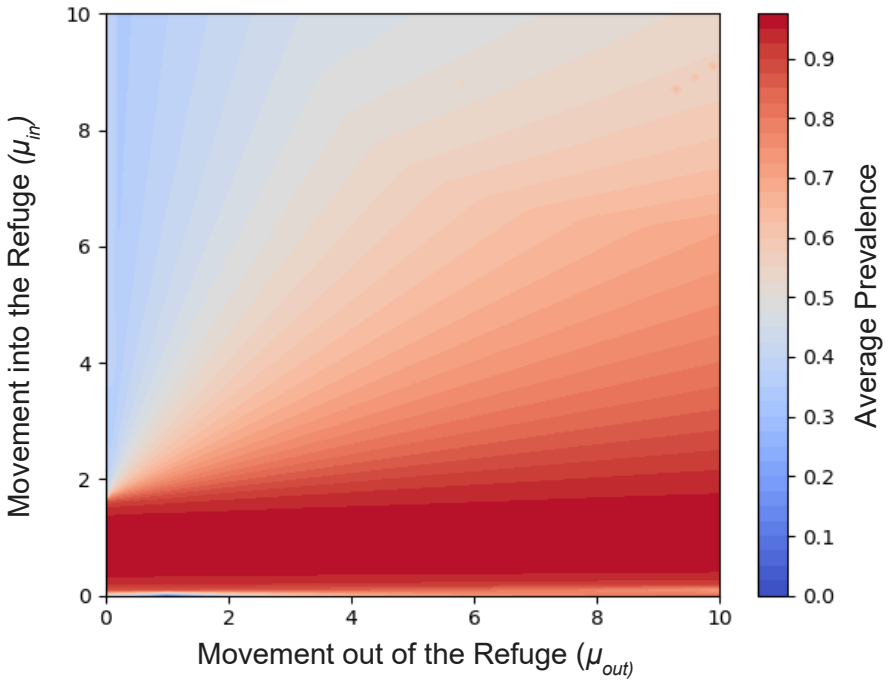

***Figure 3**: Heatmap showing the average prevalence of the parasite population as the movement rates of susceptibles into (μin) and out of (μout) the refuge are varied. The colour gradient represents the average infection prevalence, with blue indicating low prevalence and red indicating high prevalence.*

While refuges are typically thought to offer protection to susceptible populations, exceeding certain thresholds in movement rates (μ_{in} and μ_{out}) can diminish the refuge's protective effect. At very high movement rates, the refuge ceases to function as a true refuge, as susceptibles spend little time sheltered from infection before re-entering the main population. To better understand how refuge properties shape these dynamics, we explored the impact of refuge size, measured by its carrying capacity (m), on population cycling and disease prevalence.

Figure 4 illustrates how refuge size influences population dynamics and cycling intensity. Refuge size has a substantial effect on both the cycling threshold and the severity of outbreaks, as seen in **Figure 4c** (m = 5000), larger refuges lead to more intense disease cycles, particularly when susceptible individuals can easily move into the refuge (high μ_{in}). In contrast, smaller refuges (**Figure 4a**, m = 50) promote equilibrium across a broader range of movement parameters (μ_{in} and μ_{out}), suggesting that smaller refuges can help stabilize populations more effectively. This pattern is likely due to the fact that larger refuges not only shelter more susceptible but can also act as a source population when movement out of the

refuge is high. A highly productive refuge can replenish susceptibles in the main population, indirectly increasing the availability of hosts for infection, thereby sustaining or even intensifying parasite outbreaks. This dynamic resembles predator-prey systems where an abundant prey refuge can fuel predator persistence by supporting periodic prey release.

Further investigation (**Figure S1**) suggests that increased host mortality due to infection also contributes to greater fluctuations. When infected individuals experience higher mortality, disease cycles become more pronounced, whereas lower infected mortality rates promote stability across a wider range of movement conditions. This finding suggests that both refuge size (as a proxy for habitat productivity) and infection-related mortality shape host-parasite stability. Under certain conditions, larger refuges and higher infected mortality rates can amplify population fluctuations rather than suppress them. These results emphasize that refuges are not inherently stabilizing; rather, their effects depend on movement rates, mortality, and how the refuge functions as a population source or sink.

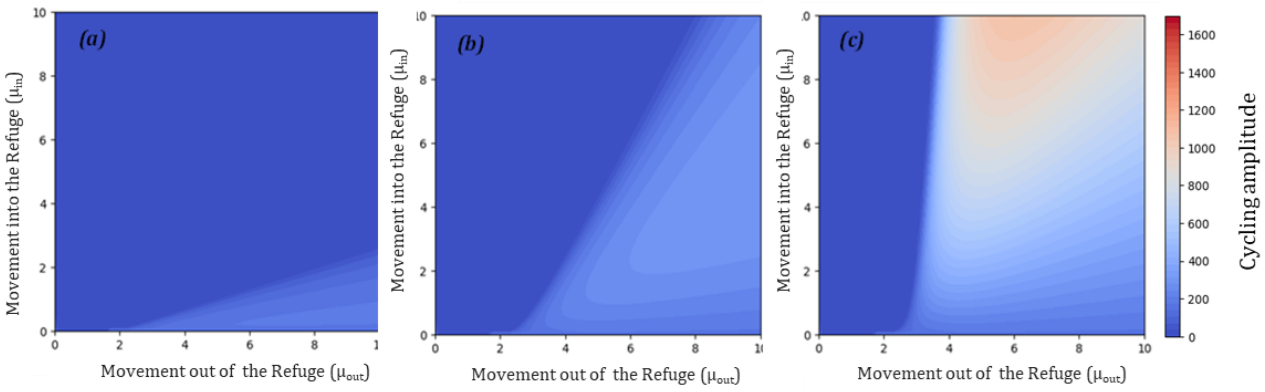

***Figure 4**: **(a-c)** Showing what happens to the threshold of when populations stop/start cycling, when varying the carrying capacity of the refuge m. The colour bar indicates the population density, where there is dark blue at 0 there is no cycling, the redder colours show the intensity of the cycles. Where **a)** m = 50, **b)** m = 500, **c)** m = 5000.*

Since population recovery is also influenced by how infected individuals contribute to the growth of the susceptible population, we examined the role of fecundity in parasite dynamics. Overall host fecundity is determined by the sum of population growth in the susceptible class and the additional contribution from infected individuals, represented as fI. Changes in

fecundity affect how quickly the susceptible population can rebound and how this, in turn, influences infection cycles.

Figure 5 illustrates how varying the fecundity rates (f) of the infected population affects system dynamics. When fecundity is low but non-zero (f =0.1)(**Figure 5a**), the system exhibits noticeable cycles, suggesting that when the infected individuals contribute minimally to the growth of the susceptible population, population fluctuations remain prominent (as seen in **Figure 2**. As the fecundity increases (**Figure 5b** and **5c**, f = 0.2, f = 0.3), the cycles diminish, leading to more stable equilibrium state. This stabilization is likely due to the increased replenishment of susceptibles, which offsets losses due to infection. However, while higher fecundity compensates for population declines, it could also increase the pool of susceptibles available for infection, which in some scenarios might sustain or even amplify cycling. The net effect depends on the balance between host replenishment and parasite transmission dynamics. More generally, if infected individuals retain the ability to contribute to overall population growth, the system may become more resilient to population crashes, promoting stability under certain conditions. However, this effect is contingent on whether the rate of new infections remains lower than the replenishment of susceptibles. This highlights the dual role of infected host fecundity in shaping host-parasite population dynamics.

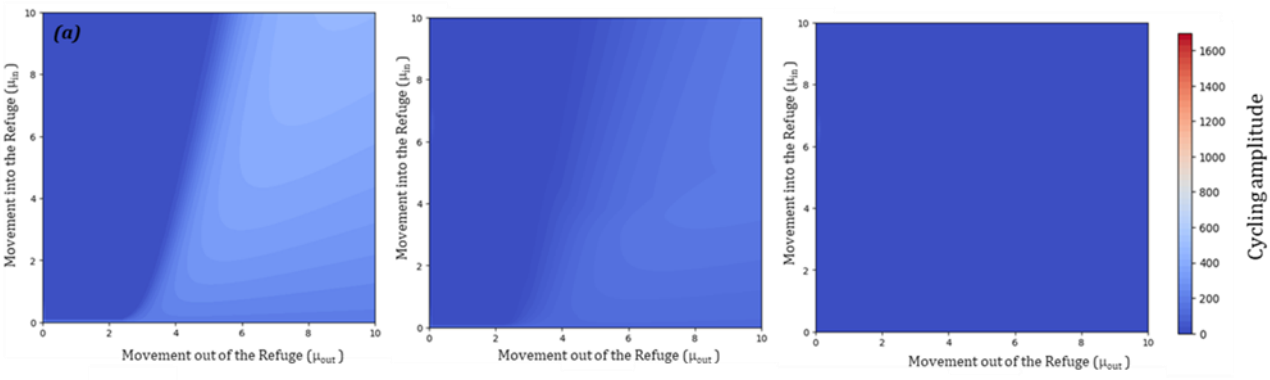

Figure 5: (a-c) *Showing what happens to the threshold of when the fecundity (f) of the infected population is affected by infection. Fecundity (f) represents the rate at which infected individuals contribute to the growth of the susceptible population. It is a ratio relative to the growth rate of the susceptible population. The colour bar indicates the population density, where there is dark blue at 0, there is no cycling; the redder colours show the intensity of the cycles. Where;* ***a)*** *f = 0.1;* ***b)*** *f = 0.2;* ***c)*** *= 0.3.*

While larger refuges and unrestricted movement may offer protection, they can also lead to amplified outbreaks under certain conditions. Similarly, managing movement rates and refuge accessibility becomes critical, particularly when parasite pressure is low, to avoid destabilizing population dynamics. These findings highlight the complex nature of refuge effects, which, under certain thresholds, can lead to counterintuitive outcomes like intensified outbreaks. Careful consideration of refuge size, movement patterns, and host fecundity is crucial when applying refuges in disease mitigation strategies.

4.5 Discussion

This study investigated the impact of a refuge for susceptible hosts on population dynamics in a system with a free-living parasite, using a Susceptible–Infected (SI) model that differentiates between susceptible hosts in the main population, infected hosts, and susceptible hosts within a refuge. The model was inspired by the rhizobia–phage system, where rhizobia can inhabit protective root nodules that temporarily shield them from phage infection. We simulate movement between host states, where susceptible individuals can transition into and out of the refuge but are protected from infection while inside.

Our results demonstrate that refuges can both stabilize and destabilize disease dynamics, depending on the interactions between refuge size, accessibility, and movement rates. Reducing host exposure to parasites can dampen outbreaks and promote equilibrium, but when refuge capacity is high or movement rates are rapid, refuges can paradoxically intensify outbreaks by acting as reservoirs for susceptibles. If a large pool of susceptible individuals accumulates within the refuge and later re-enters the main population, this can fuel a surge in infections. Furthermore, when movement rates are high, the system becomes more similar to one without a refuge, as individuals spend little time sheltered before re-entering the infected environment.

Firstly, our results show that introducing a refuge can disrupt the cyclic fluctuations driven by the free-living parasite, promoting population equilibrium under certain conditions. However, this stabilizing effect depends on factors like movement rates, refuge capacity, and host demography. Refuges can reduce parasite transmission by limiting contact between susceptible hosts and infectious stages (Hatcher, Dick and Dunn, 2006) and may improve host survival and reproduction by providing favourable conditions. This allows hosts to re-join the main population in greater numbers, which can either buffer against outbreaks or, conversely, reinforce cycles by increasing parasite production. The overall effect depends on whether the refuge functions primarily as a protective barrier or inadvertently sustains larger outbreaks by acting as a reservoir of susceptibles. While movement to and from the refuge may initially dampen population fluctuations, long-term effects are shaped by movement rates and refuge capacity. In some cases, refuges may help maintain stability; in others, they may amplify disease cycles through periodic reintroduction of susceptibles.

The availability of a refuge stabilizes population dynamics, with the transition from cycles to equilibrium depending on movement rates into and out of the refuge. As long as movement out remains sufficiently low, the system remains stable, but exceeding this threshold reintroduces cyclic dynamics by increasing the flow of susceptibles back into the main population. Similar thresholds have been observed in predator-prey models, where low prey dispersal from refuges promotes stability (Hassell and May, 1973; Oaten and Murdoch, 1975). Additionally, a low movement rate out of the refuge allows the refuge population to grow over time, as individuals remain sheltered for longer periods, leading to a larger pool of susceptibles that may later re-enter the main population. Likewise, in predator-prey models, prey sheltered in refuges often exhibit higher reproductive output due to reduced predation risk (Anderson and May, 1981). This effect could be even stronger if the refuge itself provides greater resource availability than the external environment, increasing host reproduction within the refuge. The stabilizing effect of refuges in predator-prey systems is shaped by prey dispersal, predator efficiency, resource availability, and refuge characteristics. In our model, movement rates in

and out of the refuge and refuge carrying capacity represent comparable factors, influencing whether stability or cyclic dynamics emerge.

While refuges can stabilize populations by limiting exposure to infection, we also find that high movement rates into and out of the refuge can create counterintuitive dynamics, leading to more frequent and intense outbreaks compared to scenarios without a refuge. When movement rates are relatively high, a steady influx of susceptible individuals enters the refuge, where they may grow in number, even if they stay there for a shorter time. This dynamic creates a larger pool of susceptibles within the refuge. When these individuals leave the refuge and re-enter the main population, they significantly increase the pool of susceptibles, fuelling larger outbreaks. A similar effect is observed in studies of wildlife corridors, which connect fragmented populations. While corridors help maintain population connectivity, they can also facilitate the spread of disease when increasing interactions between populations. Hess (1996) found that movement between subpopulations in fragmented habitats can destabilize populations by promoting disease spread (Zhang *et al.*, 2015). Similarly, in our model, higher movement rates between the refuge and the main population increase the number of susceptible individuals re-entering the infected population, which drives more intense outbreaks. This effect has also been documented in studies of social contact networks, where increasing connections between individuals enhances the spread of disease. Zhang et al. found that outbreaks were more likely when individuals had more social connections, paralleling the way a larger susceptible population in our model contributes to bigger outbreaks. This is further illustrated by pandemic control measures, such as social distancing bubbles, where restricted contact initially offers protection but movement between bubbles can lead to outbreaks if not managed carefully (Li, Yin and Chen, 2023; Zhu *et al.*, 2023). While refuges can dampen disease spread under low movement rates, higher movement rates between the refuge and the main population can lead to larger outbreaks due to the accumulation of susceptible individuals in the refuge and their subsequent reintroduction into the main population.

In addition to movement rates, our model shows that the fecundity of the infected population plays a significant role in shaping system stability and cycling dynamics. At low fecundity, the system exhibits larger amplitude cycles, suggesting that when infected individuals contribute little to the production of susceptibles, population oscillations are more pronounced—even compared to scenarios where infected individuals contribute nothing at all. As fecundity increases, these cycles diminish, and the system moves toward equilibrium. This occurs because infected individuals begin to function more like susceptibles in terms of reproductive output, lessening the demographic impact of infection. With losses due to disease more readily offset by reproduction, susceptible hosts are replenished more quickly, reducing fluctuations in disease prevalence. Unlike high movement out of the refuge, which can destabilise the system by reintroducing susceptibles en masse, increased fecundity can promote stability by buffering the population against the costs of infection. These findings are supported by both empirical and theoretical studies. Albon et al. (2002) showed that parasite-induced reductions in fecundity were sufficient to regulate populations, while Lively (2006) demonstrated that parasites can reduce host population growth purely through effects on reproduction, without increasing mortality, ultimately promoting stability via density-dependent feedback. In line with these results, our model suggests that higher fecundity helps the host population recover more quickly from infection-driven declines, mitigating population crashes and supporting a more stable, endemic disease state. Additionally, Hudson et al. found that lowering the reproductive costs of parasitism in red grouse populations reduced population fluctuations, emphasizing the role of fecundity in maintaining stability during disease outbreaks. In general, higher reproductive output buffers host populations against infection-induced crashes, reducing the amplitude of disease-driven cycles (Anderson and May, 1981; Keeling and Rohani, 2008).

Our results also reveal an important interaction between refuge carrying capacity and parasite dynamics. While larger refuges may seem beneficial by sheltering more susceptibles, they can amplify parasite population cycles, particularly when movement rates of susceptibles are high. This is not just due to a higher number of susceptible individuals entering the refuge but

also because increasing the refuge's carrying capacity allows local population growth within the refuge itself. When these individuals later re-enter the main population, they contribute to a surge in susceptibles, acting as a catalyst for rapid disease spread and leading to larger and more frequent outbreaks. This pattern aligns with models of carrying capacity and disease persistence, where larger host populations sustain longer outbreaks due to the greater availability of susceptibles (Gubbins and Gilligan, 1997). Similarly, spatial heterogeneity in host-parasite systems has been shown to delay outbreaks but intensify them when large refuge areas harbour susceptibles (Grenfell and Harwood, 1997). Comparable effects have also been observed in conservation biology, where protected areas acting as refuges lead to population booms that destabilize the system when individuals are reintroduced into non-protected areas. This aligns with findings from Ball, Mollison, and Scalia-Tomba (1997), who showed that in spatially structured populations, the reintroduction of susceptibles intensifies disease transmission and drives larger outbreaks, much like in our model. Similarly, Keeling and Rohani (2008), demonstrated that mixing between sub-populations can increase disease persistence by continuously reintroducing susceptibles into infected areas, prolonging transmission cycles.

In our model, the interaction between refuge dynamics and outbreak severity mirrors patterns observed in predator-prey systems, where refuges influence the intensity of species interactions (Hochberg and Holt, 1995). While refuge size can affect long-term population stability, the movement rates into and out of the refuge play a crucial role in shaping disease dynamics. When movement into the refuge is low but outward movement is high, infection prevalence remains consistently high, as susceptibles spend less time in the refuge and quickly return to the infected population. Conversely, when movement into the refuge is high and outward movement is low, susceptibles remain protected for longer periods, leading to lower infection prevalence. Thus, the timing and frequency of movement between the refuge and the main population are key drivers of overall disease dynamics.

Excessive movement between the refuge and the main population disrupts stability and can intensify outbreaks. This raises the question: why do individuals leave the refuge at all? Refuges offer benefits like reduced predation or parasitism risk, potentially increasing prey population sizes. However, these refuges often come with trade-offs. They may have lower carrying capacities due to limited resources, leading to increased competition. Some refuges also require venturing out for essential resources, exposing individuals to threats. For example, freshwater mussels burrow to avoid parasitic trematodes but must emerge to filter food, risking exposure (Vaughn and Hakenkamp, 2001). This trade-off between safety and resource acquisition illustrates the complexities of refuge usage, which can vary among ecological systems and be influenced by resource distribution and life cycles.

Our model's key limitation, and a path for future work, is its simplicity. We assumed a 'perfect' refuge for susceptible only and did not include host evolution. This overlooks two critical, real-world complexities: 1) If infected hosts (like lysogens) entered the refuge, it could become a *source* of new parasites, worsening disease. 2) If hosts could evolve resistance, this new 'genetic refuge' would likely compete with the ecological refuge, dampening outbreaks. Integrating these evolutionary dynamics is a critical next step. The key message is that refuges have a dual role, defined by a critical movement threshold. Our model shows that while low-turnover refuges stabilize populations and suppress disease, high-turnover or large-capacity refuges are destabilizing. They act as 'reservoirs' for susceptible, rebuilding and releasing them to fuel paradoxically larger outbreaks. This implies that for systems like rhizobia-phage, the rate of release from nodules is as important as the protection itself. For disease management, this serves as a warning: poorly managed refuges can worsen, not mitigate, epidemics.

4.6 Supplementary Materials

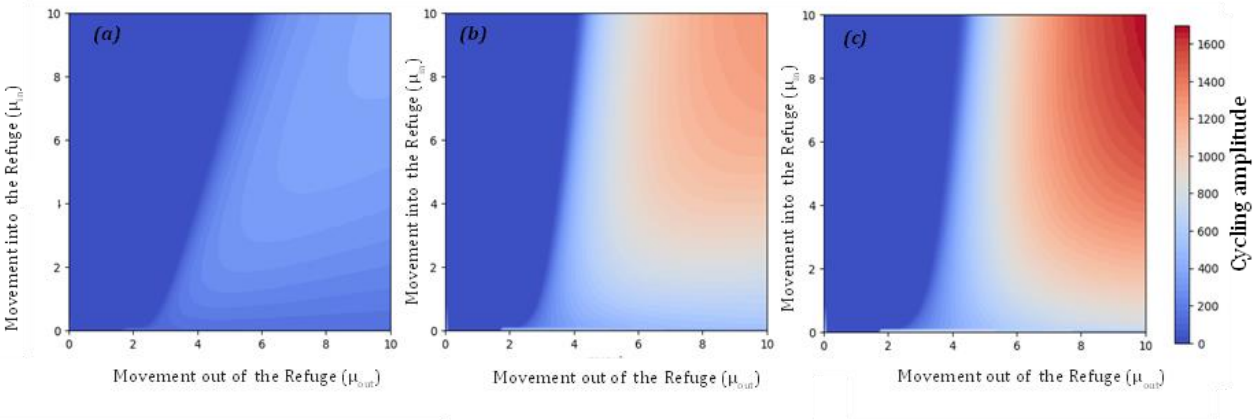

***Figure S1**: **(a-c)** Showing what happens to the threshold of when populations stop/start cycling, when varying the additional death rate when infected, γ. The colour bar indicates the population density, where there is dark blue at 0 there is no cycling, the redder colours show the intensity of the cycles. Where **a)** γ = 0.1, **b)** γ = 0.5, **c)** γ = 1.*

4.7 References

Albon, S.D. *et al.* (2002) 'The role of parasites in the dynamics of a reindeer population', *Proceedings. Biological Sciences*, 269(1500), pp. 1625–1632. Available at: https://doi.org/10.1098/rspb.2002.2064.

Anderson RM, May RM. Infectious diseases and population cycles of forest insects. Science. 1980;210(4470):658-61. Available from: https://doi.org/10.1126/science.210.4470.658

Bailey DJ, Otten W, Gilligan CA. Empirical evidence of spatial thresholds to control invasion of fungal parasites and saprotrophs. New Phytol. 2004;163(1):125-32. Available from: https://doi.org/10.1111/j.1469-8137.2004.01086.x

Ball, F., Mollison, D. and Scalia-Tomba, G. (1997) 'Epidemics in populations with two levels of mixing', in. Available at: https://www.semanticscholar.org/paper/Epidemics-in-populations-with-two-levels-of-mixing-Ball-Mollison/4b573de7808e99b3fda3fc265c346bef7280cc01

Briggs CJ, Nisbet RM, Murdoch WW, Collins JJ. Dynamical effects of host-feeding in parasitoids. J Anim Ecol. 1995;64(3):403-16. Available from: https://doi.org/10.2307/5900

Cervino JM, Hayes RL, Polson SW, Polson SC, Goreau TJ, Martinez RJ, et al. Relationship of Vibrio species infection and elevated temperatures to yellow blotch/band disease in Caribbean corals. Appl Environ Microbiol. 2004;70(11):6855-64. Available from: https://doi.org/10.1128/AEM.70.11.6855-6864.2004

Cohen LP, Baums IB, Hernandez-Agreda A, Baker AC. Genomic characterization of Symbiodinium communities in bioeroding sponges. Coral Reefs. 2023;42(1):23-36.

Costerton JW, Stewart PS, Greenberg EP. Bacterial biofilms: a common cause of persistent infections. Science. 1999;284(5418):1318-22. Available from: https://doi.org/10.1126/science.284.5418.1318

Crawford RD, O'Keefe JM. Improving the science and practice of using artificial roosts for bats. Conserv Biol. 2024;38(1). Available from: https://doi.org/10.1111/cobi.14170

Daversa DR, Bosch J, Romero D, Fisher MC, Garner TW. Routine habitat switching alters the likelihood and persistence of infection with a pathogenic parasite. Funct Ecol. 2018;32(5):1262-70. Available from: https://doi.org/10.1111/1365-2435.13038

Denlinger DL. Dormancy in tropical insects. *Annu Rev Entomol*. 1986;31(1):239-264.

Donelan SC, Grabowski JH, Trussell GC. Refuge quality impacts the strength of nonconsumptive effects on prey. Ecology. 2017;98(2):403-11. Available from: https://doi.org/10.1002/ecy.1647

Dulvy NK, Sadovy Y, Reynolds JD. Extinction vulnerability in marine populations. Fish and Fisheries. 2003;4(1):25-64.

Fillinger U, Knols BG, Becker N. Efficacy and efficiency of new sand fly control strategies for malaria vector management. Bull World Health Organ. 2009;87(9):655-66. Available from: https://doi.org/10.2471/BLT.08.055632

Gage KL, Kosoy MY. Recent trends in plague ecology. In: Recovery of the Black-footed Ferret – Progress and Continuing Challenges. US Geological Survey Scientific Investigations Report; 2005.

Gillespie TR, Nunn CL, Leendertz FH. Integrative approaches to the study of primate infectious disease: implications for biodiversity conservation and global health. Am J Phys Anthropol. 2008;137(Suppl 47):53-69. Available from: https://doi.org/10.1002/ajpa.20949

Gillespie TR, Nunn CL, Leendertz FH. Primate diseases and human health at the wild-domestic animal interface. Am J Primatol. 2008;70(8):741-57. Available from: https://doi.org/10.1002/ajp.20570

Goniewicz K, Khorram-Manesh A. Maintaining social distancing during the COVID-19 outbreak. Soc Sci. 2021;10(1):14. Available from: https://doi.org/10.3390/socsci10010014

Grenfell BT, Harwood J. (Meta)population dynamics of infectious diseases. Trends in Ecology & Evolution. 1997;12(10):395-399.

Gubbins S, Gilligan CA. Invasion thresholds in spatially structured host–parasite systems. Philos Trans R Soc Lond B Biol Sci. 1997;352(1353):851-858.

Hassell MP, May RM. Stability in insect host-parasite models. J Anim Ecol. 1973;42(3):693-726. Available from: https://doi.org/10.2307/3133

Hatcher MJ, Dick JTA, Dunn AM. How parasites affect interactions between competitors and predators. Ecol Lett. 2006;9(11):1253-71. Available from: https://doi.org/10.1111/j.1461-0248.2006.00964.x

Hess GR. Disease in metapopulation models: Implications for conservation. Ecology. 1996;77(5):1617-1632. https://doi.org/10.2307/2265556

Hochberg ME, Holt RD. Refuge use and dynamic behavior: a theoretical exploration of life-history evolution in predator-prey systems. Oikos. 1995;74(2):301-12. Available from: https://doi.org/10.2307/3545667

Holt RD, Hochberg ME. When is biological control evolutionarily stable (or is it)? Ecology. 1997;78(6):1673-83. Available from: https://doi.org/10.1890/0012-9658(1997)078(1673:WIBCES)2.0.CO;2

Holt RD. Prey communities in patchy environments. Oikos. 1987;50(3):276-90. Available from: https://doi.org/10.2307/3565488

Hudson PJ, Dobson AP, Newborn D. Prevention of population cycles by parasite removal. Science. 1998;282(5397):2256-8. Available from: https://doi.org/10.1126/science.282.5397.2256

Keeling MJ, Rohani P. Modeling Infectious Diseases in Humans and Animals. Princeton University Press; 2008.

Lafferty KD, Porter JW, Ford SE. Infectious diseases affect marine fisheries and aquaculture economics. Annu Rev Mar Sci. 2015;7:471-96. Available from: https://doi.org/10.1146/annurev-marine-010814-015646

Leng T, White C, Hilton J, Kucharski AJ, Pellis L, Stage HB, et al. The effectiveness of social bubbles as part of a Covid-19 lockdown exit strategy, a modelling study. Wellcome Open Res. 2021;5:213. Available from: https://doi.org/10.12688/wellcomeopenres.16164.2

Li C-Y, Yin J, Chen L. Impact of social distancing on disease transmission risk in the context of a pandemic. Phys Rev E. 2023;108(5):054115. Available from: https://doi.org/10.1103/PhysRevE.108.054115

Lively, C.M. (1999) 'Migration, Virulence, and the Geographic Mosaic of Adaptation by Parasites', *The American Naturalist*, 153(S5), pp. S34–S47. Available at: https://doi.org/10.1086/303210.

López, D., Vlamakis, H. and Kolter, R. (2010) 'Biofilms', *Cold Spring Harbor Perspectives in Biology*, 2(7), p. a000398. Available at: https://doi.org/10.1101/cshperspect.a000398.

McCallum H, Barlow N, Hone J. How should pathogen transmission be modelled? Trends Ecol Evol. 2001;16(6):295-300. Available from: https://doi.org/10.1016/s0169-5347(01)02144-9

Moore RA. Bat roost selection in multiuse landscapes of the Ozark Mountains. Ph.D. dissertation. Missouri State University; 2012.

Murdoch WW, Chesson J, Chesson PL. Biological control in theory and practice. Am Nat. 1985;125(3):344-66. Available from: https://doi.org/10.1086/284347

Oaten A, Murdoch WW. Switching, functional response, and stability in predator-prey systems. Am Nat. 1975;109(967):299-318. Available from: https://doi.org/10.1086/282999

Orrock JL, Danielson BJ, Burns CE. Refuge-mediated apparent competition in insect-ivorous birds. Oikos. 2013;122(7):1062-72. Available from: https://doi.org/10.1111/j.1600-0706.2012.20717.x

Ostfeld RS, Levi T, Keesing F, Oggenfuss K, Fleischman F. Tick-borne disease risk in a forest food web. Ecol Monogr. 2018;88(2):215-32. Available from: https://doi.org/10.1002/ecm.1292

Ruxton GD. Short term refuge use and stability of predator-prey models. Theor Popul Biol. 1995;47(1):1-17. Available from: https://doi.org/10.1006/tpbi.1995.1001

Schönberg CHL, Loh WKW. Bioeroding sponges and coral reefs: monitoring and new technologies. In: International Coral Reef Symposium. Okinawa, Japan; 2004.

Tusting LS, Thwing J, Sinclair D, Fillinger U, Gimnig JE, Bonner KE, et al. Mosquito larval source management for controlling malaria. Cochrane Database Syst Rev. 2013;(8). Available from: https://doi.org/10.1002/14651858.CD008923.pub2

Van Cauwenberghe J, Andrade-Sanchez JL, Robledo-Olivo A, Batstone RT, Frederickson ME, Geurts R. Spatial patterns in phage-Rhizobium coevolutionary interactions across regions of common bean domestication. ISME J. 2021;15(7):2092-106. Available from: https://doi.org/10.1038/s41396-021-00907-z

Vaughn CC, Hakenkamp CC. The functional role of burrowing bivalves in freshwater ecosystems. Freshw Biol. 2001;46(11):1431-46. Available from: https://doi.org/10.1046/j.1365-2427.2001.00771.x

Warburton L, MacDiarmid A, Freeman D, Gardner J, Curry M, Shears N, et al. A large-scale ecological intervention to restore long-term collapse of kelp forests: Can artificial reefs be effective in community recovery? J Appl Ecol. 2018;55(1):1244-56. Available from: https://doi.org/10.1111/1365-2664.13089

Zhang Z, Fu X, Wang W. Modeling epidemics spreading on social contact networks. IEEE Trans Emerg Top Comput. 2015;3(3):410-9. Available from: https://doi.org/10.1109/TETC.2015.2398353

Zhu P, Qin T, Fang H, Wu J. The impact of mass gatherings on the local transmission of COVID-19 and the implications for social distancing policies: evidence from Hong Kong. PLoS One. 2023;18(2). Available from: https://doi.org/10.1371/journal.pone.0279539

Chapter 5: Escaping the Arms Race: How Root Nodules Shape Rhizobia-Phage Coevolution

5.1 Abstract

Bacteria-phage interactions significantly shape microbial evolution, driving rapid change often characterized as an evolutionary arms race. However, symbiotic associations can provide ecological refuges that temporarily shield bacteria from phage predation, thereby relaxing selection for resistance. Rhizobia, nitrogen-fixing bacteria that form symbioses with legumes, alternate between phage-exposed free-living phases in soil and protected phases within root nodules. These nodules act as temporary refuges, allowing rhizobia to escape coevolutionary pressures. Here, we experimentally investigated how symbiosis within root nodules influences rhizobia-phage coevolution and affects symbiont competitiveness. Our results show that rhizobia colonizing nodules early evolved lower resistance to phages, while those remaining in the soil, under continuous phage exposure, developed higher resistance. However, this refuge is short-lived; once reintroduced into the phage-rich soil, early nodulators exhibited reduced competitiveness, suggesting that the benefits of refuge are negated when susceptible bacteria return to high phage pressure. Genome sequencing revealed mutations primarily in metabolic pathways unique to phage-exposed populations, indicating that phage-driven evolution can involve broader physiological adaptations. Overall, our findings highlight how spatial heterogeneity and host associations shape bacteria–phage dynamics and may constrain long-term evolutionary trajectories.

5.2. Introduction

Bacteria-phage interactions play a fundamental role in microbial evolution, driving continuous cycles of adaptation and counter-adaptation (Koskella and Brockhurst, 2014). Phages impose strong selective pressures on bacterial populations, shaping resistance dynamics and contributing to microbial diversity and population structure (Labrie, Samson and Moineau, 2010; Paterson *et al.*, 2010; Hampton, Watson and Fineran, 2020). These dynamics are a key part of how phages influence ecosystem functioning, especially in structured environments.

However, phage-driven selection is not uniformly distributed across all bacterial populations. Symbiotic bacteria, such as rhizobia, which form nitrogen-fixing mutualisms with leguminous plants, can temporarily escape phage predation by colonizing root nodules. Rhizobia transition between free-living states in the soil, where they are exposed to phage attack, and symbiotic states inside plant root nodules, where they are protected from phages (Oldroyd *et al.*, 2011; Poole, Ramachandran and Terpolilli, 2018). These nodules act as spatial refuges, reducing the selective pressure for novel resistance traits, this refuge, however, is transient. Upon plant senescence and nodule decay, rhizobia are released back into the soil, reintroducing previously protected bacteria into environments where phage pressure is high (Ratcliff, Underbakke and Denison, 2011; Remigi *et al.*, 2016). While these nodule-associated rhizobia have been shielded from selection, free-living rhizobia in the soil remain engaged in ongoing coevolution with phages. As a result, returning symbionts may be poorly adapted to the current phage population, effectively reintroducing susceptible hosts into a coevolving system. This repeated cycling between protected and exposed states may have important consequences for bacterial-phage dynamics, influencing genetic diversity, resistance evolution, and the long-term stability of their interaction. Instead of a straightforward coevolutionary trajectory toward increasing resistance within the bacterial population, the continual return of susceptible rhizobia may help sustain phage populations and maintain a dynamic equilibrium between resistance and susceptibility (Hall *et al.*, 2011; Simmons *et al.*, 2020).

Understanding how nodulation and host association alter bacterial-phage coevolution is necessary for a broader understanding of microbial evolution within structured environments. In this chapter, we investigate the ecological and evolutionary consequences of nodulation acting as a refuge, assessing its impact on the interplay between rhizobia and phages. Because nodules provide a temporary refuge from phage exposure, we focused on how host association reshapes rhizobium–phage co-evolution; experimental timings and plant developmental staging are detailed in Methods (***Section 5.3.2.2***). By acting as a temporary refuge from phage predation, the plant host shapes the evolutionary trajectories of rhizobial populations, preserving susceptible strains that would otherwise be lost and, in turn, driving variation in resistance, fitness, and symbiotic capacity upon re-entry into the soil.

5.3. Methods

5.3.1 Bacterial and phage strains

All experiments were conducted on *Rhizobium ruizarguesonis bv trifolii* (Rlt) host strain TRX19, a member of the R. leguminosarum species complex. This strain was isolated from the root nodules of Trifolium repens (clover) growing in one 1m sq site in York (Kumar et al., 2015). Fluorescently tagged derivatives were used to enable strain tracking; TRX19 with GFP (carries GFP and gentamycin resistant markers) and TRX19 with MC (carries mCherry and gentamycin resistant markers). Both tagged strains exhibited identical colony morphology, growth rate in TY medium, and phage sensitivity, confirming that the markers did not affect bacterial phenotype.

Phage strains used, *Phage 1,* which was isolated from environmental soil in the UK. Phages were isolated from rhizosphere soil from Trifolium repens (clover) (**Chapter 2**). This phage was previously used in Chapter 3, where co-evolution between Phage 1 and TRX19 led to reduced symbiotic efficiency when introduced to the host plant, resulting in lower plant biomass. Phage 1 was therefore selected for use in this chapter because it represents a well-

characterised antagonist, capable of driving measurable evolutionary and functional changes in the rhizobia–legume system.

All bacterial culturing was performed in TY media (3 g/L yeast extract, 6 g/L tryptone, 0.5 g/L calcium chloride) in 6 ml culture volumes under shaken (180 rpm) conditions at 28◦C. Colony forming units (CFUs) were enumerated on solid TY agar (13 g/L) and plaque forming units (PFUs) on soft TY agar overlays after cells were removed through filtration (using 0.45 µM syringe filters). Soft agar overlays consist of 5 ml of 6 g/L agar containing 100 µl of a growing culture of phage free TRX19 poured directly onto 5ml of 13 g/L of TY agar.

5.3.2 Plant Evolution Assay

5.3.2.1 Experimental design

A pot experiment was designed to evolve the TRX19 GFP clones with *Phage 1*. Clover (T. repens) plants were inoculated with rhizobia, with or without phages, to test the effect of nodulation as a refuge from phage selection. In total, there were six plants inoculated with TRX19 + Phage 1 (MOI = 1), six plants with TRX19 only, six with Phage 1 only, and six uninoculated controls.

5.3.2.2 Germination, planting, inoculation and culture conditions

White clover plants (variety = Avoca, DLF seeds Ltd.) were grown in 1 L tricorn pots containing 900 g of twice autoclaved vermiculite and sharp sand mix (2:3 ratio). Seeds were sterilised by immersing and shaking in 3% household (HH) bleach for 30 minutes at room temperature. The seeds were washed 4 times with sterile dH20 to remove any traces of bleach, spread on sterile filter paper, watered with 5ml of sterile dH20 and left to germinate for 5 days at room temperature. Single seedlings were randomly selected and placed in the tricorn pots, along with 5ml sterile nitrogen free Jensen media (Howieson and Dilworth, no date) and 5ml sterile dH20. Each tricorn pot was sealed inside a sterile sunbag, equipped with a sterile polypropylene tube that extended from the soil to the top, functioning as a watering tube with

a screw cap; all pots were placed in a controlled environment chamber (16/8-hour day/night cycle at 22^0C/20^0C, 500 µmol/m2/s1 light).After one week of growth, pots were inoculated with 800ul of bacterial culture by pipetting at the base of the seedling. Bacterial cultures were grown for 72 hours in TY media standardised at OD 600nm, centrifuged at 13,000 x g and resuspended in 800ul of rhizobia wash buffer (sterilised 10

mM MgSO4 and 0.01% Tween 40). Bacterial inoculation was applied directly at the seedling base. For Phage 1 treatments, an equal volume of phage lysate was added immediately after bacterial inoculation to achieve a multiplicity of infection (MOI) = 1. Phage-only pots received the same PFU load without bacteria with buffer in its place, and control pots received buffer only.

The plants were watered with 20mL of sterile water and Jensen's media mix every week, with Jensen increasing 1ml extra per week. Plants were grown for a further 7 weeks after inoculation.

Under these growth conditions, it is assumed that rhizobial infection began within 1–7 days post-inoculation, and visible nodules appeared by 10–14. Nodule senescence occurred around at week 8, coinciding with harvest.

5.3.2.3 Weekly phage and rhizobia sampling

Rhizosphere substrate from each plant was sampled each week during plant growth (8 weeks), to monitor population densities of free-living phage and rhizobia, as well as isolating evolving phage over the plant growth period.

A 5cm sterile soil corer (5cm length x 10mm diameter), per pot, was used to sample 5g of substrate from each pot, sampled substrate was put directly into a 15ml falcon tube containing 5ml of rhizobia wash buffer (10mM MgSO4 and 0.1% Tween) and 5g of sterile glass bead mix (diameters 2mm and 4mm). Samples were vortexed for 1 minute, left to stand for 30 minutes. 200ul of sample was taken for stocks, 200ul was taken for bacterial plating and 200ul was taken for phage plating and isolation. 200ul for phage was first filtered through a 0.22um filter tip. Bacterial CFU/ml counts were plated on TY + 3mg/ml gentamicin, at a 10^{-6} dilution. Phage

PFU/ml counts were plated with a soft agar overlay, as above, with serial dilutions to 10^{-7}. Phage were isolated by picking individual plaques into 1ml of SM buffer and stored at 4'C. This sampling repeated each week of plant growth, with substrate samples being taken from areas around the plant as in **Figure 1a**, so not to harm the young plant roots. This targeted rhizosphere material (soil adhering to roots) and therefore measured free-living communities. Plants showed no difference in growth or nodulation, indicating that weekly coring did not affect plant performance. All treatments including controls were sampled for consistency.

5.3.2.4 Harvest

At harvest, rhizobia were isolated from three compartments representing different symbiotic interaction and phage exposure (see **Figure 1b** for visual representation),

- Primary root nodules (BN) - large nodules on the main root, formed early.
- Lateral root nodules (SN) - smaller nodules on first- and second-order lateral roots, formed later.
- Rhizosphere soil (Soil) - free-living rhizobia not engaged in symbiosis.

"Primary" and "lateral" designations are based on nodule position; T. repens forms nodules on both root types. Clover plants typically developed 10–60 nodules per plant under these conditions.

Primary root nodules are located on the main 'primary' root of the plant, and were assumed to contain rhizobia that colonised early in the plant's development, whereas smaller 'lateral' root nodules, on first- and second-order lateral roots, likely contained rhizobia that established later in the growth cycle. The rhizosphere was expected to contain free-living rhizobia that had not undergone symbiosis. These environments can therefore be seen as representing a gradient of interaction from high symbiosis and low phage exposure, to no symbiosis and high phage exposure. All nodules on a plant were counted and then a maximum of 12 primary nodules

and 12 lateral nodules were removed from the roots, sterilised (3 mins at 70% EtOH, 6 sterile dH20 washes) and individually crushed in 150ul of rhizobia wash buffer, each in a well of a 96 well plate, before plating on TY + 3mg/ml gentamicin. End point rhizobia from the rhizosphere were isolated via serial dilution plating on selective TY medium to ensure recovery of the inoculated TRX19 background.

Shoot biomass was separated from roots and both were and dried in a hot air oven at 80'C for 48 hours then weighed.

Each treatment experienced some level of plant mortality, these surviving plants were harvested as above. To ensure consistency in comparisons, plants from the TRX19-only, phage-only and control groups were matched against the surviving experimental plants.

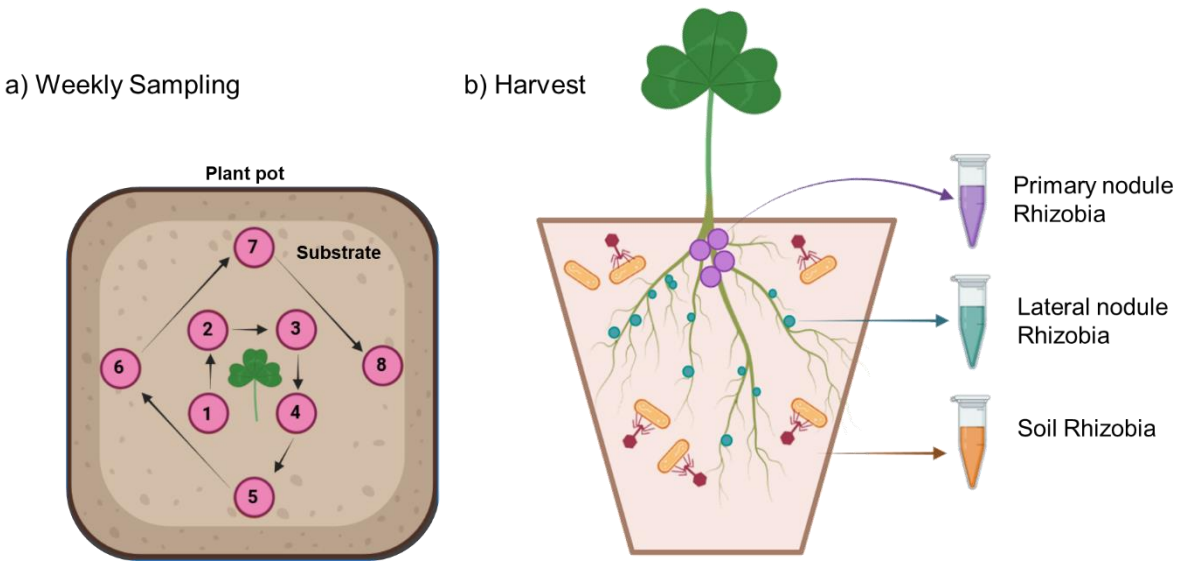

***Figure 1**: a) shows the locations of rhizosphere substrate sampling each week. The numbers represent the week the sample was taken. b) shows the sample compartment locations in the plant pot for where primary nodules, lateral nodules and endpoint rhizobia were taken from. Image created with biorender.*

5.3.3 Cross infection assay

Rhizobia isolates from each sample compartment were tested against phageisolates from its corresponding plant. Isolates from phage-free plants were also tested against phage-evolved samples for comparison. This assay measured bacterial susceptibility using the Reduction in Bacterial Growth (RBG) index (Formula 1), where higher values indicate greater sensitivity to infection.

Each rhizobia isolate was inoculated into 150ul of TY media in a 96 well plate and left to grow for 72 hours under 28'C/180RPM. After 72 hours, grown cultures were standardised to OD600nm ~0.6 and diluted 1 in 10.Each clone was then exposed to the following conditions:

- No Phage (Ty media)
- Ancestral *Phage 1* (Week 0 phage)
- Week 2 sampled phage (respective to plant
- Week 4 sampled phage (respective to plant)
- Week 6 sampled phage (respective to plant)
- Week 8 sampled phage (respective to plant)

Each of the clones were grown for 72 hours at 28'c/180RPM and at hours 0, 10, 20, 40 and 60 the Optical Density (OD) at a wavelength of 600nm was measured in a Tecan Spark microplate reader. Bacterial susceptibility to infection was measured as Reduction in bacterial growth (RBG) for each strain (**Formula 1**). A higher RBG value indicated higher bacterial susceptibility to phage infection.

Formula 1. $$RBG = 1 - \left(\frac{OD600\ phage\ tn - OD600\ phage\ t0}{OD600\ phage\ free\ tn - OD600\ phage\ free\ t0}\right)$$

5.3.4 Symbiosis experiment

5.3.4.1 Experimental design

A plant experiment in 50ml Falcon tubes was designed to assess the symbiont quality of evolved rhizobia clones from different sample compartments. The most phage-resistant clone (lowest RBG) from each compartment per plant was selected to avoid sampling bias toward susceptible strains.

In total, 9 clones evolved with phage (3 plants × 3 compartments), 9 clones evolved without phage, plus the ancestral TRX19 and an uninoculated control. All treatments were triplicated.

5.3.4.2 Germination, planting and harvesting

Germination was carried out as above, using white clover plants (variety = Avoca, DLF seeds Ltd.). They were grown in 50 ml falcon tubes, containing 35ml of twice autoclaved vermiculite and sharp sand mix (2:3 ratio), with parafilm wrapped over the top of the tube, and sliced open when plants grew to the top. Plants were inoculated with 100ul of standardised bacterial culture (OD600nm 0.6) at planting. Bacterial cultures were grown for 72 hours in TY media standardised at OD 600nm, centrifuged at 13,000 x g and resuspended in 800ul of rhizobia wash buffer (sterilised 10mM MgSO4 and 0.01% Tween 40). Plants were watered at planting with 2ml sterile nitrogen free Jensen media (Howieson and Dilworth, 2016) and 2ml sterile dH20, and then watered weekly with the same measurements.

At harvest, shoot biomass was separated from roots and both were and dried at 80’C for 48 hours then weighed.

5.3.5 Competition experiment

A competition experiment was conducted within clover plants using phage-evolved rhizobia clones from primary nodules (early colonizers with minimal phage exposure) and endpoint soil (free-living rhizobia with prolonged phage exposure) harvested from the previous experiment. These clones were competed against a phage-resistant reference strain, in phage-present and phage-absent environments. Using a resistant strain allowed competition within phage environments to be assess. Fitness was assessed in both the soil and root nodules to compare how differing levels of phage exposure influenced competitive success.

5.3.5.1. Strains used

Strains used in this experiment were TRX19 GFP, a phage-evolved TRX19 MC (used as the phage-resistant reference strain, verified by cross-infection), and the most resistant clones from the phage-evolved primary root nodule and soil compartments from the previous assay The MC strain was generated by evolving TRX19-mCherry in vitro with Phage 1 over two sequential transfers (each 72 h), producing a highly phage-resistant lineage. This strain served as a standard reference to enable direct competition with the GFP-labelled rhizobia that had evolved within the plant system. Using different fluorescent markers (GFP and mCherry) allowed both strains to be grown and analysed together while remaining distinguishable during co-culture and imaging.

The primary nodule clones and the endpoint soil clones were chosen to investigate the impact of nodulating early vs not at all and what effect this has on their fitness in soil and nodules.

5.3.5.2. Experimental Design

In total, three phage-evolved clones from primary nodules, three from endpoint soil, and three TRX19 control clones were competed against the TRX19-MC reference strain under both phage-present and phage-free conditions. All treatments were inoculated into pots and replicated in triplicate.

5.3.5.3. Germination and planting

White clover plants (variety = Avoca, DLF seeds Ltd.) were grown in 1 L tricorn pots containing 900 g of twice autoclaved vermiculite and sharp sand mix (2:3 ratio). Seeds were sterilised, germinated and planted as above. At time of planting, seeds were watered with 5ml sterile nitrogen free Jensen media (Howieson and Dilworth, 2016) and 5ml sterile dH20, then placed in a sterile sunbag and allowed to grow for one week all in a controlled environment chamber (16/8-hour day/night cycle at 22^0C/20^0C, 500 µmol/m2/s1 light). After one week of growth, each pot was inoculated with 200ul of TRX19-MC (reference strain) and 200ul of focal TRX19-GFP strain; inoculants were pipetted at the base of the seedlings Bacterial cultures were

grown for 72 hours in TY media standardised at OD 600nm to 0.6, centrifuged at 13,000 x g and resuspended in 800ul of rhizobia wash buffer (sterilised 10mM MgSO4 and 0.01% Tween 40).

5.3.5.4. Harvest and imaging

Plants were first harvested by removing the above ground biomass. To estimate CFU/ml from nodule populations nodules from each plant were counted and then pooled, sterilised (3 mins at 70% EtOH, 6 sterile dH20 washes) and crushed in 750ul of rhizobia wash buffer before plating on TY + 3mg/ml gentamicin, at dilutions of 10^4, 10^5 and 10^6. Plates were incubated at 28'C for 72 hours and then kept at 4'C for 24 hours.

Plates were visualised using GBOX-ChemiXX9 imager and images were analysed using the GeneTools software, where both GFP and MC markers could be identified.

Colonies for both strains were counted and relative fitness for each strain calculated using **Formula 2**. Where v is the competitive fitness of the focal strain, here x_1 is the starting proportion of the focal strain and x_2 is the final proportion of the focal strain (Ross-Gillespie et al. 2009; Bird et al., 2023).

Formula 2.

$$v = \frac{x_2(1-x_1)}{x_1(1-x_2)}$$

5.3.6. Genome sequencing

Rhizobia evolved clones were extracted using the Qiagen DNeasy PowerSoil Pro kit using 250mg of input material (6ml of saturated culture spun down and pellet was taken, up to 250mg) and quality checked on a Nanodrop 8000 (Nanodrop ™) and Qubit 4 fluorometer (Qubit ™). Rhizobia evolved clone samples were used to generate whole genome sequences for each clone. In total, 18 evolved clones (9 phage-exposed, 9 phage-free) plus the ancestral TRX19 strain underwent whole genome sequencing, this was performed using Illumina MiSeq (2 × 150 bp) at Centre for Genomic Research (University of Liverpool).

5.3.7. Analysis

Data were analysed in R (v4.1.3) with R studio (R Studio Team 2020) using tidyverse packages (Wickham, et al. 2019).

Coefficients (t and p-values) within linear mixed models are compared to the Ancestral strain TRX19 unless stated otherwise. Linear mixed effects (lmer, in lm4 (Bates et al., 2015)) models were used to investigate effects of phage presence and sample compartments, on phage susceptibility and fitness, accounting for repeated biological and technical measures. Random effects were evaluated using likelihood ratio tests, and where they did not significantly improve model fit, Type III ANOVA and appropriate post hoc tests were used instead.

Mutations in evolved rhizobia clone genomes were predicted using Breseq v0.37.0 (Deatherage and Barrick, 2014) aligned to the reference genome. Mutations that appeared in 100% of the samples were assumed to be ancestral and filtered out.

5.4. Results/Discussion

To explore the impact of spatial refuges created through symbiotic interactions on bacteria-phage coevolution, we evolved rhizobia in plant mesocosms with and without phages. Rhizobia were sampled from three compartments representing a gradient of symbiotic association and phage exposure: primary root nodules (early colonizers, low phage exposure), lateral root nodules (later colonizers, intermediate exposure), and the surrounding soil (free-living, high phage exposure). Plants were sampled weekly to track population dynamics of both rhizobia and phages. By the end of the experiment, all populations persisted, phage did not drive rhizobia populations to extinction but co-existed instead, and control populations of phage only did not persist as expected (**Figure S1**)**.** This coexistence likely arose from spatial and ecological heterogeneity within the plant–soil system, where root nodules acted as a spatial refuge for rhizobia to temporailry escape to. Moreover, resistance–infectivity trade-offs and temporal fluctuations in bacterial susceptibility may have maintained a pool of partially sensitive hosts, allowing phages to persist without collapsing their host population (Brockhurst

et al., 2006; Heilmann, Sneppen and Krishna, 2012; Schrag and Mittler, 1996).. The presence of phage in the soil did not affect the ability of the rhizobia to form root nodules, and had no significant effect on plant biomass, (**Figure S2**).

5.4.1 Phage Exposure and Resistance Evolution in Rhizobia

Cross-infections of end point rhizobia from different compartments with phage samples collected throughout the experiment revealed a gradient in resistance. Isolates from the soil, which experienced prolonged phage exposure, evolved the highest levels of resistance. In contrast, rhizobia that colonized root nodules early exhibited significantly lower resistance (*soil* × *phage* interaction: $t = –6.24$, $p < 0.001$, compared to primary nodule × phage). Rhizobia from secondary root nodules, which likely entered later after some time in the soil, displayed intermediate resistance levels (*lateral nodule* × *phage* interaction: $t = –3.57$, $p < 0.001$) (**Figure 2**). For all rhizobia isolates, susceptibility increased when exposed to phages from later time points, consistent with ongoing phage evolution and directional selection over time. Reflecting both spatial and temporal dynamics of exposure, with early nodule entry limiting both the intensity and duration of phage-driven selection. This spatial separation created a clear evolutionary divergence, with soil isolates adapting to persistent phage pressure and nodule inhabitants experiencing relaxed selection.

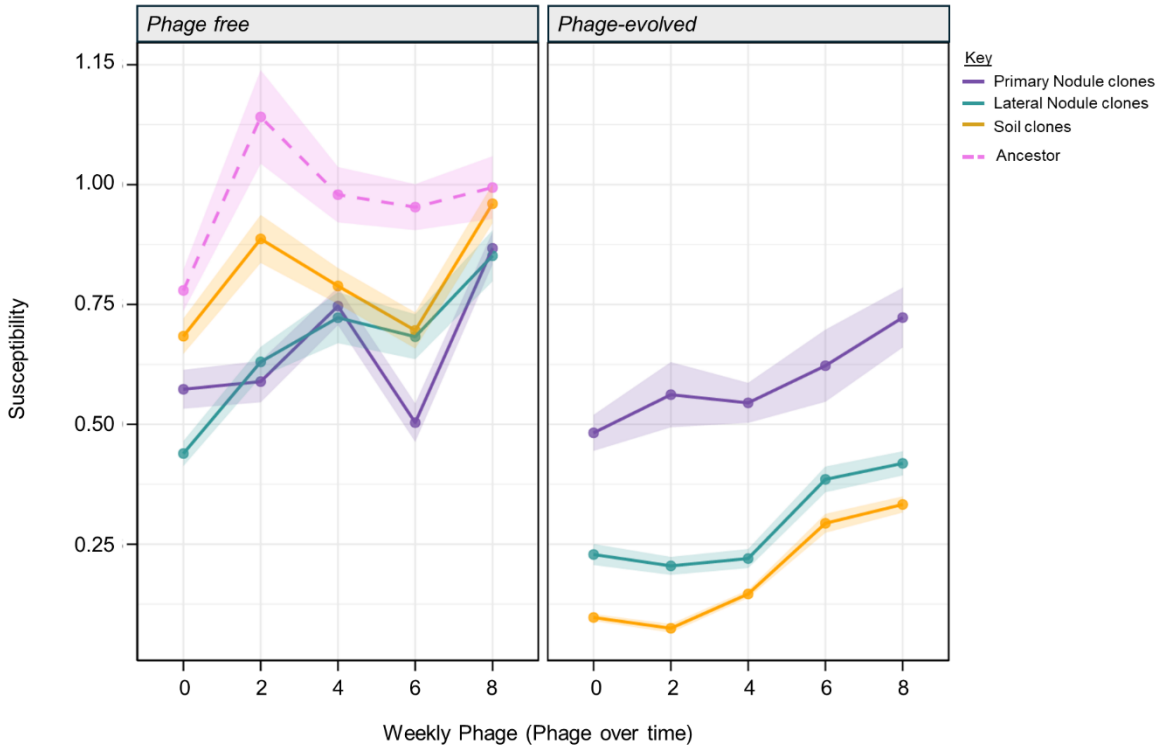

***Figure 2**: Rhizobia susceptibility to Phage sampled weekly from rhizobia-phage evolving plants. The y-axis shows the susceptibility to Phage (calculated as the Reduction in Bacterial Growth (RBG)), and the x-axis shows the phage rhizobia have been crossed with (phage weekly sampling time). The plot is split by phage free and phage-evolved Rhizobia sampled from different sample compartments, Primary nodules (purple), lateral nodules (teal), Soil (orange); with the susceptibility of the Ancestral strain (pink) being displayed on the plot for reference.*

This pattern is consistent with broader ecological theories on spatial refuges and predator–prey dynamics, where physical or ecological barriers reduce exposure to antagonists (Koskella & Brockhurst, 2014). In microbial systems, structured environments such as biofilms, intracellular niches, or symbiotic associations can shield bacteria from phage attack, reducing the intensity of selection for resistance (Heilmann, Sneppen and Krishna, 2012). Our findings suggest that nodulation provides a similar form of protection, where rhizobia that enter nodules early, experience reduced exposure to phage and evolve lower resistance, while bacteria remaining in the soil continue to evolve resistance under strong phage selection.

5.4.2 Genomic and Symbiotic Consequences of Phage-Driven Evolution

Based on phage susceptibility (RBG) values, the most resistant clones from each sample compartment were selected and tested for symbiotic performance. Phage exposure significantly reduced plant growth (t = –2.55, p = 0.025), and plant biomass also varied by sample compartment (F(7, 52) = 3.15, p = 0.0085; **Figure S3**). Within the phage-evolved groups, isolates from the soil and lateral nodules produced significantly lower biomass compared to early-colonising primary nodule isolates, with p = 0.0106 and p = 0.0367, respectively. Suggesting, that extended exposure to phage, particularly in the soil, compromises symbiotic performance. Phage-driven reductions in plant growth likely reflect the fitness costs of bacterial resistance. Resistance mutations that block phage adsorption often alter surface molecules such as LPS, EPS, pili, or flagella, structures that are also essential for root attachment and infection-thread formation (Hall et al., 2011). Such surface changes can reduce nodule initiation and nitrogen fixation, leading to lower host biomass (Gibson et al., 2008; Kiers and Denison, 2008). Additionally, mutations in metabolic and respiratory genes suggest a reallocation of resources that promotes bacterial survival under phage pressure but compromises efficiency during symbiosis (Li, Yin and Chen, 2023; Gurney et al., 2020; Oono, Denison and Kiers, 2009). Resistance linked surface and metabolic changes may disrupt multiple stages of symbiosis. Alterations to outer membrane components, such as LPS and EPS, may weaken Nod-factor perception and infection-thread formation, reducing nodule initiation and quality (Gibson et al., 2008). Meanwhile, mutations affecting respiration and carbon metabolism may also restrict energy available for bacteroid differentiation and nitrogenase activity, leading to reduced nitrogen fixation and overall host biomass (Poole et al., 2018; Oono, Denison and Kiers, 2009). These combined effects could explain how rhizobia that survive phage pressure may remain poor mutualists within the host plant, highlighting a trade-off between resistance and symbiotic efficiency. Similar patterns have been observed in other bacteria–phage systems, where resistance evolution comes with

costs to competitive ability or host association (Gómez and Buckling, 2011; Meaden and Koskella, 2017).

Whole-genome sequencing of these evolved clones revealed 106 mutations across 28 unique genes (**Table S1**). Of these, 22 loci were shared across phage and no-phage treatments, one was unique to phage-free clones, and six were exclusive to phage-exposed clones (**Figure 3a**). Phage-exposed isolates accumulated more mutations overall than those evolved without phage (**Figure 3b**), consistent with phage-driven selection. Mutation counts also varied by sample compartment, where clones from phage-evolved primary nodules carried approximately half as many mutations as those from the soil. Suggesting that sustained exposure to phages in the soil led to greater genomic change, while early entry into nodules reduced phage-mediated selection. Only a small number of loci were unique to the phage-exposed lines after removing those shared with phage-free controls. This suggests that most mutations reflect general adaptation to the plant–soil environment rather than phage-specific selection. The few phage-only loci likely represent multiple, independent routes to resistance, targeting genes linked to surface structure and metabolism rather than a single, conserved genetic pathway. A similar pattern has been observed in experimental systems where coevolution is shown to accelerate molecular evolution and increases genetic divergence between populations (Paterson *et al.*, 2010; Scanlan, Buckling and Hall, 2015).

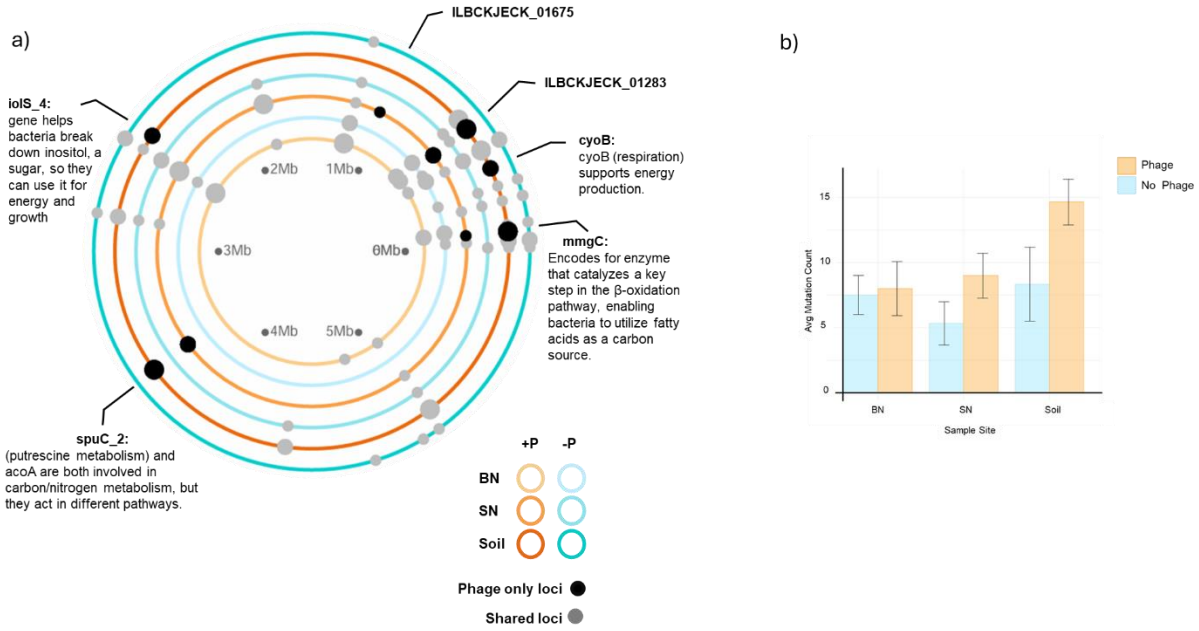

Figure 3: a) *Gene-level parallelisms where mutations have occurred within each Sample Compartment, for phage-free and phage-evolved clones. Each ring represents a treatment group. Black dots represent phage only loci, and the grey dots represent loci shared between phage-evolved and phage-free; the size of the dot represents the frequency at which this mutation occurs within samples;* ***b)*** *The average mutation counts between clones sampled from different sample compartments and for phage-evolved and phage-free.*

Specific mutations were detected only in phage-treated samples (**Figure 3a**), with many targeting metabolic pathways, particularly genes such as mmgC, *cyoB*, *spuC*_2, and iolS_4.

In some bacterium, the mmgC gene encodes a methylmalonyl-CoA mutase, a key enzyme involved in fatty acid metabolism and the methylcitrate cycle, which allows bacteria to utilize alternative carbon sources (Bryan, Beall and Moran, 1996; Reddick *et al.*, 2017) .

The *cyoB* gene encodes a subunit of cytochrome o ubiquinol oxidase, a key component of the aerobic respiratory chain involved in maintaining energy production under varying oxygen conditions (Chepuri *et al.*, 1990; Lunak and Noel, 2015). In *Rhizobium etli*, *cyoB* expression is upregulated under microaerobic conditions and plays a role in early symbiotic development, suggesting that mutations in this gene may alter respiratory flexibility and adaptation to environmental stress (Lunak and Noel, 2015).

The *spuC* gene encodes putrescine aminotransferase, an enzyme involved in polyamine metabolism. While its function is well characterised in *Pseudomonas aeruginosa*, where it contributes to stress responses, biofilm formation, and host interactions (Lu *et al.*, 2002),its role in rhizobia is less clear. However, polyamines such as putrescine and homospermidine are important for rhizobial growth, motility, exopolysaccharide production, and stress tolerance (Becerra-Rivera and Dunn, 2019). Mutations in polyamine biosynthesis and transport genes in rhizobia have been linked to impaired symbiosis and environmental adaptability (Becerra-Rivera and Dunn, 2019). Thus, disruption of *spuC* may reflect a metabolic shift that supports adaptation to phage pressure.

The *iolS_4* gene is linked to inositol metabolism, which supports carbon and energy acquisition in plant-associated bacteria. Inositol isomers, are abundant in legume root exudates and nodules, offering a rich nutrient source in the rhizosphere. In *Rhizobium leguminosarum*, inositol catabolism promotes competitive nodulation (Fry, Wood and Poole, 2001), and in *Sinorhizobium meliloti*, related genes are required for utilizing inositol and promoting host interactions (Kohler, Choong and Rossbach, 2011). Mutations in *iolS_4* may reflect adaptive shifts in metabolism that enhance symbiotic fitness. Genes involved in inositol catabolism may also face phage pressure, as they often intersect with transport and signalling systems involved in environmental stress responses (Price *et al.*, 2018).

These mutations, mainly targeting genes within metabolic pathways, suggest that phage-driven evolution can lead to broad physiological shifts beyond direct resistance mechanisms. Phage predation imposes strong selective pressures that may drive metabolic adaptations in bacteria, as seen in *Escherichia coli* and *Pseudomonas aeruginosa*, where aktered resource utilization strategies emerged under phage selection, as an indirect consequence of resistance evolution (Gurney *et al.*, 2020). These shifts may represent compensatory adaptations that offset the high fitness costs of resistance, such as biofilm production or membrane modification, by optimizing energy use or redirecting metabolic flux (Li, Yin and Chen, 2023). Moreover, metabolic changes may offer advantages beyond phage survival,

improving fitness under nutrient limitation or enhancing interactions with plant hosts (Lenski, 1988). Thus, phage exposure may reshape rhizobial metabolism in ways that influence not only resistance, but also ecological function and symbiotic potential, with lasting impacts on their evolutionary trajectory within soil microbial communities.

5.4.3 Competition experiment

Importantly, this escape from phage pressure is temporary. Once plants senesce and nodules decay, rhizobia are released back into the soil, where they must compete with phage-resistant strains. This ecological transition could reintroduce susceptible bacteria into phage-rich environments, potentially maintaining long-term coexistence between phage and host populations (Schrag and Mittler, 1996). In our system, soil-dwelling rhizobia evolved under sustained antagonistic selection, while nodule-associated strains experienced relaxed selection, potentially preserving traits that enhance symbiosis at the expense of resistance. To explore whether this ecological divergence creates fitness trade-offs, we conducted competition experiments between strains from different compartments. To test the impact of escaping phage pressure, by entering the root nodules, a plant-based competition experiment was carried out using rhizobia strains from different compartments that had evolved with phage. Strains from (1) primary nodules, which likely avoided prolonged phage exposure, and (2) the soil, which evolved under continuous phage selection. Each was competed against a phage-evolved reference strain in both phage-absent and phage-present environments. For comparison, the ancestral strain was also included in both conditions.

In the soil, phage presence significantly affected bacterial fitness ($F_{(1,38)} = 12.30$, $p < 0.001$), with the effect varying depending on the evolutionary history of the competing strain (Phage × Sample Site interaction: $F_{(2,36)} = 4.44$, $p = 0.019$; **Figure 4a**). In phage-absent environments, all strains performed similarly to the phage-evolved reference, regardless of the compartment they were isolated from. However, when phages were present in the environment, the soil-evolved strain maintained high fitness, while both the ancestral and primary nodule isolates experienced significant reductions. This pattern suggests that prolonged phage exposure

selected for robust resistance in soil strains, while early nodule colonization limited the opportunity for resistance evolution, reducing competitiveness when re-introduced to a phage-rich environment.

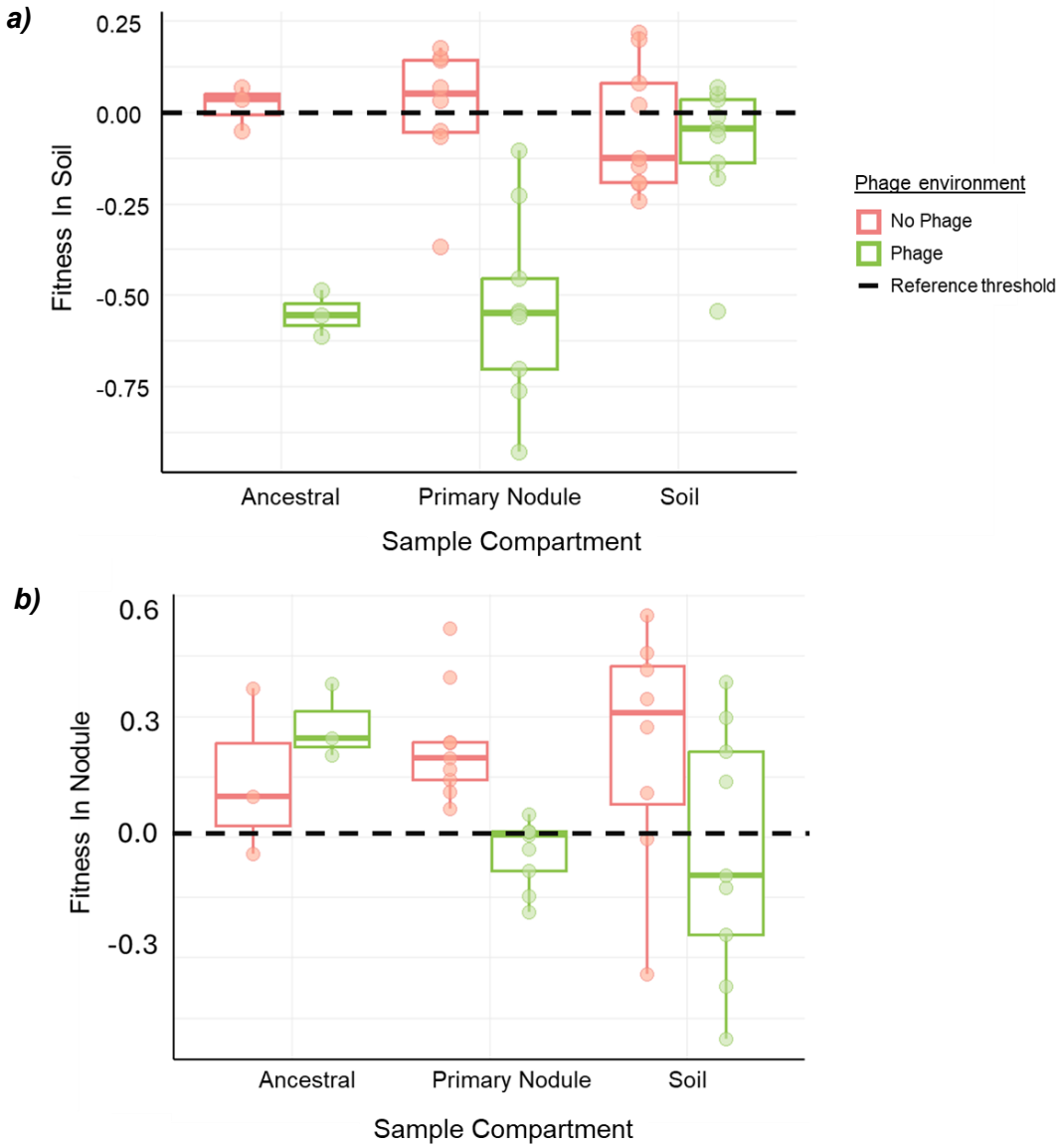

Figure 4: *Competitive fitness of the Ancestral strain, phage-evolved rhizobia from the primary Nodules and phage-evolved rhizobia from the substrate, against the phage-evolved TRX19-MC reference strain. Phage free environment is shown in red, and phage present environment is shown in green.* ***a)*** *shows the fitness in the soil (log10);* ***b)*** *shows the fitness in the root nodules (log10).*

In nodules, the competitive dynamics shifted, where competitive strain fitness was influenced by both phage presence ($F(1,41) = 5.69$, $p = 0.022$) and the sample compartment ($F(4,41) =$

2.87, p = 0.035), with a significant interaction between these factors (F(2,41) = 3.41, p = 0.043; **Figure 4b**). Indicating that the effect of phage presence on fitness in the nodules depends on where the strain originated, reflecting distinct evolutionary responses to phage exposure across compartments. The ancestral strain, which was at a severe disadvantage in the soil, consistently performed well in nodules, outcompeting both phage-evolved strains regardless of whether phages were present in the surrounding environment. Primary nodule isolates, those that had evolved with minimal phage exposure, showed a clear context-dependent response, where in the presence of phages, they experienced reduced fitness in the nodules, demonstrating high susceptibility. However, in the absence of phages, their fitness increased substantially, comparable to the ancestral strain. Suggesting, that susceptibility to phages is offset by a competitive advantage in nodule colonization under phage-free conditions. By contrast, soil isolates, those that evolved under continuous phage pressure, showed greater variability in nodule fitness. While some clones remained competitive, others exhibited reduced fitness when phages were present. These reductions were not observed in the soil, suggesting that maintaining fitness under phage pressure may come at a cost to symbiotic performance. Although not consistent across all isolates, this points to a potential trade-off between resistance and nodulation efficiency.

These findings highlight a clear evolutionary trade-off, where rhizobia that evolved resistance to phages in soil became better adapted to phage-rich environments but, in some cases, showed reduced symbiotic performance. In contrast, strains that avoided strong phage selection by colonizing nodules early remained competitive within the host but were more susceptible to phage when reintroduced to the soil. This pattern is consistent with previous work showing that spatial refuges, such as root nodules or intracellular environments, can allow susceptible bacteria to persist under predation pressure (Schrag and Mittler, 1996; Brockhurst *et al.*, 2006). However, escaping selection in one context may come at a cost in another, particularly when resistance-conferring modifications, impair host recognition and compromise symbiotic compatibility (Kiers *et al.*, 2003; Kiers and Denison, 2008).

5.5 Conclusions

Our work demonstrates how the presence of a plant host disrupts bacterial-phage coevolution by providing an ecological refuge that creates heterogenous selective pressures on rhizobia within one population. By partitioning bacterial populations between root nodules and the surrounding soil, the host exposes subpopulations to contrasting levels of phage pressure. Rhizobia that remained in the soil evolved high levels of resistance, while those that entered nodules early escaped sustained antagonistic selection and retained lower resistance.

This divergence led to environment-specific fitness outcomes. In phage-rich soil environments, phage-resistant strains had a clear competitive advantage, whereas early-colonising strains, despite evolving under phage presence, showed reduced performance. Soil-evolved strains likely maintained high fitness because resistance mutations that emerged under prolonged phage selection were accompanied by compensatory adaptations that offset their metabolic costs. Extended exposure to both phage predation and fluctuating soil conditions would have favoured clones that not only resist infection but also optimise growth and resource use in nutrient-variable environments. This interpretation is consistent with the genomic data, where soil isolates accumulated mutations in metabolic and respiratory genes (e.g., mmgC, cyoB, $iolS_4$), suggesting adaptive shifts enhancing carbon utilisation and energy efficiency. Such compensatory or pleiotropic changes may restore fitness while maintaining resistance, explaining how soil-evolved strains remain competitive despite the typical costs associated with phage resistance (Gurney et al., 2020; Li, Yin and Chen, 2023).

In nodules, by contrast, the competitive dynamics were reversed: primary nodule isolates performed well in the absence of phages, while several soil-evolved strains suffered reduced nodule fitness, particularly when phages were present. These results indicate a trade-off, where adaptation to resist phage in the soil may come at a cost to symbiotic efficiency, a pattern echoed in other systems where resistance carries metabolic or ecological costs (Oono, Denison and Kiers, 2009; Hall *et al.*, 2011)). Genomic analysis supports this functional divergence, revealing that phage-evolved clones, particularly those from the soil, accumulated

more mutations, including in genes linked to metabolism and stress response. Suggesting broader physiological costs associated with resistance (Gurney et al., 2020). Importantly, these adaptations were not uniform across sample compartments, highlighting how spatial structure constrains the paths available for adaptation.

Coevolutionary dynamics in bacteria-phage interactions are therefore not uniform but shaped by ecological heterogeneity. Different environments favour different adaptive solutions, leading to distinct fitness trade-offs. While early nodule colonisation may help maintain genetic diversity by enabling escape from strong selection, it can also create vulnerabilities when bacteria return to phage-rich conditions. Similar trade-offs have been reported in other systems, where adaptation to specific stressors (e.g., antibiotics or phages) compromises other vital functions like metabolic efficiency or symbiosis (Hall et al., 2011; Oono et al., 2009). By interrupting bacterial-phage coevolution, nodulation alters the typical arms race between bacteria and phages. Instead of a continuous cycle of adaptation and counter-adaptation, coevolution is periodically reset as bacteria transition between soil and nodules. This dynamic may help maintain genetic and phenotypic diversity within rhizobial populations, influencing the long-term stability of phage–bacteria coexistence and the structure of microbial communities in the soil.

5.5.1 Future Directions

While this study provides key insights into how nodulation alters bacterial-phage coevolution, yet the long-term effects of escaping coevolution remain unclear. Future work should explore how the continual release of susceptible rhizobia from decaying nodules affects phage persistence, bacterial community structure, and ecosystem function over successive plant generations. Moreover, because rhizobia interact with a complex soil microbiome, it would be beneficial to investigate how their adaptive responses to phage pressure ripple through microbial competition, nutrient cycling, and plant–microbe interactions. Such work will deepen our understanding of how structured environments shape microbial adaptation and clarify the broader ecological and evolutionary consequences of escaping coevolution.

5.6 Supplementary Materials

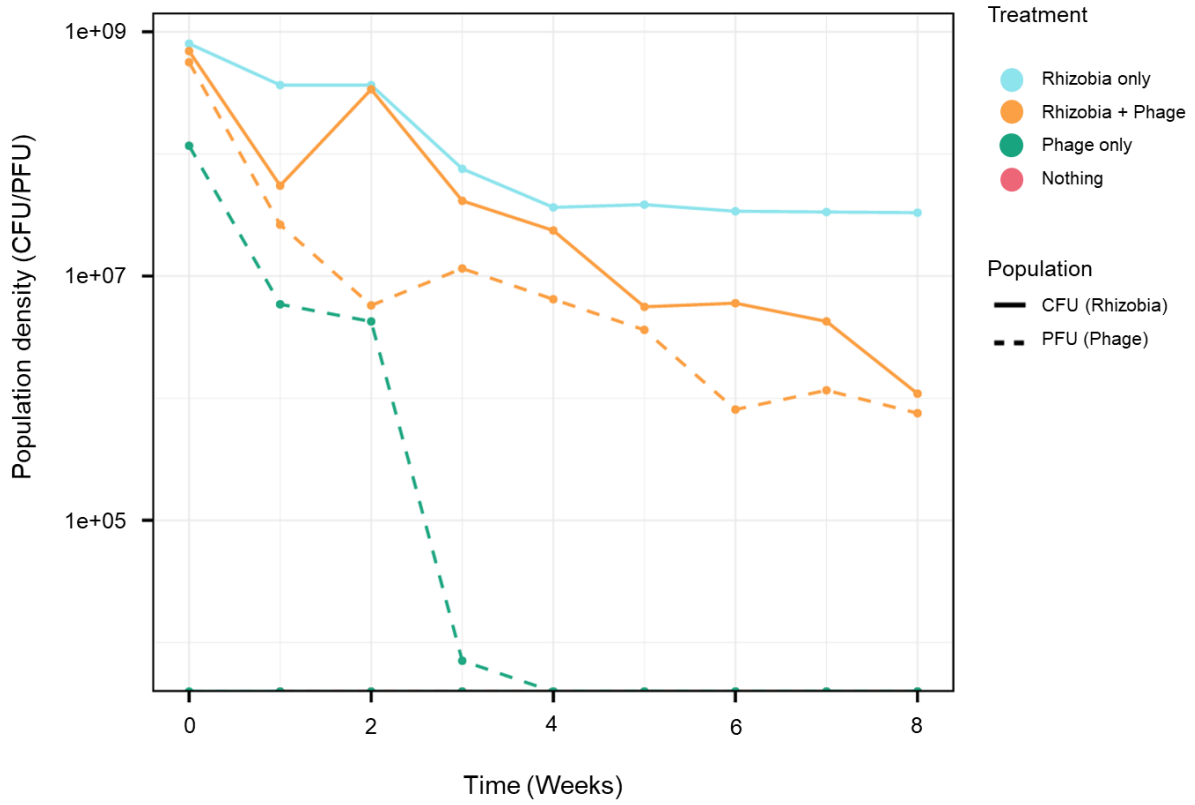

Supplementary Figure S1: *Shows the CFU and PFU of rhizobia and phage populations, based on treatment, across the 8 weeks of plant growth.*

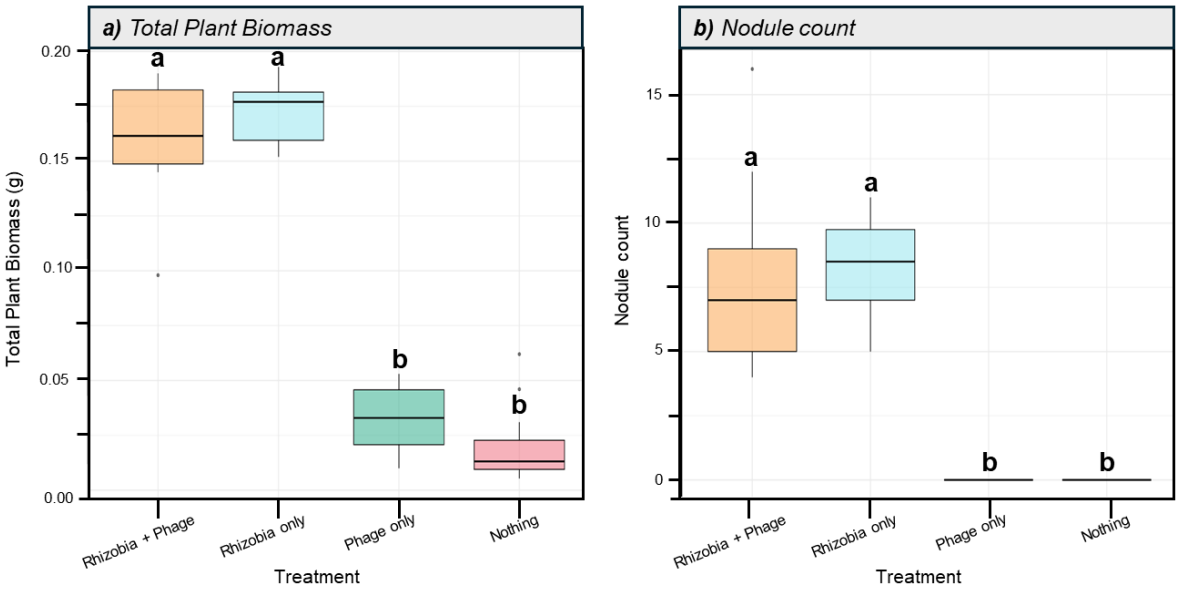

Figure S2*: Plants grown in 50ml falcon tubes;* ***a)*** *the total plant biomass (dried weight, g);* ***b)*** *nodule count, harvested from plants after 8 weeks of growth. Where there is a different letter, p<0.05. Overall harvest does not show differences between phage vs no phage.*

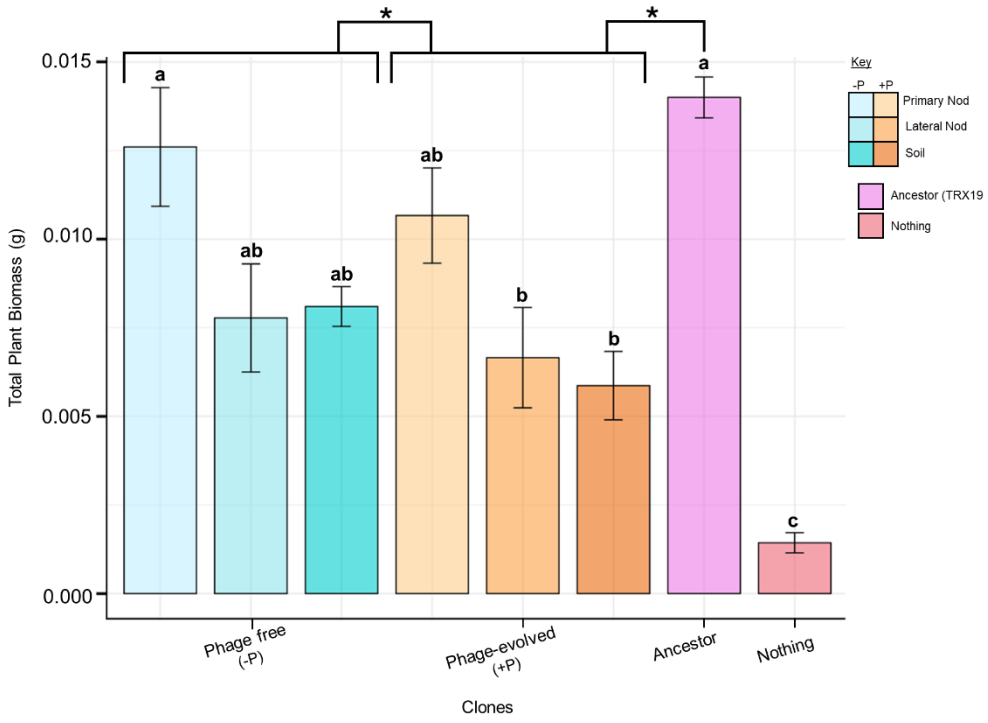

***Figure S3**: Total plant biomass (dried weight) (g), for the most resistant clones from each phage-evolved and phage-free sample compartments (Primary nodule, lateral nodule and soil). Black bars long the top show which groups are statistically different if labelled with a '*'. Letters show post-hoc analysis for between sample compartments and ancestral strain and control, where bars share the same letter there is no significant differences.*

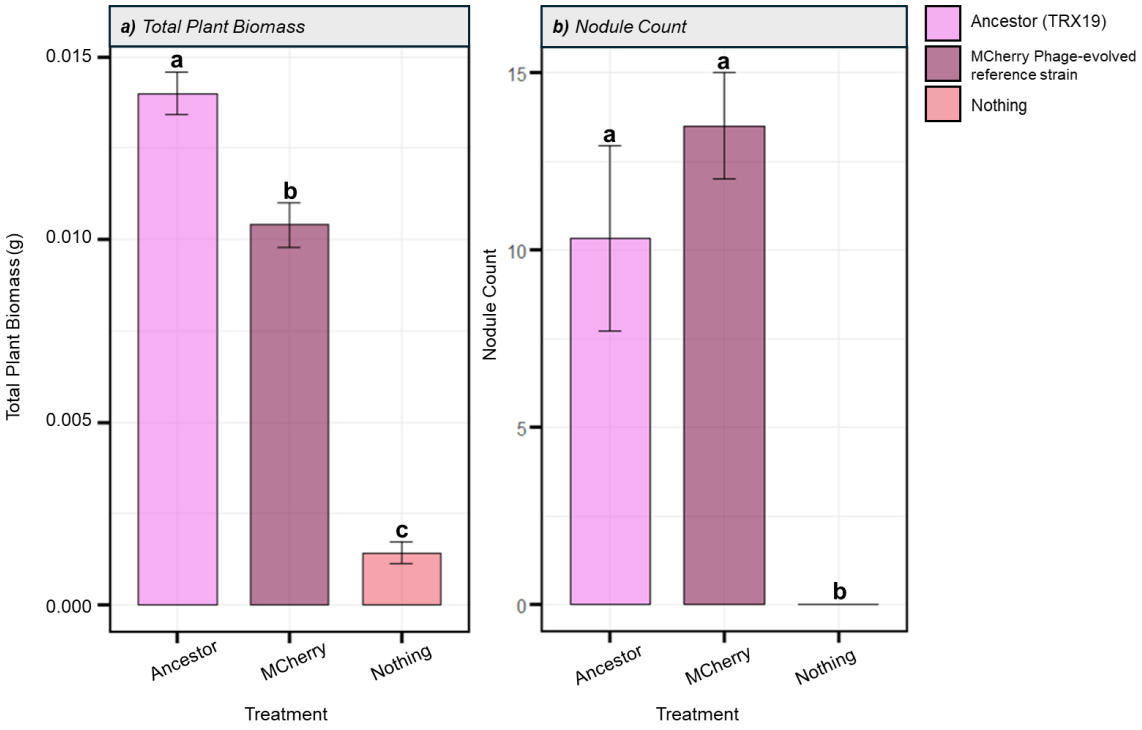

Figure S4: *MCherry evolved reference strain and how it performs in isolated symbiosis vs TRX19 and a negative control* ***a)*** *total plant biomass (g);* ***b)*** *Nodule count. Where there is a different letter p<0.005.*

***Table S1**: Full list of mutations for each Phage treatment sampled from each plant root compartment.*

Sample	Gene	Position	Annotation	Mutation Type	Sequence ID	Treatment	Sample Site
Sample_5-PB2S	cyoB	414990	A416A (GCC?GCT)	non-synonymous	contig_1	phage	Soil
Sample_5-PB2S	cyoB	415053	V395V (GTC?GTG)	non-synonymous	contig_1	phage	Soil
Sample_6-PB4S	cyoB	414962	L426V (CTG?GTG)	non-synonymous	contig_1	phage	Soil
Sample_6-PB4S	cyoB	414993	coding (1243-1245/2004 nt)	frameshift	contig_1	phage	Soil
Sample_6-PB4S	cyoB	415014	G408G (GGT?GGC)	non-synonymous	contig_1	phage	Soil
Sample_22-B5SN	dgoD_1	698670	A275A (GCC?GCT)	non-synonymous	contig_2	nophage	SN
Sample_6-PB4S	dgoD_1	698670	A275A (GCC?GCT)	non-synonymous	contig_2	phage	Soil
Sample_14-B2S	dgoD_1	698697	T266T (ACC?ACT)	non-synonymous	contig_2	phage	Soil
Sample_7-PB5S	dgoD_1	698697	T266T (ACC?ACT)	non-synonymous	contig_2	phage	Soil
Sample_16-B5S	dnaK_2	5013056	I140I (ATT?ATC)	non-synonymous	contig_2	nophage	Soil
Sample_16-B5S	dnaK_2	5013167	L177L (CTC?CTG)	non-synonymous	contig_2	nophage	Soil
Sample_15-B4S	echA8	4783816	coding (363-364/774 nt)	frameshift	contig_2	nophage	Soil
Sample_9-PB2BN	echA8	4783816	coding (363-364/774 nt)	frameshift	contig_2	phage	BN
Sample_22-B5SN	edd	4369814	coding (386/1824 nt)	frameshift	contig_2	nophage	SN
Sample_6-PB4S	edd	4369803	E125E (GAG?GAA)	non-synonymous	contig_2	phage	Soil
Sample_7-PB5S	edd	4369824	D132E (GAC?GAA)	non-synonymous	contig_2	phage	Soil
Sample_11-PB2SN	gabD_1	247434	coding (430-432/1539 nt)	frameshift	contig_2	phage	SN
Sample_16-B5S	gabD_1	247410	T136S (ACC?TCC)	non-synonymous	contig_2	nophage	Soil
Sample_16-B5S	gabD_1	247419	coding (415/1539 nt)	frameshift	contig_2	nophage	Soil
Sample_16-B5S	gabD_1	247423	E140G (GAG?GGG)	non-synonymous	contig_2	nophage	Soil
Sample_16-B5S	gabD_1	247434	coding (430-432/1539 nt)	frameshift	contig_2	nophage	Soil
Sample_22-B5SN	gabD_1	247418	coding (414/1539 nt)	frameshift	contig_2	nophage	SN
Sample_6-PB4S	gabD_1	247379	L125L (CTT?CTG)	non-synonymous	contig_2	phage	Soil
Sample_14-B2S	glgE	690470	A729A (GCA?GCC)	non-synonymous			
Sample_18-B4BN	glgE	690470	A729A (GCA?GCC)	non-synonymous	contig_4	nophage	BN
Sample_19-B5BN	glgE	690481	coding (2175-2176/3225 nt)	frameshift	contig_4	nophage	BN
Sample_21-B4SN	glgE	690458	S733S (TCG?TCC)	non-synonymous	contig_4	nophage	SN
Sample_8-PB4BN	glgE	690428	P743P (CCC?CCG)	non-synonymous	contig_4	phage	BN
Sample_8-PB4BN	glgE	690446	P737P (CCC?CCA)	non-synonymous	contig_4	phage	BN
Sample_8-PB4BN	glgE	690452	D735D (GAT?GAC)	non-synonymous	contig_4	phage	BN
Sample_8-PB4BN	glgE	690475	L728F (CTC?TTC)	non-synonymous	contig_4	phage	BN
Sample_9-PB2BN	glgE	690458	S733S (TCG?TCC)	non-synonymous	contig_4	phage	BN
Sample_9-PB2BN	glgE	690470	A729A (GCA?GCC)	non-synonymous	contig_4	phage	BN
Sample_18-B4BN	glnP_1	523747	T154K (ACG?AAG)	non-synonymous	contig_4	nophage	BN
Sample_19-B5BN	glnP_1	523745	I155F (ATC?TTC)	non-synonymous	contig_4	nophage	BN
Sample_19-B5BN	glnP_1	523770	N146N (AAC?AAT)	non-synonymous	contig_4	nophage	BN
Sample_8-PB4BN	glnP_1	523745	I155F (ATC?TTC)	non-synonymous	contig_4	phage	BN
Sample_8-PB4BN	glnP_1	523747	T154K (ACG?AAG)	non-synonymous	contig_4	phage	BN
Sample_8-PB4BN	glnP_1	523770	N146N (AAC?AAT)	non-synonymous	contig_4	phage	BN
Sample_16-B5S	gsiA_13	323054	D459D (GAC?GAT)	non-synonymous	contig_5	nophage	Soil
Sample_16-B5S	gsiA_13	323131	S434C (AGC?TGC)	non-synonymous	contig_5	nophage	Soil
Sample_5-PB2S	gsiA_13	323072	P453P (CCG?CCT)	non-synonymous	contig_5	phage	Soil
Sample_19-B5BN	gsiB_4	321389	E438A (GAA?GCA)	non-synonymous	contig_5	nophage	BN
Sample_21-B4SN	gsiB_4	321439	H421H (CAC?CAT)	non-synonymous	contig_5	nophage	SN
Sample_16-B5S	hslU	19282	T90T (ACC?ACT)	non-synonymous	contig_2	nophage	Soil
Sample_16-B5S	hslU	19318	coding (232-234/1317 nt)	frameshift	contig_2	nophage	Soil
Sample_20-B2SN	hslU	19282	T90T (ACC?ACT)	non-synonymous	contig_2	nophage	SN
Sample_20-B2SN	hslU	19282	T90T (ACC?ACT)	non-synonymous	contig_2	nophage	SN
Sample_7-PB5S	hslU	19308	I82L (ATC?CTC)	non-synonymous	contig_2	phage	Soil
Sample_13-PB5SN	ILBCKJEK_I	513282	A283S (GCC?TCC)	non-synonymous	contig_1	phage	SN
Sample_14-B2S	ILBCKJEK_I	513283	A283D (GCC?GAC)	non-synonymous	contig_1	nophage	Soil
Sample_15-B4S	ILBCKJEK_I	513262	S276N (AGC?AAC)	non-synonymous	contig_1	nophage	Soil
Sample_20-B2SN	ILBCKJEK_I	513282	coding (847-848/1857 nt)	frameshift	contig_1	nophage	SN
Sample_22-B5SN	ILBCKJEK_I	513224	A263A (GCC?GCT)	non-synonymous	contig_1	nophage	SN
Sample_6-PB4S	ILBCKJEK_I	513251	T272T (ACC?ACG)	non-synonymous	contig_1	phage	Soil
Sample_7-PB5S	ILBCKJEK_I	513179	L248L (CTG?CTT)	non-synonymous	contig_1	phage	Soil
Sample_14-B2S	ILBCKJEK_I	513251	T272T (ACC?ACG)	non-synonymous	contig_1	phage	Soil
Sample_9-PB2BN	ILBCKJEK_I	513282	coding (847-848/1857 nt)	frameshift	contig_1	phage	BN
Sample_12-PB4SN	ILBCKJEK_I	638798	noncoding (1036/1477 nt)	frameshift	contig_2	phage	SN
Sample_12-PB4SN	ILBCKJEK_I	638814	noncoding (1052/1477 nt)	frameshift	contig_2	phage	SN
Sample_12-PB4SN	ILBCKJEK_I	638816	noncoding (1054/1477 nt)	frameshift	contig_2	phage	SN
Sample_12-PB4SN	ILBCKJEK_I	638825	noncoding (1063/1477 nt)	frameshift	contig_2	phage	SN
Sample_13-PB5SN	ILBCKJEK_I	638798	noncoding (1036/1477 nt)	frameshift	contig_2	phage	SN
Sample_13-PB5SN	ILBCKJEK_I	638814	noncoding (1052/1477 nt)	frameshift	contig_2	phage	SN
Sample_13-PB5SN	ILBCKJEK_I	638816	noncoding (1054/1477 nt)	frameshift	contig_2	phage	SN
Sample_5-PB2S	ILBCKJEK_I	638798	noncoding (1036/1477 nt)	frameshift	contig_2	phage	Soil
Sample_5-PB2S	ILBCKJEK_I	638816	noncoding (1054/1477 nt)	frameshift	contig_2	phage	Soil
Sample_6-PB4S	ILBCKJEK_I	638798	noncoding (1036/1477 nt)	frameshift	contig_2	phage	Soil
Sample_7-PB5S	ILBCKJEK_I	638798	noncoding (1036/1477 nt)	frameshift	contig_2	phage	Soil
Sample_10-PB5BN	ILBCKJEK_I	642280	noncoding (1929/2931 nt)	frameshift	contig_2	phage	BN
Sample_12-PB4SN	ILBCKJEK_I	642291	noncoding (1940/2931 nt)	frameshift	contig_2	phage	SN
Sample_20-B2SN	ILBCKJEK_I	642270	noncoding (1919/2931 nt)	frameshift	contig_2	nophage	SN
Sample_5-PB2S	ILBCKJEK_I	642275	noncoding (1924/2931 nt)	frameshift	contig_2	phage	Soil
Sample_6-PB4S	ILBCKJEK_I	642275	noncoding (1924/2931 nt)	frameshift	contig_2	phage	Soil
Sample_9-PB2BN	ILBCKJEK_I	642396	noncoding (2045-2046/2931 nt)	frameshift	contig_2	phage	BN
Sample_9-PB2BN	ILBCKJEK_I	642399	noncoding (2048/2931 nt)	frameshift	contig_2	phage	BN
Sample_11-PB2SN	ILBCKJEK_I	1066069	noncoding (1919/2931 nt)	frameshift	contig_2	phage	SN
Sample_11-PB2SN	ILBCKJEK_I	1066074	noncoding (1924/2931 nt)	frameshift	contig_2	phage	SN
Sample_11-PB2SN	ILBCKJEK_I	1803408	P245A (CCC?GCC)	non-synonymous	contig_2	phage	SN
Sample_12-PB4SN	ILBCKJEK_I	1803408	P245A (CCC?GCC)	non-synonymous	contig_2	phage	SN
Sample_13-PB5SN	ILBCKJEK_I	1803408	P245A (CCC?GCC)	non-synonymous	contig_2	phage	SN
Sample_20-B2SN	ILBCKJEK_I	1803408	P245A (CCC?GCC)	non-synonymous	contig_2	nophage	SN
Sample_9-PB2BN	ILBCKJEK_I	1803413	D246D (GAT?GAC)	non-synonymous	contig_2	phage	BN
Sample_9-PB2BN	ILBCKJEK_I	1803425	Y250Y (TAT?TAC)	non-synonymous	contig_2	phage	BN
Sample_16-B5S	ILBCKJEK_I	5094540	noncoding (42/76 nt)	frameshift	contig_2	nophage	Soil
Sample_16-B5S	ILBCKJEK_I	5094554	noncoding (28/76 nt)	frameshift	contig_2	nophage	Soil
Sample_8-PB4BN	ILBCKJEK_I	5094532	noncoding (50/76 nt)	frameshift	contig_2	phage	BN
Sample_19-B5BN	ILBCKJEK_I	570652	R143R (CGA?CGC)	non-synonymous	contig_5	nophage	BN
Sample_6-PB4S	iolS_4	2401325	E195E (GAA?GAG)	non-synonymous	contig_2	phage	Soil
Sample_6-PB4S	iolS_4	2401460	coding (449-450/990 nt)	frameshift	contig_2	phage	Soil
Sample_7-PB5S	iolS_4	2401313	G199G (GGT?GGC)	non-synonymous	contig_2	phage	Soil
Sample_7-PB5S	iolS_4	2401328	coding (579-582/990 nt)	frameshift	contig_2	phage	Soil
Sample_12-PB4SN	malK_10	5113667	A167A (GCC?GCT)	non-synonymous	contig_2	phage	SN
Sample_22-B5SN	malK_10	5113757	G137G (GGC?GGT)	non-synonymous	contig_2	nophage	SN
Sample_6-PB4S	malK_10	5113667	A167A (GCC?GCT)	non-synonymous	contig_2	phage	Soil
Sample_7-PB5S	malK_10	5113661	L169L (CTG?CTT)	non-synonymous	contig_2	phage	Soil
Sample_14-B2S	malK_10	5113733	I145I (ATC?ATT)	non-synonymous	contig_2	phage	Soil
Sample_15-B4S	mkl	2480737	L175F (CTC?TTC)	non-synonymous	contig_2	nophage	Soil
Sample_9-PB2BN	mkl	2480773	S187A (TCC?GCC)		contig_2	phage	BN
Sample_8-PB4BN	mkl	2480715	A167A (GCA?GCC)		contig_2	phage	BN
Sample_10-PB5BN	mkl	2480715	A167A (GCA?GCC)		contig_2	phage	BN
Sample_11-PB2SN	mkl	2480760	L182L (CTG?CTC)		contig_2	phage	SN
Sample_12-PB4SN	mkl	2480799	coding (585-586/846 nt)		contig_2	phage	SN
Sample_13-PB5SN	mkl	2480822	N203T (AAC?ACC)		contig_2	phage	SN
Sample_21-B4SN	mkl	2480754	Sample_21-B4SN		contig_2	nophage	SN
Sample_20-B2SN	mkl	2480737	L175F (CTC?TTC)	non-synonymous	contig_2	nophage	SN
Sample_19-B5BN	mkl	2480773	S187A (TCC?GCC)		contig_2	nophage	BN
Sample_5-PB2S	mkl	2480822	N203T (AAC?ACC)		contig_2	phage	Soil
Sample_13-PB5SN	mmgC_1	96828	coding (554/1188 nt)	frameshift	contig_1	phage	SN

Sample_13-PB5SN	mmgC_1	96848	A178A (GCC?GCT)	non-synonymous	contig_1	phage	SN
Sample_5-PB2S	mmgC_1	96788	E198E (GAA?GAG)	non-synonymous	contig_1	phage	Soil
Sample_5-PB2S	mmgC_1	96791	L197L (CTC?CTG)	non-synonymous	contig_1	phage	Soil
Sample_5-PB2S	mmgC_1	96796	I196V (ATC?GTC)	non-synonymous	contig_1	phage	Soil
Sample_6-PB4S	mmgC_1	97085	R99R (CGT?CGC)	non-synonymous	contig_1	phage	Soil
Sample_6-PB4S	mmgC_1	96815	coding (566-567/1188 nt)	frameshift	contig_1	phage	Soil
Sample_7-PB5S	mmgC_1	97070	V104V (GTC?GTG)	non-synonymous	contig_1	phage	Soil
Sample_10-PB5BN	oqxB2	1225542	S629T (TCC?ACC)	non-synonymous	contig_2	phage	BN
Sample_10-PB5BN	oqxB2	1225551	A632T (GCC?ACC)	non-synonymous	contig_2	phage	BN
Sample_13-PB5SN	oqxB2	1225542	coding (1885-1886/3201 nt)	frameshift	contig_2	phage	SN
Sample_15-B4S	oqxB2	1225551	A632T (GCC?ACC)	non-synonymous	contig_2	nophage	Soil
Sample_18-B4BN	oqxB2	1225565	F636F (TTT?TTC)	non-synonymous	contig_2	nophage	BN
Sample_19-B5BN	oqxB2	1225542	coding (1885-1886/3201 nt)	frameshift	contig_2	nophage	BN
Sample_20-B2SN	oqxB2	1225542	S629T (TCC?ACC)	non-synonymous	contig_2	nophage	SN
Sample_8-PB4BN	oqxB2	1225571	T638T (ACG?ACC)	non-synonymous	contig_2	phage	BN
Sample_9-PB2BN	oqxB2	1225545	S630P (TCG?CCG)	non-synonymous	contig_2	phage	BN
Sample_12-PB4SN	spuC_2	3613518	E171E (GAG?GAA)	non-synonymous	contig_2	phage	SN
Sample_12-PB4SN	spuC_2	3613539	G164G (GGC?GGT)	non-synonymous	contig_2	phage	SN
Sample_13-PB5SN	spuC_2	3613458	E191E (GAG?GAA)	non-synonymous	contig_2	phage	SN
Sample_13-PB5SN	spuC_2	3613518	E171E (GAG?GAA)	non-synonymous	contig_2	phage	SN
Sample_13-PB5SN	spuC_2	3613521	H170H (CAT?CAC)	non-synonymous	contig_2	phage	SN
Sample_13-PB5SN	spuC_2	3613557	V158V (GTC?GTG)	non-synonymous	contig_2	phage	SN
Sample_5-PB2S	spuC_2	3613458	E191E (GAG?GAA)	non-synonymous	contig_2	phage	Soil
Sample_5-PB2S	spuC_2	3613557	V158V (GTC?GTG)	non-synonymous	contig_2	phage	Soil
Sample_6-PB4S	spuC_2	3613458	E191E (GAG?GAA)	non-synonymous	contig_2	phage	Soil
Sample_7-PB5S	spuC_2	3613465	Y189F (TAC?TTC)	non-synonymous	contig_2	phage	Soil
Sample_7-PB5S	spuC_2	3613521	H170H (CAT?CAC)	non-synonymous	contig_2	phage	Soil
Sample_10-PB5BN	stcD_1	116675	coding (825/2037 nt)	frameshift	contig_4	phage	BN
Sample_18-B4BN	stcD_1	116957	L181L (CTC?CTG)	non-synonymous	contig_4	nophage	BN
Sample_8-PB4BN	stcD_1	116963	S179S (TCT?TCA)	non-synonymous	contig_4	phage	BN
Sample_11-PB2SN	trpB	51594	L92L (CTG?CTT)	non-synonymous	contig_2	phage	SN
Sample_15-B4S	trpB	51548	I107I (ATC?ATT)	non-synonymous	contig_2	nophage	Soil
Sample_16-B5S	trpB	51593	L92L (CTG?CTT)	non-synonymous	contig_2	nophage	Soil
Sample_18-B4BN	trpB	51593	L92L (CTG?CTT)	non-synonymous	contig_2	nophage	BN
Sample_6-PB4S	trpB	51548	I107I (ATC?ATT)	non-synonymous	contig_2	phage	Soil
Sample_6-PB4S	trpB	51593	L92L (CTG?CTT)	non-synonymous	contig_2	phage	Soil
Sample_7-PB5S	trpB	51548	I107I (ATC?ATT)	non-synonymous	contig_2	phage	Soil
Sample_7-PB5S	trpB	51593	L92L (CTG?CTT)	non-synonymous	contig_2	phage	Soil
Sample_11-PB2SN	ugpC_7	2830453	L168L (CTG?CTT)	non-synonymous	contig_2	phage	SN
Sample_16-B5S	ugpC_7	2830453	L168L (CTG?CTT)	non-synonymous	contig_2	nophage	Soil
Sample_22-B5SN	ugpC_7	2830453	L168L (CTG?CTT)	non-synonymous	contig_2	nophage	SN
Sample_6-PB4S	ugpC_7	2830453	L168L (CTG?CTT)	non-synonymous	contig_2	phage	Soil
Sample_7-PB5S	ugpC_7	2830453	L168L (CTG?CTT)	non-synonymous	contig_2	phage	Soil
Sample_15-B4S	ydeP_2	129488	A156A (GCG?GCC)	non-synonymous	contig_4	nophage	Soil
Sample_18-B4BN	ydeP_2	129488	A156A (GCG?GCC)	non-synonymous	contig_4	nophage	BN
Sample_19-B5BN	ydeP_2	129488	A156A (GCG?GCC)	non-synonymous	contig_4	nophage	BN
Sample_5-PB2S	ydeP_2	129488	A156A (GCG?GCC)	non-synonymous	contig_4	phage	Soil
Sample_8-PB4BN	ydeP_2	129488	A156A (GCG?GCC)	non-synonymous	contig_4	phage	BN

5.7 References

Bates, D. *et al.* (2015) 'Fitting Linear Mixed-Effects Models Using lme4', *Journal of Statistical Software*, 67, pp. 1–48. Available at: https://doi.org/10.18637/jss.v067.i01.

Becerra-Rivera, V.A. and Dunn, M.F. (2019) 'Polyamine biosynthesis and biological roles in rhizobia', *FEMS Microbiology Letters*, 366(7), p. fnz084. Available at: https://doi.org/10.1093/femsle/fnz084.

Brockhurst, M.A. *et al.* (2006) 'The impact of phages on interspecific competition in experimental populations of bacteria', *BMC Ecology*, 6(1), p. 19. Available at: https://doi.org/10.1186/1472-6785-6-19.

Bryan, E.M., Beall, B.W. and Moran, C.P. (1996) 'A sigma E dependent operon subject to catabolite repression during sporulation in Bacillus subtilis', *Journal of Bacteriology*, 178(16), pp. 4778–4786. Available at: https://doi.org/10.1128/jb.178.16.4778-4786.1996.

Chepuri, V. *et al.* (1990) 'The sequence of the cyo operon indicates substantial structural similarities between the cytochrome o ubiquinol oxidase of Escherichia coli and the aa3-type family of cytochrome c oxidases.', *Journal of Biological Chemistry*, 265(19), pp. 11185–11192. Available at: https://doi.org/10.1016/S0021-9258(19)38574-6.

Deatherage, D.E. and Barrick, J.E. (2014) 'Identification of mutations in laboratory-evolved microbes from next-generation sequencing data using breseq', *Methods in Molecular Biology (Clifton, N.J.)*, 1151, pp. 165–188. Available at: https://doi.org/10.1007/978-1-4939-0554-6_12.

Fry, J., Wood, M. and Poole, P.S. (2001) 'Investigation of myo-Inositol Catabolism in Rhizobium leguminosarum bv. viciae and Its Effect on Nodulation Competitiveness', *Molecular Plant-Microbe Interactions®*, 14(8), pp. 1016–1025. Available at: https://doi.org/10.1094/MPMI.2001.14.8.1016.

Gómez, P. and Buckling, A. (2011) 'Bacteria-Phage Antagonistic Coevolution in Soil', *Science*, 332(6025), pp. 106–109. Available at: https://doi.org/10.1126/science.1198767.

Gurney, J. *et al.* (2020) 'Phage steering of antibiotic-resistance evolution in the bacterial pathogen, Pseudomonas aeruginosa', *Evolution, Medicine, and Public Health*, 2020(1), pp. 148–157. Available at: https://doi.org/10.1093/emph/eoaa026.

Hall, A.R. *et al.* (2011) 'Host–parasite coevolutionary arms races give way to fluctuating selection', *Ecology Letters*, 14(7), pp. 635–642. Available at: https://doi.org/10.1111/j.1461-0248.2011.01624.x.

Hampton, H.G., Watson, B.N.J. and Fineran, P.C. (2020) 'The arms race between bacteria and their phage foes', *Nature*, 577(7790), pp. 327–336. Available at: https://doi.org/10.1038/s41586-019-1894-8.

Heilmann, S., Sneppen, K. and Krishna, S. (2012) 'Coexistence of phage and bacteria on the boundary of self-organized refuges', *Proceedings of the National Academy of Sciences of the United States of America*, 109(31), pp. 12828–12833. Available at: https://doi.org/10.1073/pnas.1200771109.

Howieson, J.G., Dilworth, M.J., 2016. Working with rhizobia, Australian Centre for International Agricultural Research. Canberra.

Kiers, E.T. *et al.* (2003) ‘Host sanctions and the legume–rhizobium mutualism’, *Nature*, 425(6953), pp. 78–81. Available at: https://doi.org/10.1038/nature01931.

Kiers, E.T. and Denison, R.F. (2008) ‘Sanctions, Cooperation, and the Stability of Plant-Rhizosphere Mutualisms’, *Annual Review of Ecology, Evolution, and Systematics*, 39(Volume 39, 2008), pp. 215–236. Available at: https://doi.org/10.1146/annurev.ecolsys.39.110707.173423.

Kohler, P.R.A., Choong, E.-L. and Rossbach, S. (2011) ‘The RpiR-Like Repressor IolR Regulates Inositol Catabolism in Sinorhizobium meliloti’, *Journal of Bacteriology*, 193(19), pp. 5155–5163. Available at: https://doi.org/10.1128/jb.05371-11.

Koskella, B. and Brockhurst, M.A. (2014) ‘Bacteria–phage coevolution as a driver of ecological and evolutionary processes in microbial communities’, *FEMS Microbiology Reviews*, 38(5), pp. 916–931. Available at: https://doi.org/10.1111/1574-6976.12072.

Labrie, S.J., Samson, J.E. and Moineau, S. (2010) ‘Bacteriophage resistance mechanisms’, *Nature Reviews Microbiology*, 8(5), pp. 317–327. Available at: https://doi.org/10.1038/nrmicro2315.

Lenski, R.E. (1988) ‘Experimental studies of pleiotropy and epistasis in escherichia coli. i. variation in competitive fitness among mutants resistant to virus t4’, *Evolution; International Journal of Organic Evolution*, 42(3), pp. 425–432. Available at: https://doi.org/10.1111/j.1558-5646.1988.tb04149.x.

Li, C.-Y., Yin, J. and Chen, L. (2023) ‘Impact of social distancing on disease transmission risk in the context of a pandemic’, *Physical Review E*, 108(5), p. 054115. Available at: https://doi.org/10.1103/PhysRevE.108.054115.

Lu, C.-D. *et al.* (2002) ‘Functional analysis and regulation of the divergent spuABCDEFGH-spuI operons for polyamine uptake and utilization in Pseudomonas aeruginosa PAO1’, *Journal of Bacteriology*, 184(14), pp. 3765–3773. Available at: https://doi.org/10.1128/JB.184.14.3765-3773.2002.

Lunak, Z.R. and Noel, K.D. (2015) ‘A quinol oxidase, encoded by cyoABCD, is utilized to adapt to lower O2 concentrations in Rhizobium etli CFN42’, *Microbiology*, 161(Pt 1), pp. 203–212. Available at: https://doi.org/10.1099/mic.0.083386-0.

Meaden, S. and Koskella, B. (2017) ‘Adaptation of the pathogen, Pseudomonas syringae, during experimental evolution on a native vs. alternative host plant’, *Molecular Ecology*, 26(7), pp. 1790–1801. Available at: https://doi.org/10.1111/mec.14060.

Oldroyd, G.E.D. *et al.* (2011) ‘The rules of engagement in the legume-rhizobial symbiosis’, *Annual Review of Genetics*, 45, pp. 119–144. Available at: https://doi.org/10.1146/annurev-genet-110410-132549.

Oono, R., Denison, R.F. and Kiers, E.T. (2009) ‘Controlling the reproductive fate of rhizobia: how universal are legume sanctions?’, *New Phytologist*, 183(4), pp. 967–979. Available at: https://doi.org/10.1111/j.1469-8137.2009.02941.x.

Paterson, S. *et al.* (2010) ‘Antagonistic coevolution accelerates molecular evolution’, *Nature*, 464(7286), pp. 275–278. Available at: https://doi.org/10.1038/nature08798.

Poole, P., Ramachandran, V. and Terpolilli, J. (2018) ‘Rhizobia: from saprophytes to endosymbionts’, *Nature Reviews Microbiology*, 16(5), pp. 291–303. Available at: https://doi.org/10.1038/nrmicro.2017.171.

Price, M.N. *et al.* (2018) 'Mutant phenotypes for thousands of bacterial genes of unknown function', *Nature*, 557(7706), pp. 503–509. Available at: https://doi.org/10.1038/s41586-018-0124-0.

R Studio Team, 2020. RStudio: Integrated Development for R.

Ratcliff, W.C., Underbakke, K. and Denison, R.F. (2011) 'Measuring the fitness of symbiotic rhizobia', *Symbiosis*, 55(2), pp. 85–90. Available at: https://doi.org/10.1007/s13199-011-0150-2.

Reddick, J.J. *et al.* (2017) 'First Biochemical Characterization of a Methylcitric Acid Cycle from Bacillus subtilis Strain 168', *Biochemistry*, 56(42), pp. 5698–5711. Available at: https://doi.org/10.1021/acs.biochem.7b00778.

Remigi, P. *et al.* (2016) 'Symbiosis within Symbiosis: Evolving Nitrogen-Fixing Legume Symbionts', *Trends in Microbiology*, 24(1), pp. 63–75. Available at: https://doi.org/10.1016/j.tim.2015.10.007.

Scanlan, P.D., Buckling, A. and Hall, A.R. (2015) 'Experimental evolution and bacterial resistance: (co)evolutionary costs and trade-offs as opportunities in phage therapy research', *Bacteriophage*, 5(2), p. e1050153. Available at: https://doi.org/10.1080/21597081.2015.1050153.

Schrag, S.J. and Mittler, J.E. (1996) 'Host-Parasite Coexistence: The Role of Spatial Refuges in Stabilizing Bacteria-Phage Interactions', *The American Naturalist*, 148(2), pp. 348–377.

Simmons, E.L. *et al.* (2020) 'Biofilm Structure Promotes Coexistence of Phage-Resistant and Phage-Susceptible Bacteria', *mSystems*, 5(3), pp. e00877-19. Available at: https://doi.org/10.1128/mSystems.00877-19.

Wickham H, Averick M, Bryan J, Chang W, McGowan LD, François R, Grolemund G, Hayes A, Henry L, Hester J, Kuhn M, Pedersen TL, Miller E, Bache SM, Müller K, Ooms J, Robinson D, Seidel DP, Spinu V, Takahashi K, Vaughan D, Wilke C, Woo K, Yutani H (2019). "Welcome to the tidyverse." *Journal of Open Source Software*, **4**(43), 1686. doi:10.21105/joss.01686.

Chapter 6: The Ecology of Escape: Refuge-Mediated Trade-offs in Structured Bacteria–Phage Systems

6.1 Abstract

Microbial communities are shaped by ecological interactions, with bacteriophages imposing strong selection on bacteria, driving resistance evolution. However, resistance often carries fitness costs, particularly in structured environments where spatial refuges, such as bacterial biofilms or root nodules, allow susceptible bacteria to persist. In rhizobia-phage interactions, resistant rhizobia have been seen to be less competitive inside root nodules. Using mathematical modelling, we show that resistance associated trade-offs (increased mortality and exit rates from refuges), are necessary for susceptible bacteria to persist and dominate in the refuge. Without these costs, resistant strains dominate in refuge and external environments. We also incorporate seasonal fluctuations in resource availability, demonstrating that high seasonal variation in the refuge temporarily favours susceptible bacteria by increasing their dispersal into the external environment. However, resistant strains ultimately recover, indicating that seasonality slows competitive exclusion but does not permanently shift the balance. These findings suggest that structured habitats and environmental variability play a key role in maintaining microbial diversity. By integrating resistance trade-offs and seasonal dynamics, our model provides insights into bacterial-phage coexistence. Future research should incorporate bacterial replication dynamics to enhance ecological realism and further explore how seasonal cycles within and out of agriculture influence long term microbial stability in the rhizobia-legume system.

6.2. Introduction

Microbial populations are shaped by ecological interactions and evolutionary pressures, particularly in environments where predator-prey relationships drive rapid adaptations. Bacteriophages (phages), as the primary predators of bacteria, impose strong selective pressures that lead to the evolution of bacterial resistance (Scanlan, Buckling and Hall, 2015). However, in structured environments, where bacteria can temporarily escape phage predation, coevolutionary dynamics become more complex, influenced by spatial heterogeneity, eco-evolutionary feedbacks, and genetic constraints (Buckingham and Ashby, no date). Such structured environments include biofilms, intracellular niches, and host-associated refuges, all of which can significantly alter the expected evolutionary trajectories. Theoretical models highlight how these spatial structures can prevent resistance from rapidly becoming fixed within bacterial populations, slowing the pace of evolutionary arms races and maintaining genetic diversity over extended periods (Brockhurst *et al.*, 2007; Heilmann, Sneppen and Krishna, 2012; Best *et al.*, 2017). Thus, spatial refuges provide critical ecological contexts in which susceptible bacterial populations can persist despite strong phage selection, buffering them from extinction, and actively shaping long term bacterial-phage coexistence (Schrag and Mittler, 1996). This dynamic is particularly relevant for facultative symbionts like rhizobia, which are not dependent on their legume host for survival. They are adapted to persist and replicate in the soil (the free-living state) but can also enter root nodules (the refuge state). This dual lifestyle means the refuge is not essential for survival, but rather an alternative ecological niche that offers protection at the cost of different selection pressures.

In previous work (**chapter 4)**, we have shown, using a modelling approach, the presence of a spatial refuge can promote the stability of susceptible populations and their co-existence with a free-living parasite (phage). However, in this previous model, bacterial populations were homogeneous in their susceptibility, where only a single population coexisted with a parasitic population through refuge dynamics. While the previous chapter (**chapter 4**) established that spatial refuges stabilize susceptible bacteria, the presence of resistant bacteria introduces a

new competitive dynamic. Unlike susceptible strains, which rely on the refuge to persist, resistant bacteria can survive in the phage-exposed soil environment. This changes the fundamental ecological question from whether refuges promote bacterial persistence to whether refuges, in combination with fitness trade-offs, can maintain diversity between competing bacterial populations in the presence of phage predation. Experimental evidence from **chapter 5** strongly suggests that resistance to phage carries fitness costs. Specifically, competition experiments demonstrated that phage-resistant rhizobia were less competitive inside root nodules compared to susceptible rhizobia, and vice versa in the external environment, likely due to fitness burdens associated with maintaining resistance mechanisms. This aligns with findings from Chapter 3, which showed that coevolution with some phages led to a complete loss of symbiotic function, including the ability to form nodules. These results imply that spatial refuges not only offer susceptible bacteria protection from phages but also favour strains that maintain higher fitness inside the refuge. While the experimental data strongly suggest the presence of fitness trade-offs, they do not define their exact nature or quantify their effects on bacterial coexistence. This limitation necessitates the use of mathematical modelling to systematically explore different potential trade-offs and determine the conditions under which susceptible and resistant bacteria can coexist.

6.2.2 Competition, predation and spatial structures

Competition between multiple prey species facing a shared predator is a fundamental ecological concept often described through predator-mediated coexistence models (Holt, 1977; Levin, Stewart and Chao, 1977). Such models emphasize that prey persistence is influenced not only by competitive abilities but also by differential predation pressures. In microbial ecosystems, particularly bacteria-phage interactions, these dynamics are characterized by trade-offs associated with resistance. Resistant bacterial strains gain rapid survival advantages under strong predation pressure but typically incur fitness costs, such as reduced growth rates or competitiveness (Bohannan and Lenski, 2000; Gómez and Buckling, 2011). These trade-offs allow susceptible strains to persist or even dominate when predation

pressures relax, thereby maintaining genetic diversity through fluctuating selection pressures. Spatial structure further influences these interactions by modifying predation risks and competition. Structured environments such as biofilms and host-associated refuges create spatial heterogeneity, significantly altering competitive outcomes. Empirical evidence shows that these refuges effectively protect susceptible bacteria by physically restricting phage access, enabling coexistence despite strong external predation (Heilmann et al., 2012; Brockhurst et al., 2007) (Brockhurst *et al.*, 2007; Heilmann, Sneppen and Krishna, 2012). For instance, Brockhurst et al. (2007) demonstrated that resistant bacteria within biofilms experience substantial fitness costs, facilitating susceptible strain persistence.

Building upon previous research, this study investigates competition between resistant and susceptible bacterial strains within a structured bacterial-phage system using a resident-invader modelling approach (Lenski and Levin, 1985; Holt, Grover and Tilman, 1994). This approach allows us to identify conditions under which invading susceptible strains can establish alongside resistant resident populations, explicitly examining fitness trade-offs associated with resistance, such as increased mortality within refuges or altered movement rates out of refuges. Specifically, we determine whether spatial refuges alone can sustain susceptible bacteria, or if these resistance trade-offs are necessary for coexistence. Additionally, we explore ecological conditions that enable susceptible strains to dominate within refuges while resistant strains prevail externally. Overall, our study aims to clarify how spatial structure, and evolutionary constraints interact to shape bacterial coexistence and community stability under phage predation.

6.3. Methods

6.3.1 Model assumptions

This model describes the population dynamics of susceptible and resistant bacteria in the presence of a free-living parasite population, incorporating both competition and refuge-mediated interactions. The system accounts for bacterial growth, infection, parasite

replication, and population movement into and out of a spatial refuge, which provides temporary protection from parasite infection. As the model is expanded, seasonal variability is introduced, allowing an exploration of how fluctuations in environmental conditions impact coexistence and competitive outcomes between susceptible and resistant bacteria populations. By incorporating competition, refuge effects, and seasonal variation, this model provides a framework for testing under what conditions susceptible bacteria persist alongside resistant populations despite parasite infection.

The model is shown and described as:

$$\frac{dS}{dt} = r\left(1 - \frac{S+E+I}{k(t)}\right)S - cS - \beta_S SP - \mu_{in,S}S + \mu_{out,S}R_S$$

$$\frac{dE}{dt} = r\left(1 - \frac{S+E+I}{k(t)}\right)E - cE - \beta_E EP - \mu_{in,E}E + \mu_{out,E}R_E$$

$$\frac{dI}{dt} = \beta_S SP + \beta_E EP - cI - \gamma I$$

$$\frac{dP}{dt} = \gamma \mathrm{n} I - bP$$

$$\frac{dR_S}{dt} = r\left(1 - \frac{R_S+R_E}{m(t)}\right)R_S + \mu_{in,S}S - \alpha_S R_S - \mu_{out,S}R_S$$

$$\frac{dR_E}{dt} = r\left(1 - \frac{R_S+R_E}{m(t)}\right)R_E + \mu_{in,E}E - \alpha_E R_E - \mu_{out,E}R_E$$

The susceptible *(S)* and resistant *(E)* bacterial populations compete for the same resources in the external environment and within the spatial refuge. Both populations share a common carrying capacity in the external environment, represented by $k(t)$, and a common carrying capacity in the refuge, represented by $m(t)$. The competitive interaction between the two populations is captured in the growth terms, $r\left(1 - \frac{S+E+I}{k(t)}\right)$ (external environment and

$r\left(1-\frac{R_S+R_E}{m(t)}\right)$ (refuge). Initially, these carrying capacities are assumed to be constant, with, $k(t)= k_0$ and $m(t)= m_0$, meaning that resource availability remains stable over time. However, later in the model, seasonal fluctuations in environmental conditions are incorporated by introducing time-dependent carrying capacities, allowing an exploration of how periodic changes in resource availability influence competition between the two populations.

Both susceptible (S) and resistant (E) populations grow at rate r, and all populations experience a natural death rate of c. However, infection by parasite (P) occurs when either S or E comes into contact with P, with infection parameters given by β_S and β_E, respectively. Once infected, the individual experiences an accelerated death rate of γ and do not recover, meaning they are removed from the system. In this system when infected hosts die at an accelerated death due to the infection, this directly increases the parasite population by n, while natural parasite death is represented by b.

A subset of both S and E populations can escape parasite infection by moving into a parasite free spatial refuge. These refuge populations R_S (susceptible population in refuge) and R_E (resistant population in refuge) grow at the same rate r as their external counterparts, but they still compete for limited refuge space/recourses, as captured by their shared carrying capacity, $m(t)$. The refuge susceptible and resistant populations experience natural death rates at α_S and α_E (respectively). The rate at which susceptible and resistant individuals move into the refuge is represented by $\mu_{in,S}$ and $\mu_{in,E}$ (respectively) while $\mu_{out,S}$ and $\mu_{out,E}$ denotes the rate at which individuals leave the refuge and return to the susceptible and resistant populations outside. These rates reflect the speed/frequency at which individuals from the susceptible population migrate to and from the refuge. Both movement rates are assumed to be completely passive, where there is no choice or decision to enter a refuge based on infection prevalence.

6.3.2 Sensitivity analysis

To replicate the empirical results from **chapter 5**, where susceptible bacteria (S) outcompete resistant bacteria (E) in the refuge but not in the external environment, we conducted a sensitivity analysis to explore the trade-offs necessary for this outcome (**Figure S1-S2**). Since empirical data suggest that resistant strains dominate in the soil but are outcompeted in the refuge (**chapter 5**), we explored two biologically plausible mechanisms that could explain this pattern. The first mechanism, adjusted mortality of both strains in the refuge (α_S and α_E), where differing death rates in the refuge could reflect metabolic costs, inefficient symbiosis, or other fitness burdens associated with resistance mechanisms. The second mechanism, is altered exit rate of strains from the refuge ($\mu_{out,S}$ and $\mu_{out,E}$). The second mechanism involves altering the exit rates of bacterial strains from the refuge ($\mu_{out,S}$ and $\mu_{out,E}$), reflecting differences in how well susceptible and resistant bacteria are adapted to refuge conditions due to resistance costs. For example, a key phage resistance mechanism (as discussed in Chapter 3) is the modification of flagella or surface polysaccharides, which would also result in reduced motility. In this model, such a strain would have a higher effective exit rate because its reduced motility would make it less likely to successfully infect a root and enter the refuge in the first place.

While adjusting the mortality rates (α_S and α_E) within the refuge could potentially allow susceptible strains to dominate, relying exclusively on mortality differences might impy biologically unrealistic fitness costs for resistant strains. (**Figure S2**), Resistance mechanisms may also impose other fitness costs beyond increased mortality, such as reduced motility or altered behaviour, affecting bacterias ability to exit the refuge. Therefore, variations in exit rates ($\mu_{out,S}$ and $\mu_{out,E}$) were also explored, capturing a broader range of biologically plausible trade-offs and providing a more comprehensive understanding of how fitness costs shape coexistence between phage populations, susceptible and resistant bacterial populations within a spatial refuge.

These parameters were chosen as they represent fitness costs that could selectively disadvantage resistant bacteria within the refuge. The selected trade-off values for these

parameters are shown in **Table 1**, providing a baseline framework for further analysis of bacterial coexistence in a spatial refuge.

Table 1: *Description of parameters.*

Parameter	Description	Default value
E	Resistant Bacteria Population	
S	Susceptible Bacteria Population	
I	Infected Bacteria Population	
P	Parasite population	
R_E	Resistant Bacteria Refuge population	
R_S	Susceptible Bacteria Refuge Population	
r	Growth rate	2
c	'Normal' death rate	1
β_E	Resistant infection rate	0.01
β_S	Susceptible infection rate	0.04
γ	Infection induced death	0.1
n	Parasite growth	5
b	Parasite 'death'	0.3
k	Carrying capacity	1000
δ_k	Amplitude of seasonal fluctuations in main population	0.0
m	Carrying capacity of refuge	1000
δ_k	Amplitude of seasonal fluctuations in refuge populations	0.0
	Refuge - resistant population specific parameters	
$\mu_{in,E}$	Movement into the refuge from the resistant	0.1
$\mu_{out,E}$	Movement out of the refuge to the resistant	0.5
α_E	Death in the refuge for resistant	1.5
	Refuge – susceptible population specific parameters	

$\mu_{in,S}$	Movement into the refuge from the susceptible	0.1
$\mu_{out,S}$	Movement out of the refuge to the susceptible	0.01
α_S	Death in refuge for susceptible	0.5

6.3.3 Incorporating seasonal variation

The carrying capacities for both the external, $k(t)$, and refuge, $m(t)$, environments are modelled as time-dependent functions to reflect seasonal fluctuations in environmental conditions, these are represented as:

$$k(t) = k_0(1 + \delta_k \sin(2\pi t))$$

$$m(t) = m_0(1 + \delta_m \sin(2\pi t))$$

The baseline carrying capacities, $k0$ and $m0$, represent the maximum population sizes that the soil and refuge can sustain in the absence of fluctuations. The parameters δk and δm introduce periodic fluctuations, where their values determine the amplitude of the seasonal variation.

Initially, the model assumes no seasonal variation, setting $\delta_k = 0$ and $\delta_m = 0$, meaning that the carrying capacities remain constant over time. However, as we investigate effects of seasonal fluctuations in resourced availability and environmental conditions, these parameters take nonzero values, allowing the carrying capacities to vary periodically. The function $\mathbf{sin(2\pi t)}$ ensures that carrying capacities follow a smooth repeating seasonal cycle, where, in this system, resource availability is lower during 'winter' months and higher during 'summer'. Here, one time unit corresponds to a full seasonal cycle. This framework provides a general exploration of how seasonality influences bacterial competition, rather than a precise representation of bacterial replication times.

6.4 Results

The goal of this modelling work was to determine the conditions under which susceptible strains could persist in a spatial refuge, despite the selective advantage of resistance in the presence of a parasite population.

6.4.1 Trade-offs in resistant strains

To explore the conditions under which susceptible strains could persist in a spatial refuge, we first simulated the model using parameters where the only difference between susceptible and resistant bacteria was their respective infection rates (μ_{outS} and μ_{outE} = 0.1, and α_S and α_E= 1). As expected, resistant bacteria dominated both the external and refuge environments, leading to a significant decline in susceptible bacteria populations (**Figure 1a**). This result aligns with the expectation that resistance provides a strong selective advantage in the presence of the parasite population, leading to the exclusion of more vulnerable susceptible strains. We then incorporated resistance-associated trade-offs into the model by using the default parameters established in **Table 1**, which include increased death rates and higher exit rates for resistant bacteria in the refuge. These trade-offs were identified as biologically plausible mechanisms that could explain the observed empirical pattern in **chapter 5**, where susceptible bacteria outcompete resistant bacteria in the refuge but not in the external environment. When these trade-offs were included, susceptible bacteria consistently established and maintained a dominant population in the refuge while resistant bacteria continued to dominate the external environment (**Figure 1b**). This shift demonstrates that resistance alone does not guarantee competitive superiority in all environments; rather, the costs associated with resistance within the refuge create opportunities for susceptible strains to persist.

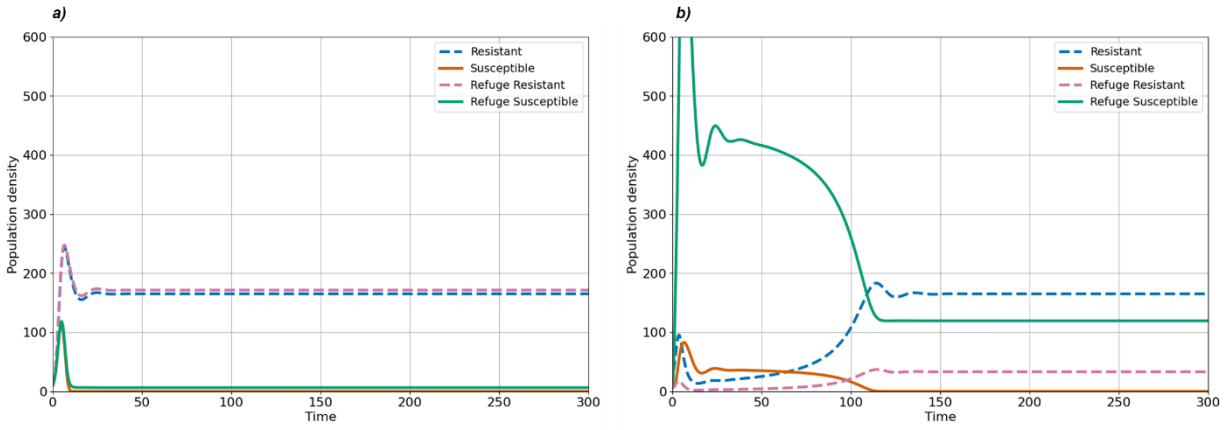

Figure 1: *Shows time series plots where the dashed lines represent resistant populations, and the solid line represents susceptible populations. Blue is resistant in the external environment, pink is resistant in the refuge. Orange is the susceptible in the external environment, green is the susceptible in the refuge.*

a) *Time series of the model, where resistant (E) and susceptible (S) populations, all parameters are the same except for their infection rates. Where β_E (resistant infection) = 0.01 and β_s (resistant infection) = 0.04.*

b) *Shows the time series with new default parameters from Table 1, that allow the susceptible populations to win in the refuge. Where $\mu_{out,E}$ (resistant exit rate from refuge) = 0.5, $\mu_{out,S}$ (susceptible exit rate from refuge) = 0.01, α_E (resistant death in refuge) = 1.5, α_E (susceptible death in refuge) = 0.5.*

To better understand the effects of these trade-offs, we systematically varied the resistant strain's mortality (α_E) and exit rate ($\mu_{out,E}$) from the refuge while keeping susceptible refuge parameters fixed. **Figure 2a** illustrates how changes in these parameters influence both susceptible and resistant bacterial densities in the refuge, by showing the net population difference between each strain. At low levels of both resistant death in refuge and movement out of refuge (α_E and $\mu_{out,E}$ respectively) resistant bacteria remain dominant in the refuge. However, as both parameters increases, the competitive balance shifts in favour of susceptible bacteria, allowing them to outcompete resistant strains within the refuge. At higher values of both parameters, susceptible bacteria completely dominate, while resistant strains fail to establish a stable population. However, when only one of these parameters increases while the other remains low, more extreme trade-offs are required to shift the competitive balance in favour of susceptible bacteria.

For instance, if only the exit rate ($\mu_{out,E}$)) increases, resistant bacteria can still persist if their mortality rate remains low, as they are not experiencing significant death within the refuge. Similarly, if only the mortality rate (α_E) increases, resistant bacteria can still maintain a presence if their exit rate is low, allowing them to remain in the refuge for extended periods. This interdependence suggests that while each parameter contributes to resistance-associated costs, a stronger effect is observed when both costs are elevated simultaneously. In cases where only one parameter is increased, a more extreme threshold is needed before susceptible bacteria can fully dominate in the refuge.

Figures 2b-d further illustrate these dynamics through time series simulations with different trade-off intensities. When resistance associated costs are low (**Figure 2b**), resistant bacteria remain dominant in the refuge. However, as the trade-offs increase (**Figures 2c-d**), susceptible bacteria become increasingly competitive, leading to their dominance in the refuge. Notably, despite these shifts within the refuge, resistant strains consistently outcompete susceptible strains in the external environment. This pattern suggests that while resistance trade-offs can impact within-refuge competition, they do not alter the broader dominance of resistant bacteria in the external environment, likely due to their advantage in surviving parasite infection.

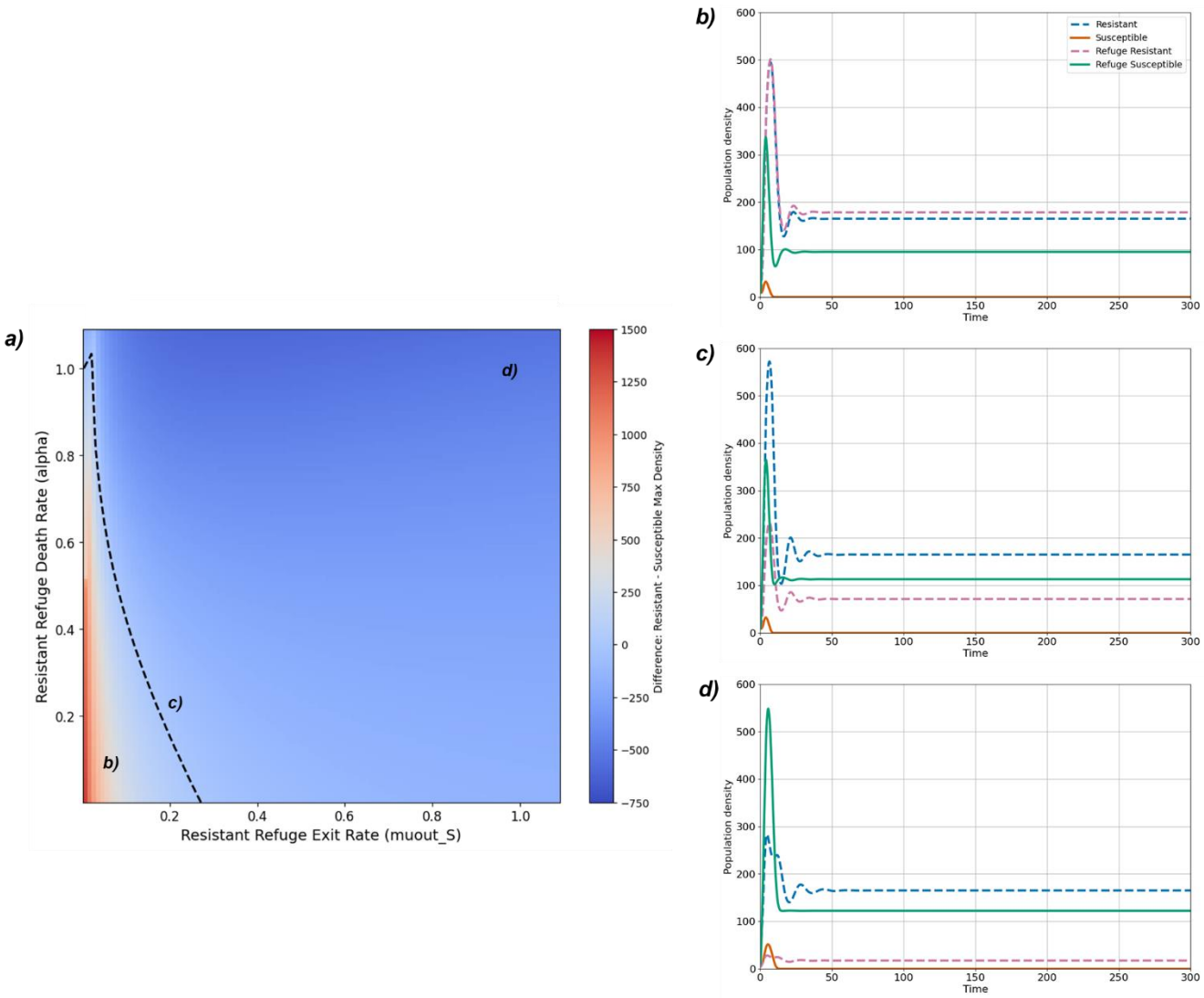

Figure 2:

a). *This heatmap illustrates the difference in maximum population densities between the resistant (R_E) and susceptible (R_S) strains within the refuge across varying resistant strain exit rate ($\mu_{out,E}$) and resistant strain death rate within refuge (α_E) ; when the susceptible refuge population has fixed parameters of exit rate ($\mu_{out,S}$) = 0.01 and death rate within refuge (α_S) = 0.5. The colour gradient represents the net population difference, calculated as $max\ R_E$ - $max\ R_S$, where positive values (red) indicate higher resistant strain densities in the refuge and negative values (blue) indicate higher susceptible strain densities. The black dashed line represents where the resistant refuge population wins.*

(b - d) *Shows a time series with fixed susceptible refuge population parameters as in a), whilst the resistant refuge population:* **b)** *exit rate ($\mu_{out,E}$) = 0.1 death rate within refuge (α_E) = 0.1;* **c)** *exit rate ($\mu_{out,E}$) = 0.25, death rate within refuged (α_E) = 0.25* **d)** *exit rate ($\mu_{out,E}$) = 1 death rate within refuge (α_E) = 1.*

6.4.2 Seasonal cycling and its impact on population dynamics

Having established that trade-offs in resistance are necessary for susceptible bacteria to persist in the refuge, we next introduced seasonal fluctuations in carrying capacity to reflect natural variations in resource availability. In a rhizobia-legume environment, bacterial populations can be influenced by seasonal changes, such as plant growth cycles and fluctuating soil conditions, which can impact both the external and refuge environments (Hirsch, 2002; Burghardt, 2018). To incorporate this ecological realism, we modelled periodic changes in carrying capacity for both habitats and examined how they affect bacterial competition. Each cycle represents one year, during which resource availability oscillates due to seasonal environmental changes. The external carrying capacity $k(t)$ and refuge carrying capacity $m(t)$ are modelled sinusoidally, with δ_k controlling seasonal variation in the external environment and δ_m controlling seasonal variation in the refuge. By incorporating sinusoidal variations in carrying capacity, we explored whether seasonal fluctuations alter the competitive interactions between susceptible and resistant bacteria.

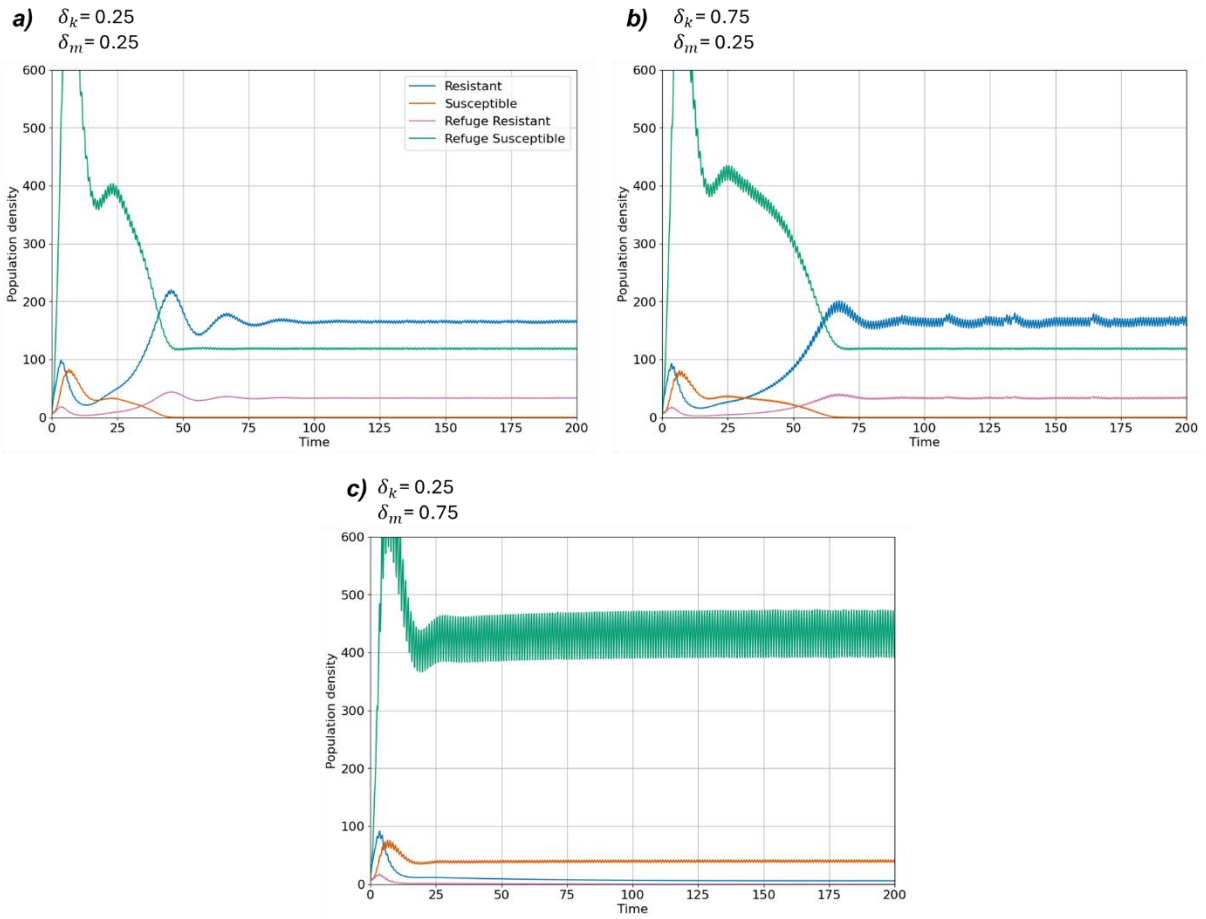

Figure 3:

These plots illustrate the population dynamics of resistant (E) and susceptible (S) populations, including their respective refuge populations (R_E and R_S), under seasonally fluctuating carrying capacities. Each cycle represents one year, where seasonal resource availability changes periodically due to fluctuations in the external ($k(t)$) and refuge ($m(t)$) carrying capacities. The carrying capacities are modelled as a function of time.

Where δ_k controls the seasonal fluctuation in the external environment and δ_m controls the seasonal fluctuation in the refuge.

a) *$\delta_k = 0.25$, $\delta_m = 0.25$: Moderate seasonal variation in both the external environment and refuge.*

b) *$\delta_k = 0.75$, $\delta_m = 0.25$: Large seasonal variation in the external environment, while the refuge remains relatively stable.*

c) *$\delta_k = 0.25$, $\delta_m = 0.75$: Moderate seasonal variation in the external environment, but large fluctuations in the refuge.*

Figure 3 illustrates how different levels of seasonal variation affect the resistant and susceptible population dynamics in both external and refuge environments, whilst trade-off conditions are maintained ensuring, that the susceptible bacteria populations can dominate in

the refuge. When both environments experience moderate seasonal variation (δ_k = 0.25, δ_m = 0.25, **Figure 3a**), resistant bacteria remain dominant in the external environment, while susceptible bacteria persist in the refuge but do not outcompete resistant strains. Increasing seasonal variation in the external environment alone (δ_k = 0.75, δ_m = 0.25, **Figure 3b**) does not shift the competitive balance, where resistant bacteria continue to dominate the external population, suggesting that fluctuations in external carrying capacity alone do not affect their competitive advantage. However, when seasonal variation in the refuge is high (δ_k = 0.25, δ_m = 0.75, **Figure 3c**), we observe a key shift, where susceptible bacteria dominate the external environment. Under these conditions, resistant bacteria do not re-establish dominance within the modelled timeframe. This prolonged dominance occurs because extreme fluctuations in refuge carrying capacity enable susceptible populations to reach exceptionally high densities during refuge expansions. When the refuge contracts, these large susceptible populations disperse into the external environment, numerically overwhelming resistant strains and preventing their recovery. Our results suggest that when refuge cycling surpasses a certain threshold, it can fundamentally reshape competitive dynamics, allowing susceptible bacteria to persist and dominate externally far longer than under moderate seasonal cycling (**Figure S3**).

These results highlight how seasonal fluctuations in resource availability can significantly alter competitive dynamics, revealing general ecological trends and providing a theoretical foundation for understanding bacterial coexistence under temporally varying conditions.

6.5. Discussion

Our results demonstrate that trade-offs associated with phage resistance in resistant bacterial populations are necessary for susceptible bacteria to persist and dominate in the refuge. Without explicitly imposing additional costs on resistant bacteria, susceptible bacteria are unable to establish themselves in the refuge, aligning with broader evolutionary theory that resistance often comes with fitness trade-offs (Lenski and Levin, 1985; Buckling and Rainey, 2002). These trade-offs arise because phage resistance is rarely cost-free and mutations

conferring resistance often impose metabolic/fitness burdens, reduce competitive ability, or interfere with other essential cellular processes. Several studies have demonstrated that resistance mechanisms can be costly. For example, resistance mutations can alter receptor proteins used for phage attachment, but these same receptors may play crucial roles in nutrient uptake or biofilm formation, leading to reduced growth rates or impaired resource acquisition (Bohannan and Lenski, 2000; Gómez and Buckling, 2011). In structured environments, resistant bacteria may also experience reduced symbiotic efficiency when engaging in mutualistic relationships. In rhizobia-phage interactions, for instance, this is the central trade-off observed in our experimental chapters, resistance mutations may decrease nitrogen-fixation efficiency or hinder the ability to establish symbiosis within root nodules, thereby reducing fitness (Heath and Tiffin, 2007; Kiers *et al.*, 2011). Our model supports this by demonstrating that increased mortality or exit rates of resistant bacteria in the refuge allow susceptible bacteria to establish themselves, preventing resistant strains from dominating in both environments. Furthermore, structured environments can actively shape the trade-offs associated with resistance, potentially preventing the rapid fixation of resistant strains and slowing the evolutionary arms race between bacteria and phages (Schrag and Mittler, 1996; Heilmann, Sneppen and Krishna, 2012). This suggests that spatial refuges act not just as a safe haven for susceptible bacteria but as a selective filter favouring bacteria with higher symbiotic efficiency.

This idea places spatial refuges, such as plant root nodules, in a central role not just as passive safe zones from phage predation, but as active ecological and evolutionary drivers shaping rhizobia-phage interactions. Root nodules effectively select for bacterial strains capable of maintaining a delicate balance between resistance mechanisms necessary for soil survival and symbiotic effectiveness crucial for successful plant colonization and nitrogen fixation (Kiers and Denison, 2008; Burghardt, 2020). Thus, spatial refuges actively mediate rhizobia evolution by imposing selection pressures fundamentally different from those experienced in the external soil environment. This dual selection regime stabilizes coexistence between

susceptible and resistant populations, preventing either group from universally dominating and thereby maintaining bacterial diversity within rhizobia communities. Contemporary coevolutionary theory emphasizes how spatial heterogeneity and ecological structure can moderate selection pressures, promoting stable coexistence rather than driving perpetual escalation in resistance and infectivity traits (Brockhurst *et al.*, 2007; Buckingham and Ashby, no date). Consequently, spatial refuges such as plant root nodules serve as ecological buffers, reducing selective pressures for resistance escalation and facilitating the stable, long-term coexistence of diverse bacterial strategies (Schrag & Mittler, 1996; Heilmann et al., 2012). Ultimately, our results strongly support the ecological and evolutionary importance of structured habitats like root nodules in rhizobia-phage systems, demonstrating their critical role in shaping bacterial communities through fitness trade-offs. By explicitly incorporating these trade-offs into our theoretical framework, we have provided a more nuanced understanding of how structured environments modulate bacterial coexistence, limit resistance fixation, and ultimately influence the evolutionary pathways taken by bacteria and their parasites.

6.5.1 Seasonal Cycling and Bacterial Competition

Our results highlight the significant role of seasonal fluctuations in shaping competition between susceptible and resistant bacterial populations. While resistance-associated trade-offs enable susceptible bacteria to persist within refuges, seasonal variation further influences coexistence. Moderate fluctuations in external carrying capacity do not significantly disrupt resistant dominance. However, substantial seasonal variation in the refuge shifts the competitive balance, temporarily favouring susceptible populations. This occurs because periodic increases in refuge capacity allow susceptible populations to grow; when the refuge contracts, more susceptibles disperse into the external environment. This pattern aligns with theoretical models predicting that fluctuating protected niches create temporary advantages for less competitive phenotypes (Lenski and Levin, 1985; Schrag and Mittler, 1996). Despite this advantage, susceptible bacteria cannot permanently dominate. Instead, our results

suggest that the resistant-dominated equilibrium is weakly stable, where oscillations repeatedly push the system away from equilibrium, delaying resistant dominance for extended periods. Similar transient coexistence has been observed in biofilm systems, where biofilm expansion slows competitive exclusion (Brockhurst et al., 2007) and in fluctuating phytoplankton and predator-prey systems (Huisman and Weissing, 1999; Becks *et al.*, 2010). This non-equilibrium perspective aligns with ecological theories suggesting that periodic disruptions promote coexistence by resetting competitive dynamics (Chesson, 2000).

6.6. Conclusion

Our work highlights the critical role of structured environments and seasonal fluctuations in shaping bacterial competition and coexistence within bacterial-phage systems. Our findings demonstrate that trade-offs associated with resistance are essential for the persistence of susceptible bacteria in spatial refuges, as resistance alone does not confer universal competitive advantage. When resistance incurs substantial costs, such as increased mortality or altered movement within refuges, susceptible populations can establish dominance, closely mirroring our empirical observations of bacterial competition within symbiotic environments. Additionally, seasonal fluctuations in resource availability emerge as key factors influencing competitive outcomes, while moderate fluctuations typically maintain resistant dominance, extreme seasonal variation within refuges can shift competitive balance in favour of susceptible populations. This shift occurs due to increased dispersal of susceptible bacteria from refuges during resource contractions, temporarily challenging resistant dominance externally.

Future research should expand upon these results by explicitly incorporating realistic bacterial replication rates and detailed growth dynamics, better connecting theoretical outcomes to empirically observed ecological patterns. Additionally, including evolutionary processes, such as evolving phage infectivity, bacterial resistance strategies, and compensatory adaptations, would significantly enhance our understanding of how coevolution influences long-term coexistence. Investigating these evolutionary interactions will provide deeper insights into the

stability of microbial communities and reveal how fluctuating selection pressures shape bacterial-phage coexistence. Such studies would further clarify how spatial and temporal heterogeneity influences microbial evolution and ecological stability in diverse natural and applied contexts, including agricultural systems and other ecosystems where bacteria-phage interactions are crucial.

6.7 Supplementary Materials

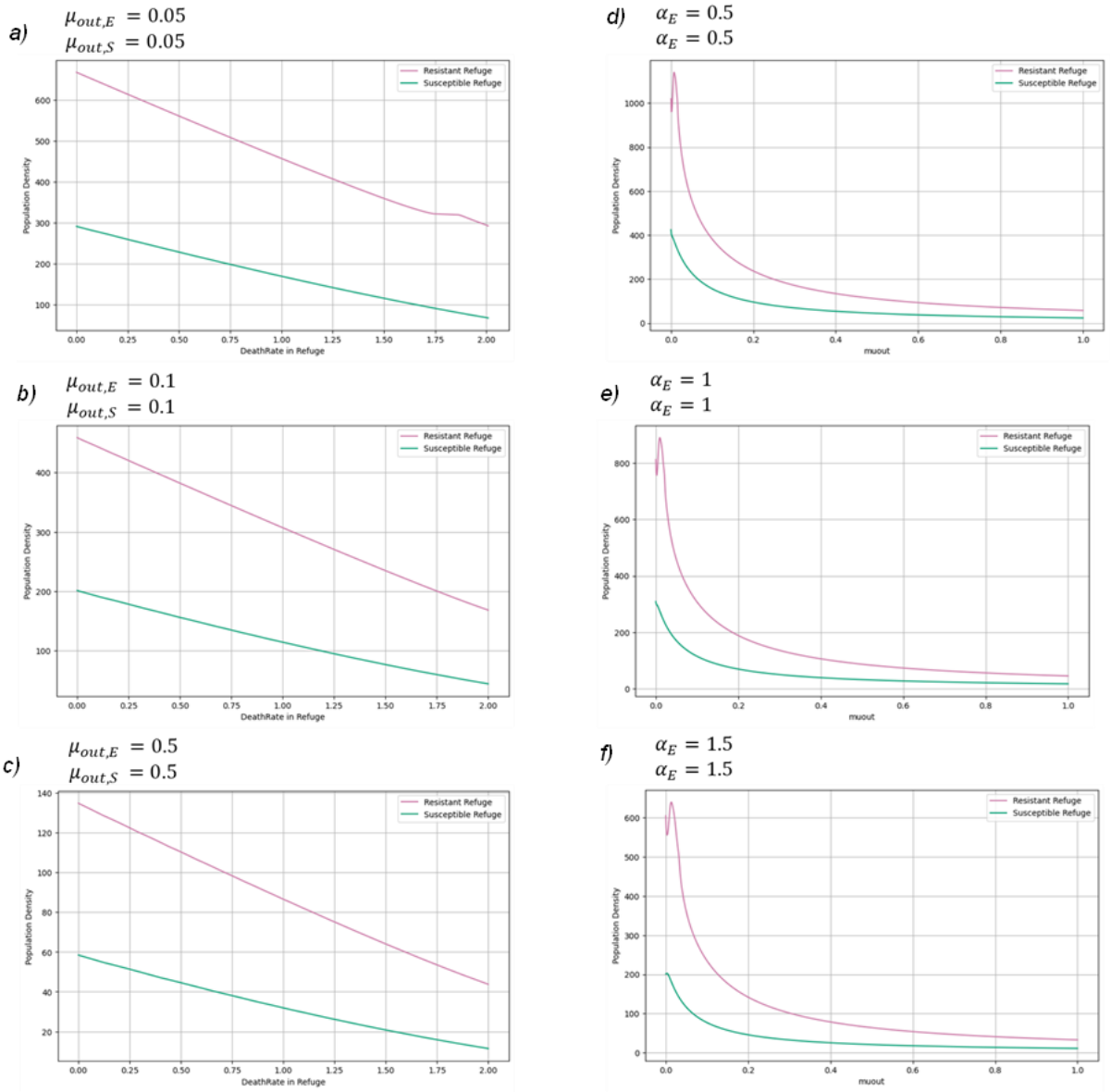

Figure S1: *Sensitivity analysis for refuge parameters:*

a-c) *Examines how varying the death rate in the refuge for susceptible and resistant populations (α_S and α_E respectively) influences their maximum population densities (R_S and R_E respectively). For each plot, exit rate from the refuge for susceptible and resistant populations ($\mu_{out,S}$ and $\mu_{out,E}$) have been modified where; a) $\mu_{out,S}$ and $\mu_{out,E}$ = 0.05; b) $\mu_{out,S}$ and $\mu_{out,E}$ = 0.1; c) $\mu_{out,S}$ and $\mu_{out,E}$ = 0.5.*

d-f) *Examines how varying the exit rate from the refuge for susceptible and resistant populations ($\mu_{out,S}$ and $\mu_{out,E}$ respectively) influences their maximum population densities (R_S and R_E respectively). For each plot, death rate in refuge for susceptible and resistant populations (α_S and α_E) have been modified where; d) α_S and α_E = 0.5; e) α_S and α_E = 1; f) α_S and α_E = 1.5.*

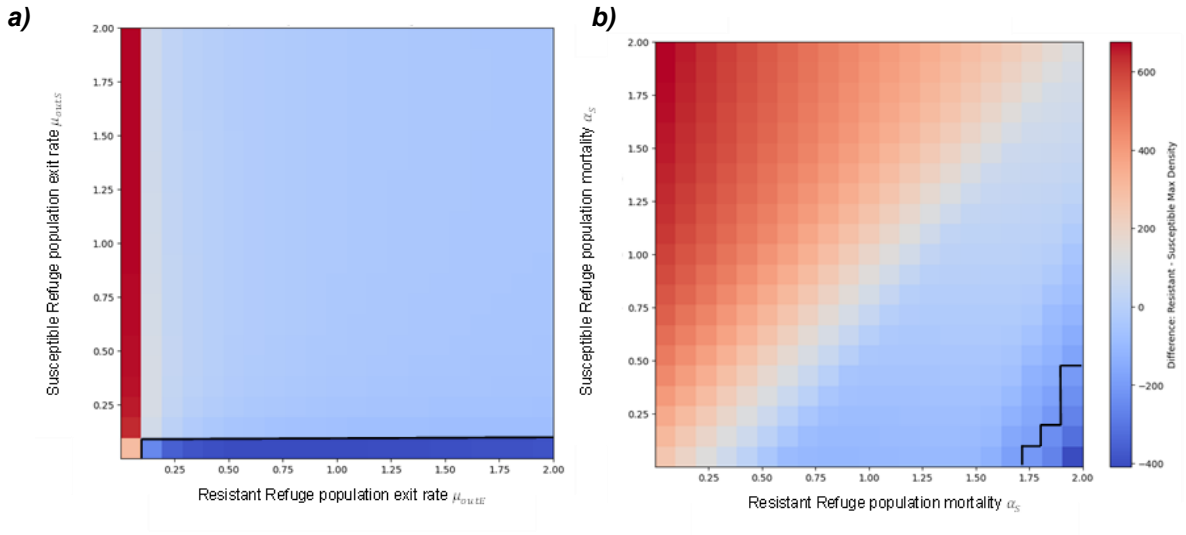

Figure S2: *The black shows when the susceptible population will start dominating in the refuge* ***a)*** *shows the effect of varying exit rates from the refuge for both bacterial populations (* μ_{out}*), when mortality for both populations in the refuge (* α_S *and* α_E*) = 1); and all other parameters follow* ***Table 1****. This shows that the susceptible population can only win when varying* μ_{out} *if* $\mu_{out\,S} = 0$*.* ***b)*** *shows the effect of varying mortality in the refuge for both populations (*α_S *and* α_E*) when exit rates for both populations (*$\mu_{out,S}$ *and* $\mu_{out,E}$ *) = 0.1. We see that as mortality for the resistant population get high, the susceptible population can win with this changed alone.*

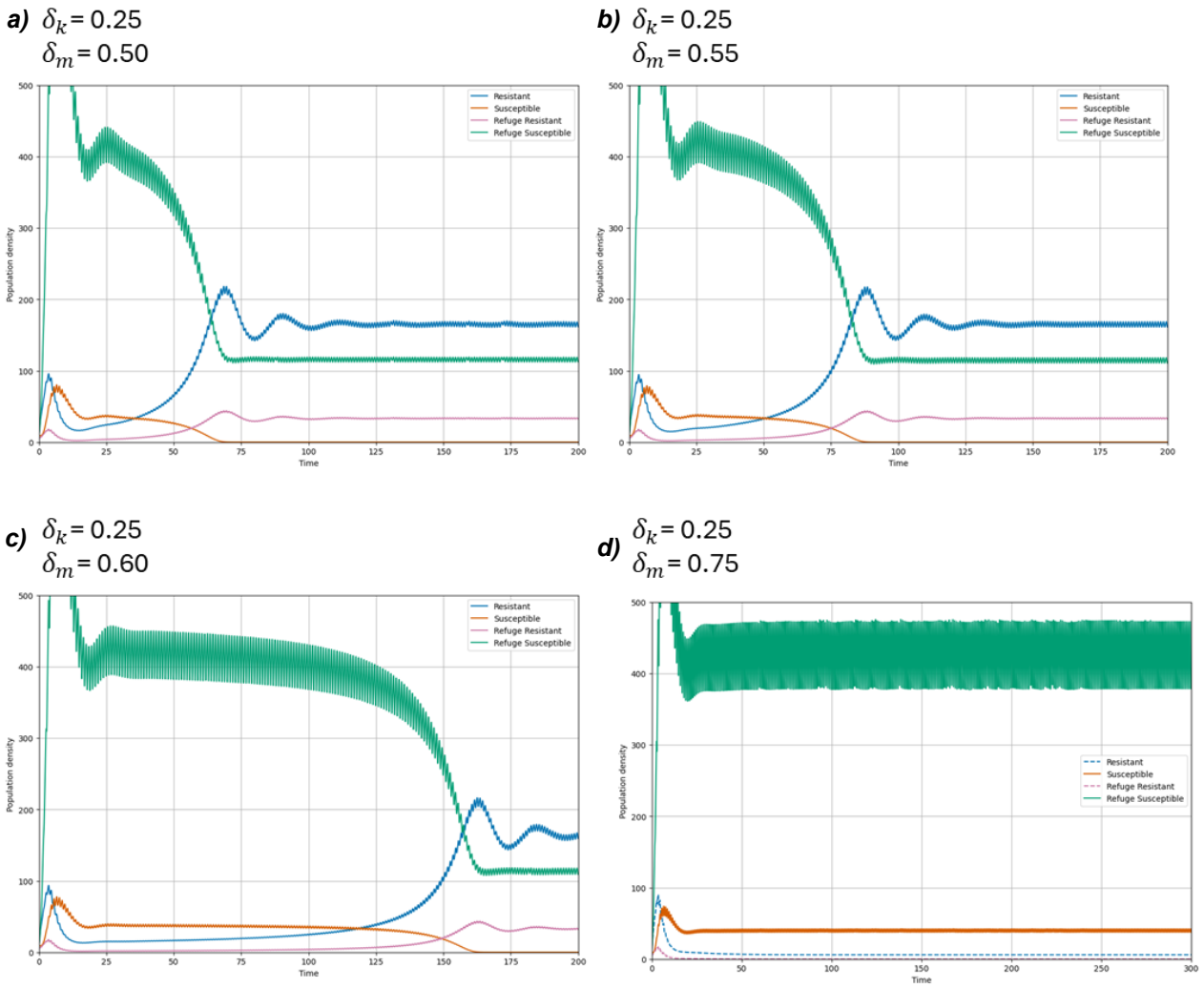

Figure S3:

These plots illustrate the population dynamics of resistant (E) and susceptible (S) populations, including their respective refuge populations (R_E and R_S), under seasonally fluctuating carrying capacities. Each cycle represents one year, where seasonal resource availability changes periodically due to fluctuations in the external ($k(t)$) and refuge ($m(t)$) carrying capacities. Where ***a)*** *$\delta_k = 0.25$, $\delta_m = 0.50$;* ***b)*** *$\delta_k = 0.25$, $\delta_m = 0.55$;* ***c)*** *$\delta_k = 0.25$, $\delta_m = 0.60$;* ***d)*** *$\delta_k = 0.25$, $\delta_m = 0.75$.*

6.8. References

Becks, L. *et al.* (2010) 'Reduction of adaptive genetic diversity radically alters eco-evolutionary community dynamics', *Ecology Letters*, 13(8), pp. 989–997. Available at: https://doi.org/10.1111/j.1461-0248.2010.01490.x.

Best, A. *et al.* (2017) 'Host–parasite fluctuating selection in the absence of specificity', *Proceedings of the Royal Society B: Biological Sciences*, 284(1866), p. 20171615. Available at: https://doi.org/10.1098/rspb.2017.1615.

Bohannan, B. j. m. and Lenski, R. e. (2000) 'Linking genetic change to community evolution: insights from studies of bacteria and bacteriophage', *Ecology Letters*, 3(4), pp. 362–377. Available at: https://doi.org/10.1046/j.1461-0248.2000.00161.x.

Brockhurst, M.A. *et al.* (2007) 'Niche Occupation Limits Adaptive Radiation in Experimental Microcosms', *PLOS ONE*, 2(2), p. e193. Available at: https://doi.org/10.1371/journal.pone.0000193.

Buckingham, L.J. and Ashby, B. (no date) 'Coevolutionary theory of hosts and parasites', *Journal of Evolutionary Biology*, n/a(n/a). Available at: https://doi.org/10.1111/jeb.13981.

Buckling, A. and Rainey, P.B. (2002) 'Antagonistic coevolution between a bacterium and a bacteriophage', *Proceedings. Biological Sciences*, 269(1494), pp. 931–936. Available at: https://doi.org/10.1098/rspb.2001.1945.

Burghardt, L.T. (2018) 'Evolving together, evolving apart: measuring the fitness of rhizobial bacteria in and out of symbiosis with leguminous plants'. Available at: https://doi.org/10.1111/nph.16045.

Burghardt, L.T. (2020) 'Evolving together, evolving apart: measuring the fitness of rhizobial bacteria in and out of symbiosis with leguminous plants', *The New Phytologist*, 228(1), pp. 28–34. Available at: https://doi.org/10.1111/nph.16045.

Chesson, P. (2000) 'Mechanisms of Maintenance of Species Diversity', *Annual Review of Ecology, Evolution, and Systematics*, 31(Volume 31, 2000), pp. 343–366. Available at: https://doi.org/10.1146/annurev.ecolsys.31.1.343.

Gómez, P. and Buckling, A. (2011) 'Bacteria-Phage Antagonistic Coevolution in Soil', *Science*, 332(6025), pp. 106–109. Available at: https://doi.org/10.1126/science.1198767.

Heath, K.D. and Tiffin, P. (2007) 'Context dependence in the coevolution of plant and rhizobial mutualists', *Proceedings. Biological Sciences*, 274(1620), pp. 1905–1912. Available at: https://doi.org/10.1098/rspb.2007.0495.

Heilmann, S., Sneppen, K. and Krishna, S. (2012) 'Coexistence of phage and bacteria on the boundary of self-organized refuges', *Proceedings of the National Academy of Sciences of the United States of America*, 109(31), pp. 12828–12833. Available at: https://doi.org/10.1073/pnas.1200771109.

Hirsch, P. (2002) 'Sprent, J.I. Nodulation in legumes', *Annals of Botany*, 89(6), pp. 797–798. Available at: https://doi.org/10.1093/aob/mcf128.

Holt, R.D. (1977) 'Predation, apparent competition, and the structure of prey communities', *Theoretical Population Biology*, 12(2), pp. 197–129. Available at: https://doi.org/10.1016/0040-5809(77)90042-9.

Holt, R.D., Grover, J. and Tilman, D. (1994) ‘Simple Rules for Interspecific Dominance in Systems with Exploitative and Apparent Competition’, *The American Naturalist*, 144(5), pp. 741–771.

Huisman, J. and Weissing, F.J. (1999) ‘Biodiversity of plankton by species oscillations and chaos’, *Nature*, 402(6760), pp. 407–410. Available at: https://doi.org/10.1038/46540.

Kiers, E.T. *et al.* (2011) ‘Reciprocal Rewards Stabilize Cooperation in the Mycorrhizal Symbiosis’, *Science*, 333(6044), pp. 880–882. Available at: https://doi.org/10.1126/science.1208473.

Kiers, E.T. and Denison, R.F. (2008) ‘Sanctions, Cooperation, and the Stability of Plant-Rhizosphere Mutualisms’, *Annual Review of Ecology, Evolution, and Systematics*, 39(Volume 39, 2008), pp. 215–236. Available at: https://doi.org/10.1146/annurev.ecolsys.39.110707.173423.

Lenski, R.E. and Levin, B.R. (1985) ‘Constraints on the Coevolution of Bacteria and Virulent Phage: A Model, Some Experiments, and Predictions for Natural Communities’, *The American Naturalist*, 125(4), pp. 585–602. Available at: https://doi.org/10.1086/284364.

Levin, B.R., Stewart, F.M. and Chao, L. (1977) ‘Resource-Limited Growth, Competition, and Predation: A Model and Experimental Studies with Bacteria and Bacteriophage’, *The American Naturalist*, 111(977), pp. 3–24. Available at: https://doi.org/10.1086/283134.

Scanlan, P.D., Buckling, A. and Hall, A.R. (2015) ‘Experimental evolution and bacterial resistance: (co)evolutionary costs and trade-offs as opportunities in phage therapy research’, *Bacteriophage*, 5(2), p. e1050153. Available at: https://doi.org/10.1080/21597081.2015.1050153.

Schrag, S.J. and Mittler, J.E. (1996) ‘Host-Parasite Coexistence: The Role of Spatial Refuges in Stabilizing Bacteria-Phage Interactions’, *The American Naturalist*, 148(2), pp. 348–377.

Chapter 7: Discussion

7.1 Summary

Bacteria-phage interactions drive rapid evolutionary change, shaping microbial communities in ways that extend beyond survival under phage predation. Resistance to phages often comes at a cost, affecting bacterial fitness in other ecological contexts, particularly in environments where bacteria engage in symbiotic relationships. In structured habitats, such as root nodules, bacterial populations can escape phage selection, altering the dynamics of resistance evolution and coevolutionary cycles. However, this escape is temporary, and when bacteria transition back into a phage-rich environment, they face strong selective pressures that influence population structure and adaptation.

Here, we suggest that phage resistance in Rhizobium carries significant trade-offs, particularly for symbiotic function. While some resistance mechanisms preserved competitive ability, others altered traits that indirectly affected symbiosis, leading to reduced benefit for the plant. This variation underscores how the evolutionary trajectory of resistance is shaped not only by phage pressure but also by ecological context. Moreover, spatial structure and environmental variation, such as seasonal changes in host availability modulate these dynamics, delaying competitive exclusion and allowing coexistence between resistant and susceptible strains. By integrating experimental evolution, competition assays, and mathematical modelling, we show that microbial evolution is not solely a product of arms-race dynamics, but is mediated by the costs of resistance, ecological structure, and fluctuating selection.

7.2 The costs of phage resistance and its impact on symbiosis

Our results show that, for one of the three phages tested, evolution of resistance in *Rhizobium* came with clear fitness costs, particularly in the ability to form effective symbioses with legumes. Experimental evolution revealed that phage-resistant rhizobia often exhibited reduced symbiotic efficiency, leading to lower plant biomass and nitrogen fixation compared to ancestral and phage-susceptible strains (**Chapter 3, Figure 6**). Whole-genome sequencing

identified mutations in *acoA*, a gene involved in the TCA cycle, in multiple resistant clones (**Chapter 3, Figure 3a**). Given that nitrogen fixation is an ATP-intensive process, disruptions to central metabolism likely impair rhizobia's ability to supply nitrogen to the host plant, representing a clear case of antagonistic pleiotropy, where adaptation to phage predation reduces fitness in a symbiotic environment (Heath and Tiffin, 2007). These findings are consistent with studies in other bacterial systems where phage resistance mutations disrupt essential metabolic pathways, leading to trade-offs in host interactions (Duffy, Turner and Burch, 2006; Gómez and Buckling, 2011). However, not all resistance mechanisms imposed the same fitness costs. Some phage-resistant rhizobia, across all phage treatments carried mutations in exopolysaccharide (EPS) biosynthesis gene, *wcaJ*, which is involved in polysaccharide assembly of biofilms (**Chapter 3, Figure 3**). These clones exhibited increased biofilm production, likely forming a physical barrier against phage adsorption. Notably, these biofilm-producing strains did not exhibit significant reductions in symbiotic efficiency, suggesting that structural resistance mechanisms may mitigate trade-offs. This pattern is supported by previous research showing that EPS-mediated phage resistance can protect bacteria without severely impairing interactions with certain hosts (Tan *et al.*, 2020; Bain *et al.*, 2024). However, increased EPS production could influence rhizobial dispersal, root colonization efficiency, and competition with native soil microbes, potentially altering rhizosphere dynamics (Gómez and Buckling, 2011; Simmons *et al.*, 2020).

A particularly striking outcome was the emergence of lysogeny via integration of temperate phages into the rhizobial genome during coevolution with Phage 3. This shift from lytic to lysogenic infection (**Chapter 3**), conferred superinfection immunity, relaxing selection for costly resistance mutations. (Feiner *et al.*, 2015; Touchon, Moura de Sousa and Rocha, 2017). As a result, lysogenized rhizobia maintained symbiotic function and avoided the fitness costs such as reduced motility, observed in clones that evolved resistance to Phages 1 and 2 (**Chapter 3, Figure 5**). These results align with broader findings that temperate phages can

act as mutualists rather than strict antagonists, stabilizing bacterial populations and even introducing beneficial genes (Bobay, Touchon and Rocha, 2014; Howard-Varona *et al.*, 2018).

Taken together, these findings highlight the diverse evolutionary responses rhizobia can adopt under phage pressure. While metabolic resistance often imposes symbiotic trade-offs, alternative resistance strategies, such as EPS production or lysogeny, allow rhizobia to evade phage predation while maintaining symbiotic function. Given that phage pressure varies across environments, it is likely that the persistence of different resistance strategies contributes to the observed variation in rhizobial symbiotic efficiency in natural and agricultural settings (Heath and Tiffin, 2007; Burghardt, 2020). For example, **Chapter 5** showed that rhizobia with minimal phage exposure due to early nodulation, evolved lower resistance but retained higher symbiotic performance. However, this came at a cost, when reintroduced into the soil, these strains were less competitive than those evolved under sustained phage selection. This context dependence highlights how spatial structure, not just resistance mechanisms themselves, can shape both ecological outcomes and evolutionary trajectories.

7.3 Root nodules disrupt phage-driven coevolution in rhizobia populations

Spatial refuges play a pivotal role in shaping host–parasite interactions, primarily by offering susceptible host populations a temporary escape from intense predation or infection (Hassell and May, 1973; Oaten and Murdoch, 1975; Schrag and Mittler, 1996). **Chapter 4** demonstrated how such refuges can buffer host populations from extinction-level parasite predation, enabling susceptible bacterial strains to coexist alongside their parasites (**Chapter 4, Figure 2**). This result aligns with ecological models showing that even a partial refuge can stabilize prey–predator or host–parasite systems by reducing overall mortality and preventing rapid population collapse (Holt, 1977; Murdoch, Chesson and Chesson, 1985; Ruxton, 1995). Notably, under certain parameter values (e.g, high rates of host movement between the refuge and external environments), the same refuge can inadvertently intensify outbreaks in the external population by repeatedly supplying susceptible hosts to the parasite and amplifying rather than mitigating disease cycles (Holt and Hochberg, 1997).This outcome reflects a

broader principle in spatial ecology, where the effects of refuges are highly context-dependent, shaped by factors such as refuge size, movement between environments, host mobility, and the timing of dispersal events (Keeling and Rohani, 2008; Koskella and Brockhurst, 2014). In systems where movement between refuge and non-refuge zones is limited, refuges can act as effective reservoirs of susceptible hosts, slowing or even halting the spread of infection (Acevedo *et al.*, 2015; Heard *et al.*, 2015). However, when movement is higher, refuges risk functioning as source habitats, continually providing the external population with susceptible individuals, which can perpetuate cycles of host and parasite abundance (Holt and Hochberg, 1997; White *et al.*, 2018). Empirical and modelling work in both microbial and macro-ecological systems supports these patterns. For example, Brockhurst *et al.*, (2007) demonstrated that increased dispersal of bacteria from biofilm refuges enabled phage-resistant strains to dominate, breaking down coexistence with susceptible strains. As a result, while spatial heterogeneity is often considered a stabilizing force in host–parasite systems, the manner in which hosts enter and leave the refuge can create ecological feedback that intensify infection peaks when conditions favour a surplus of susceptible individuals rejoining the parasite-exposed environment (Chesson, 2000).

Chapter 5 built on this theoretical foundation by providing empirical evidence that root nodules function as ecological refuges capable of altering the selective pressures imposed by phages on rhizobial populations. Rhizobia that entered nodules early experienced significantly weaker selection for resistance, while those that remained in the soil evolved higher resistance due to continuous exposure to phage (**Chapter 5, Figure 2**). This spatial separation created a clear evolutionary divergence, where nodule-associated strains retained susceptibility but higher symbiotic performance, while free-living strains traded off symbiotic quality for phage resistance (**Chapter 5, Figure S3**). Escape from co-evolution into nodules, may preserve traits that are important for effective symbiosis, acting as filters that maintain functional compatibility with the host. Preserving susceptible rhizobia through spatial refuge in nodules has important implications for phage–rhizobia coevolution. By shielding bacteria from phage exposure,

nodules interrupt the strong selection for resistance that occurs in the soil. This allows a pool of phage-susceptible but symbiotically efficient genotypes to persist, strains that would otherwise be lost under sustained antagonistic pressure (Schrag and Mittler, 1996; Heilmann, Sneppen and Krishna, 2012). Several studies have shown that in spatially structured environments, such as biofilms or host-associated niches, susceptible bacteria can persist alongside phage due to limited access or reduced phage infectivity (Brockhurst *et al.*, 2007). For example, Brockhurst *et al*. (2007) experimentally demonstrated that spatial refuges within biofilms could maintain susceptible strains by physically excluding phages, even in the absence of direct resistance. Similarly, in a soil-like system, Gómez and Buckling (2011) showed that resistant *Pseudomonas fluorescens* strains outcompeted susceptible ones under strong phage pressure, but this dominance came with clear costs in growth rate and resource competition. In contrast, other studies suggest that in well-mixed or highly connected environments, susceptible strains are rapidly driven to extinction, especially when resistance does not carry strong fitness costs (Morgan, Gandon and Buckling, 2005; Gandon *et al.*, 2008). Moreover, the reintroduction of these susceptible rhizobia into phage-rich soil upon plant senescence may slow or reset the coevolutionary process, preventing the fixation of resistance alleles and maintaining a mix of resistant and susceptible lineages. This mechanism parallels suggestions in other host–parasite systems where recurring refuges or bottlenecks interrupt arms races by continually restoring susceptible hosts or pathogens (Lively, 1999; Buckling and Rainey, 2002). However, the ultimate impact of releasing non-resistant strains can vary, while it may prolong coexistence by buffering phage-driven extinctions (Gómez & Buckling, 2011), it could also trigger larger infection peaks or intensify selective turnover in certain contexts.

Expanding on this, we explored how different trade-offs allow susceptible and resistant strains to coexist within a structured refuge system over longer time. In contrast to **Chapter 4**, where hosts were considered a single population, **Chapter 6** explicitly incorporated competition between resistant and susceptible bacterial strains and the costs of resistance (e.g., higher

mortality or exit rates in refuges). When such resistance-associated costs were significant, susceptible bacteria could dominate inside the refuge, while resistant strains maintained an advantage in the external environment (**Chapter 6, Figure 1b**), consistent with our experimental data and with theoretical predictions that trade-offs can stabilize coexistence in predator-prey or host-parasite systems(Brockhurst *et al.*, 2007; Heilmann, Sneppen and Krishna, 2012). Notably, introducing seasonal fluctuations in resource availability showed that large oscillations in refuge capacity could temporarily favour susceptible strains by facilitating mass dispersal back into the soil, delaying the recovery of resistant strains (**Chapter 6, Figure 3c**). This finding supports ecological theory that temporal variability, particularly under non-equilibrium dynamics, can promote the persistence of otherwise disadvantaged competitors (Chesson, 2000). Although the model did not explicitly track evolving phage populations, it reinforces the idea that structured habitats, coupled with ecological trade-offs, can maintain both susceptible and resistant strains across varied environmental conditions. By acting as a protective niche that favours symbiotic performance, root nodules can effectively disrupt phage-driven coevolution in the soil. In doing so, they ensure that susceptible, yet mutually beneficial, bacteria remain part of the microbial community, supporting broader microbial diversity and possibly moderating the pace and trajectory of evolutionary change.

7.4 Implications for Rhizobia–Legume Symbiosis and Future Directions

Overall, this work reveals how root nodules play a critical role in shaping how phage predation influences rhizobial evolution and the stability of symbiosis. By providing temporary escape from antagonistic selection, nodules help maintain phage-susceptible strains that retain high symbiotic quality, preserving the mutualistic benefits for the host plant. In doing so, they disrupt the trajectory of resistance fixation and slow down phage–bacteria coevolution in the surrounding soil. For rhizobia–legume symbiosis, this has important implications, the presence of refuges may help sustain a diverse pool of effective symbionts across fluctuating environmental conditions and over successive plant generations, buffering mutualism from the destabilising effects of phage pressure.

These findings also highlight the importance of considering ecological context and community structure in understanding the dynamics of rhizobial persistence and function. While this study focused primarily on phage–rhizobia interactions, natural soils harbour complex microbial communities where multiple phage types, microbial competitors, and mutualists co-occur. Future research should therefore explore how these broader community interactions modulate the effects of refuge dynamics, particularly in more ecologically realistic or agricultural settings.

Theoretical extensions of this work could also incorporate recurrent seasonal cycles, mimicking agricultural systems where legume crops are planted and harvested on an annual basis. Modelling how the periodic release of susceptible rhizobia from nodules interacts with coevolving phages in the soil would help clarify whether refuges merely delay resistance fixation or more fundamentally shape long-term coevolutionary dynamics. Similarly, extending models to track evolving phage populations, alongside bacterial costs of resistance, could offer richer insights into the durability of rhizobia–legume mutualisms in changing environments. Tracking both evolving phage populations and bacterial resistance costs could help test whether ecological feedbacks and trade-offs lead to evolutionary branching, where susceptible and resistant strains stably coexist over time

Ultimately, understanding how spatial structure, resistance trade-offs, and ecological fluctuations interact will be crucial for predicting the resilience of symbiotic systems and designing interventions that support both microbial diversity and sustainable nitrogen fixation. Root nodules may be more than just sites of nitrogen exchange, could be key ecological filters and evolutionary buffers, helping to stabilise one of nature’s most important microbial partnerships.

7.5 References

Acevedo, M.A. *et al.* (2015) 'Spatial heterogeneity, host movement and mosquito-borne disease transmission', *PloS One*, 10(6), p. e0127552. Available at: https://doi.org/10.1371/journal.pone.0127552.

Bain, W. *et al.* (2024) 'In Vivo Evolution of a Klebsiella pneumoniae Capsule Defect With wcaJ Mutation Promotes Complement-Mediated Opsonophagocytosis During Recurrent Infection', *The Journal of Infectious Diseases*, 230(1), pp. 209–220. Available at: https://doi.org/10.1093/infdis/jiae003.

Bobay, L.-M., Touchon, M. and Rocha, E.P.C. (2014) 'Pervasive domestication of defective prophages by bacteria', *Proceedings of the National Academy of Sciences*, 111(33), pp. 12127–12132. Available at: https://doi.org/10.1073/pnas.1405336111.

Brockhurst, M.A. *et al.* (2007) 'Niche Occupation Limits Adaptive Radiation in Experimental Microcosms', *PLOS ONE*, 2(2), p. e193. Available at: https://doi.org/10.1371/journal.pone.0000193.

Buckling, A. and Rainey, P.B. (2002) 'Antagonistic coevolution between a bacterium and a bacteriophage', *Proceedings. Biological Sciences*, 269(1494), pp. 931–936. Available at: https://doi.org/10.1098/rspb.2001.1945.

Burghardt, L.T. (no date) 'Evolving together, evolving apart: measuring the fitness of rhizobial bacteria in and out of symbiosis with leguminous plants'. Available at: https://doi.org/10.1111/nph.16045.

Chesson, P. (2000) 'Mechanisms of Maintenance of Species Diversity', *Annual Review of Ecology, Evolution, and Systematics*, 31(Volume 31, 2000), pp. 343–366. Available at: https://doi.org/10.1146/annurev.ecolsys.31.1.343.

Duffy, S., Turner, P.E. and Burch, C.L. (2006) 'Pleiotropic Costs of Niche Expansion in the RNA Bacteriophage Φ6', *Genetics*, 172(2), pp. 751–757. Available at: https://doi.org/10.1534/genetics.105.051136.

Feiner, R. *et al.* (2015) 'A new perspective on lysogeny: prophages as active regulatory switches of bacteria', *Nature Reviews. Microbiology*, 13(10), pp. 641–650. Available at: https://doi.org/10.1038/nrmicro3527.

Gandon, S. *et al.* (2008) 'Host–parasite coevolution and patterns of adaptation across time and space', *Journal of Evolutionary Biology*, 21(6), pp. 1861–1866. Available at: https://doi.org/10.1111/j.1420-9101.2008.01598.x.

Gómez, P. and Buckling, A. (2011) 'Bacteria-Phage Antagonistic Coevolution in Soil', *Science*, 332(6025), pp. 106–109. Available at: https://doi.org/10.1126/science.1198767.

Hassell, M.P. and May, R.M. (1973) 'Stability in Insect Host-Parasite Models', *The Journal of Animal Ecology*, 42(3), p. 693. Available at: https://doi.org/10.2307/3133.

Heard, G.W. *et al.* (2015) 'Refugia and connectivity sustain amphibian metapopulations afflicted by disease', *Ecology Letters*. Edited by C. Bradshaw, 18(8), pp. 853–863. Available at: https://doi.org/10.1111/ele.12463.

Heath, K.D. and Tiffin, P. (2007) 'Context dependence in the coevolution of plant and rhizobial mutualists', *Proceedings. Biological Sciences*, 274(1620), pp. 1905–1912. Available at: https://doi.org/10.1098/rspb.2007.0495.

Heilmann, S., Sneppen, K. and Krishna, S. (2012) ‘Coexistence of phage and bacteria on the boundary of self-organized refuges’, *Proceedings of the National Academy of Sciences of the United States of America*, 109(31), pp. 12828–12833. Available at: https://doi.org/10.1073/pnas.1200771109.

Holt, R.D. (1977) ‘Predation, apparent competition, and the structure of prey communities’, *Theoretical Population Biology*, 12(2), pp. 197–129. Available at: https://doi.org/10.1016/0040-5809(77)90042-9.

Holt, R.D. and Hochberg, M.E. (1997) ‘When Is Biological Control Evolutionarily Stable (or Is It)?’, *Ecology*, 78(6), pp. 1673–1683. Available at: https://doi.org/10.1890/0012-9658(1997)078[1673:WIBCES]2.0.CO;2.

Howard-Varona, C. *et al.* (2018) ‘Multiple mechanisms drive phage infection efficiency in nearly identical hosts’, *The ISME Journal*, 12(6), pp. 1605–1618. Available at: https://doi.org/10.1038/s41396-018-0099-8.

Keeling, M.J. and Rohani, P. (2008) *Modeling Infectious Diseases in Humans and Animals*. Princeton University Press. Available at: https://doi.org/10.2307/j.ctvcm4gk0.

Koskella, B. and Brockhurst, M.A. (2014) ‘Bacteria–phage coevolution as a driver of ecological and evolutionary processes in microbial communities’, *FEMS Microbiology Reviews*, 38(5), pp. 916–931. Available at: https://doi.org/10.1111/1574-6976.12072.

Lively, C.M. (1999) ‘Migration, Virulence, and the Geographic Mosaic of Adaptation by Parasites’, *The American Naturalist*, 153(S5), pp. S34–S47. Available at: https://doi.org/10.1086/303210.

Morgan, A.D., Gandon, S. and Buckling, A. (2005) ‘The effect of migration on local adaptation in a coevolving host-parasite system’, *Nature*, 437(7056), pp. 253–256. Available at: https://doi.org/10.1038/nature03913.

Murdoch, W.W., Chesson, J. and Chesson, P.L. (1985) ‘Biological Control in Theory and Practice’, *The American Naturalist*, 125(3), pp. 344–366. Available at: https://doi.org/10.1086/284347.

Oaten, A. and Murdoch, W.W. (1975) ‘Switching, Functional Response, and Stability in Predator-Prey Systems’, *The American Naturalist*, 109(967), pp. 299–318. Available at: https://doi.org/10.1086/282999.

Ruxton, G.D. (1995) ‘Short Term Refuge Use and Stability of Predator-Prey Models’, *Theoretical Population Biology*, 47(1), pp. 1–17. Available at: https://doi.org/10.1006/tpbi.1995.1001.

Schrag, S.J. and Mittler, J.E. (1996) ‘Host-Parasite Coexistence: The Role of Spatial Refuges in Stabilizing Bacteria-Phage Interactions’, *The American Naturalist*, 148(2), pp. 348–377.

Simmons, E.L. *et al.* (2020) ‘Biofilm Structure Promotes Coexistence of Phage-Resistant and Phage-Susceptible Bacteria’, *mSystems*, 5(3), pp. e00877-19. Available at: https://doi.org/10.1128/mSystems.00877-19.

Tan, D. *et al.* (2020) ‘A Frameshift Mutation in wcaJ Associated with Phage Resistance in Klebsiella pneumoniae’. Available at: https://doi.org/10.3390/microorganisms8030378.

Touchon, M., Moura de Sousa, J.A. and Rocha, E.P. (2017) ‘Embracing the enemy: the diversification of microbial gene repertoires by phage-mediated horizontal gene transfer’,

Current Opinion in Microbiology, 38, pp. 66–73. Available at: https://doi.org/10.1016/j.mib.2017.04.010.

White, E.C. *et al.* (2018) 'Manipulation of host and parasite microbiotas: Survival strategies during chronic nematode infection', *Science Advances*, 4(3), p. eaap7399. Available at: https://doi.org/10.1126/sciadv.aap7399.